GLUTAMATE METABOLISM REVISITED

Clarifying the pathophysiology of GLS mutations

Lynne Rumping

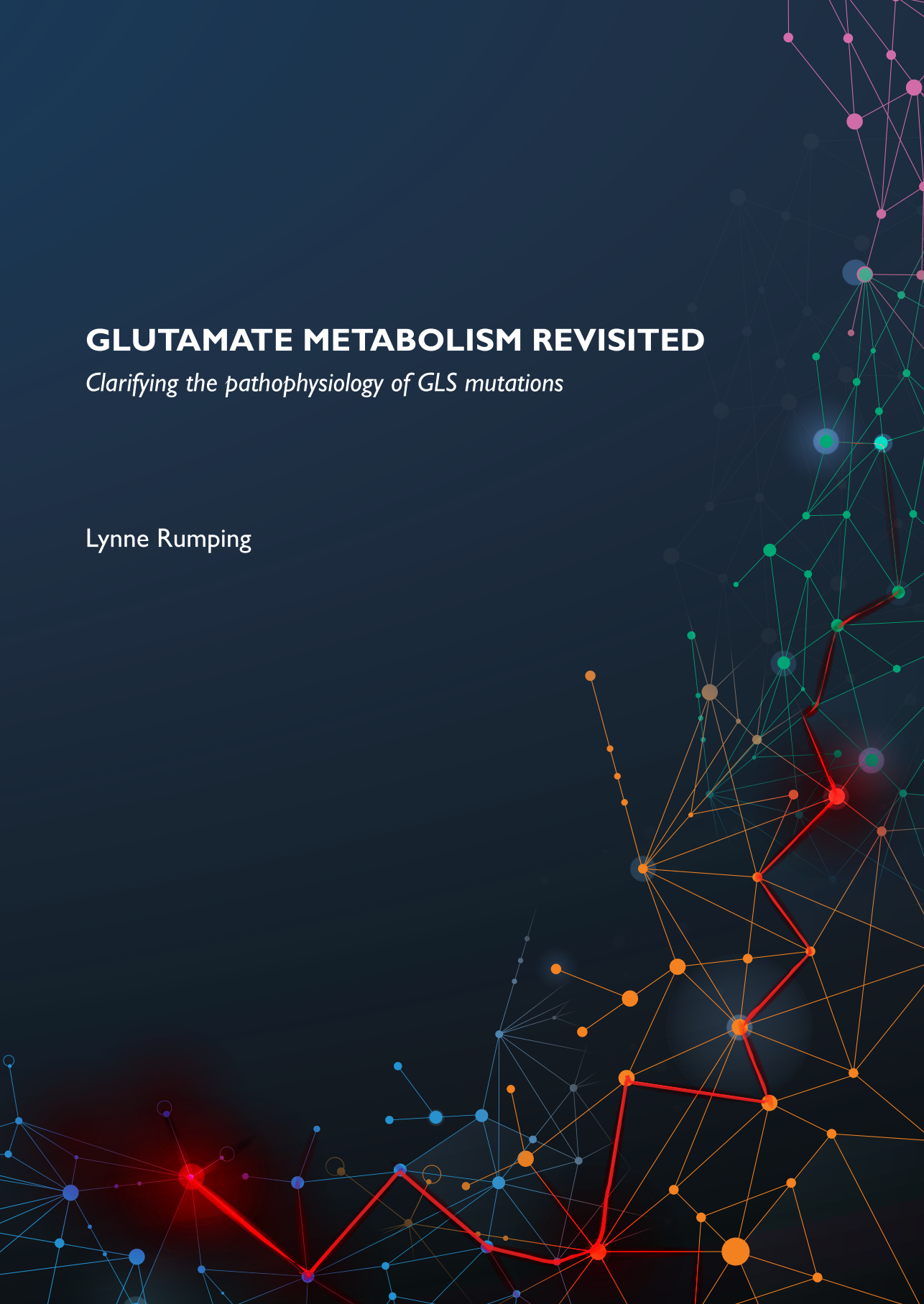

GLUTAMATE METABOLISM REVISITED

Clarifying the pathophysiology of *GLS* mutations

Lynne Rumping

ISBN: 978-94-6323-614-0
Cover: Erik Haverkort
Lay-out: Ilse Modder, www.ilsemodder.nl
Printed by: Gildeprint Eschede, www.gildeprint.nl

GLUTAMATE METABOLISM REVISITED

Clarifying the pathophysiology of *GLS* mutations

Glutamaat metabolisme opnieuw bekeken:
Opheldering van de ziektemechanismen van *GLS* mutaties

(met een samenvatting in het Nederlands)

Proefschrift

ter verkrijging van de graad van doctor aan de
Universiteit Utrecht
op gezag van de
rector magnificus, prof.dr. H.R.B.M. Kummeling,
ingevolge het besluit van het college voor promoties
in het openbaar te verdedigen op

donderdag 23 mei 2019 des ochtends te 10.30 uur

door

Lynne Rumping

geboren op 8 maart 1988
te Beverwijk

Promotoren:

Prof. dr. N.M. Verhoeven-Duif

Prof. dr. R.H.J. Houwen

Copromotoren:

Dr. P.M. van Hasselt

Dr. J.J.M. Jans

Dit proefschrift werd (mede) mogelijk gemaakt met financiële steun van Stichting ODAS, Stichting ESN, Chipsoft en de afdelingen Genetica (metabole diagnostiek) en Kindergeneeskunde (metabole ziekten) van het UMC Utrecht.

CONTENTS

Chapter 1

Introduction and scope of this thesis

INBORN ERRORS OF METABOLISM

Inborn Errors of Metabolism (IEMs) are a class of inherited genetic disorders caused by variants in genes coding for proteins that function in metabolism[1]. Genetic defects that disrupt a functional, conserved, area of the protein-encoding genome might lead to either loss, change or gain of protein function as classified by Hermann Muller (BOX I)[2]. IEMs mostly involve defects of enzymes, transporters, receptors, or complex molecules and organelles, which lead to disturbed homeostasis. As IEMs can affect a wide range of metabolic pathways, the biochemical and clinical presentations also vary widely but these patients often have early, severe onset[3]. Early diagnosis is essential for optimal outcome of children with an IEM, as disease severity and onset are influenced by environmental factors (e.g. dietary changes, infections and surgery) and treatment is possible for many inborn errors[4-6]. Knowledge on the pathophysiology of IEMs is essential for early detection and treatment. This starts with the identification of these rare IEMs and their underlying genetic defects.

IEMs follow Mendelian inheritance patterns. The vast majority of IEMs are transmitted as autosomal recessive traits. These concern bi-allelic loss-of-function (LoF) defects which in a mono-allelic state only lead to an approximate 50% activity reduction and do not lead to relevant metabolic effects[7]. The paradigm that mono-allelic variants in enzyme-encoding genes are usually harmless is however changing, since more IEMs caused by these variants are being identified. Autosomal dominant inheritance in IEMs is rare, but occurs when a minor change in enzyme activity and metabolite concentration has a functional effect (e.g. familial hypercholesterolemia caused by a mono-allelic LoF defect of the LDL-receptor) or when the mutation leads to protein gain-of-function (GoF) (e.g. congenital hyperinsulinism caused by a mono-allelic GoF defect of the enzyme glutamate dehydrogenase which, by overproduction of ATP, opens the ATP-regulated insulin channel)[3,7,8]. IEMs can also be transmitted as mitochondrial trait from mother to child (e.g. maternally inherited disabetes and deafness) and as X-linked in either recessive manner mainly affecting hemizygous males (e.g. Barth syndrome) or dominant trait mainly affecting women as hemizygosity in males is lethal (e.g. chondrodysplasia punctate 2)[3]. *De novo* variants are an example of non-Mendelian genetic defects. These are not present in somatic cells of the parents, but occur in the germline during gametogenesis and can there-after follow Mendelian inheritance patterns. These variants are a source of rapid evolutionary change[9]. As they have not been exposed to negative selection, *de novo* variants are likely to be more deleterious than inherited variation and to cause a more profound disease presentation[10,11]. Polygenic causes of IEMs, another example of non-Mendelian inheritance, have not been identified yet.

BOX I - NATURE OF GENETIC MUTATIONS

Hermann J. Muller –geneticist and Nobel prize winner for physiology or medicine in 1946- coined the terms to classify genetic mutations based on the outcome of protein alterations[2]. These are divided into variants leading to protein loss-of-functions (LoF) (amorphic and hypomorphic variants) and gain-of-functions (GoF) (antimorphic, isomorphic, neomorphic and hypermorphic). Amorphic variants cause complete loss of protein expression or function by disrupted transcription (RNA null) or translation (protein null). Hypomorphic variants cause a partial loss of protein expression or function. Isomorphic mutations are nonsense and thereby keep the same function and expression. Antimorphic and neomorphic variants cause a change of protein function, either acting in opposition or a new function respectively. Hypermorphic variants lead to increased protein activity, either by increased expression, loss of inhibition, increased binding affinity or -very rarely- by increased intrinsic activity.

IDENTIFYING NOVEL INBORN ERRORS OF METABOLISM

Identification of new IEMs is of great importance for several reasons. First, it is important for early recognition and diagnosis of the patient and to create insight into the prognosis. Second, it creates awareness of these disorders which helps future recognition of undiagnosed patients with a similar biochemical and clinical phenotype. Third, it provides both knowledge about disease mechanism and normal physiology. IEMs that belong to the same biochemical pathway often have similar clinical features, are detected by the same diagnostic procedures and might benefit from a similar treatment. Drawing parallels between diseases within a biochemical pathway thus aids recognition of the consequences of malfunctioning on the clinical phenotype. The number of known IEMs has grown substantially in recent decades, together amounting to ~1000 individual conditions. The development of Next Generation Sequencing (NGS) (BOX II) and analytical chemical techniques (BOX III) greatly contributed to this growth.

IDENTIFICATION OF PATHOGENIC GENETIC DEFECTS

Thus far, the underlying genetic defect of most IEMs have been elucidated by the “phenotype first approach” in which biochemical and clinical alterations point to candidate genes, which subsequently can be identified by targeted genetics. The introduction of NGS –particularly Whole Exome Sequencing (WES) and Whole Genome Sequencing (WGS)- has induced a shift towards a ‘genome first approach’ in which genetic variants are identified first, followed by detection of metabolic changes supporting pathogenicity[12]. Many recent examples can be found in literature. This approach is illustrated by a recent

paper describing the identification of bi-allelic variants in the *MDH2* gene (encoding malate dehydrogenase) by WES in three unrelated patients with unexplained early onset severe encephalopathy[13]. Subsequent metabolic investigations revealed elevated substrate levels, confirming loss-of-function of malate dehydrogenase as a consequence of the *MDH2* variants. The notion that the identification of novel IEMs also might provide additional information about gene function and its related pathway, is illustrated by the identification of variants in the *GOT2* gene by WES in two patients with unexplained epilepsy and developmental delay. Metabolic analyses showed a loss-of-function as well as decreased serine levels, not only identifying the underlying genetic cause, but also unveiling that *GOT2* is essential for serine biosynthesis[14]. Another example is the discovery of *MCT1* loss-of-function mutations in patients with ketoacidosis, revealing that *MCT1*-mediated ketone-body transport is needed to maintain acid–base balance[15]. WES can also contribute to the expension of the phenotypic spectrum, as is demonstrated in a study in which the combination of deep phenotyping and WES in probands with unexplained neurometabolic disease revealed previously unreported clinical features in patients with known pathogenic variants.[16]

BOX II - NEXT GENERATION SEQUENCING

DNA sequencing is possible since 1977 by the introduction of Sanger sequencing, which has been the gold standard of DNA sequencing for several decades[17]. In 2000, the human genome was fully sequenced, providing a reference human genome for comparison to DNA sequences of patients[18]. The development of "Next Generation Sequencing" (NGS) techniques since 2005 enables us to sequence multiple DNA fragments at the same time; in long read lengths; with improved scalability and cost[19]. Whole Exome Sequencing (WES) -first performed in 2009- is an untargeted NGS approach and is therefore highly effective in finding genetic variants throughout the whole exome, especially when combined with deep clinical phenotyping. It thereby enables the detection of *de novo* variants by parent-child trio analysis[20,21]. Whole Genome Sequencing (WGS) produces additional sequence information of introns (98.5% of the genome), which are non-coding regions with possible functional relevance.

UNDERSTANDING PATHOPHYSIOLOGY FROM GENETIC DEFECT TO PHENOTYPE

As the newly developed genetic techniques have simplified the detection of variants, the challenge now lies in variant interpretation. This may be challenging, as a single enzyme may be able to catalyze more than one metabolic reaction (e.g. asparaginase also expresses glutaminase activity), may be composed of multiple subunits encoded by

different genes and may have isoforms encoded by other genes (e.g. human express two iso-enzymes of glutaminase, encoded by different genes located on different chromosomes, which both exist in two splice site variants)[22,23]. Furthermore, gene and protein expression can be either ubiquitous or tissue specific and thereby genomic defects can affect specific tissues and organs. There are different levels of evidence for causality. Detected variants can be prioritized by segregation patterns correlated with the clinical phenotype within a family or between multiple unrelated patients. Variants can additionally be prioritized by low allele frequency in healthy population variant databases such as GoNl, ExaC and gnomAD, and by the predicted deleterious effect at protein level by prediction software[24-26]. RNA analyses provide information about splicing and tissue expression. *In silico* analyses create insight into the predicted effect of the genetic defect on protein level. More conclusive information about protein function can be drawn from *in vitro* analyses in cells obtained from patients or cell transfected with the variant. Animal models expressing the genetic defect can also be valuable to create insight into causality and pathophysiology. Functional evaluation of a genetic variant by the study of metabolic consequences is essential for the interpretation of a variant and for additional insight into pathophysiology. With the current technical developments, this becomes more attainable.

Technical developments in analytical chemistry enable the simultaneous analysis of an increasing amount of metabolites with increasing sensitivity and specificity (BOX III). Targeted metabolomics enables the study of a selection of metabolites with high specificity and may therefore elucidate the metabolic consequences of a known pathogenic stimulus. Untargeted metabolomics provides a broad perspective of the metabolome of a body fluid or cell system and is therefore valuable to reveal the extensive metabolic consequences of a genetic alteration, without *a priori* knowledge, within only one assay. The potential value of untargeted metabolomics in disease recognition has convincingly been illustrated by a study in which application of direct infusion high resolution mass spectrometry (DI-HRMS) to a cohort of 42 patients with 23 IEMs led to the recognition of 22 IEMs in bloodspots[27]. In plasma, 19/21 IEMs were diagnosed in 38 patients. The value of DI-HRMS based metabolomics for interpretation of variants of unknown significance (VUS) was demonstrated in the same study, as it created insight into the metabolic consequences of a VUS which supported pathogenicity of the variant. Application of a 'semi-untargeted' metabolomics method, based on chromatography-MS and 'semi-quantitative' analyses by the addition of internal standards, to a cohort of 190 patients with 21 IEMs led to the retrospective diagnostics of 20 IEMs[28]. As untargeted metabolomics provides thousands of metabolites, a selection of candidate metabolites is needed for interpretation of the data. A panel of IEM-related metabolites developed to filter untargeted data obtained by 'semi-untargeted' based on chromatography-MS, allowed the diagnosis of 42 out of 46 IEMs.[29]

BOX III – MASS SPECTROMETRY BASED METABOLOMICS. Targeted metabolomics allows quantification of metabolites with high sensitivity and specificity. Usually, prior to mass spectrometric detection, a chromatographic step is included to separate the compounds in the sample. Molecules with the same masses (isobaric compounds) can be discriminated by their different retention times on the chromatographic column[30]. Untargeted metabolomics is a novel technology that provides an extensive profile of the metabolome by measuring masses of thousands of metabolites in a single experiment[27,28,30]. Untargeted metabolomics can be performed with and without a prior chromatographic step. In direct infusion high resolution MS (DI-HRMS), samples are directly introduced in the mass spectrometry. Advantages are: more metabolites can be detected, sample preparation is technically uncomplicated and only a very small amount of sample is needed (3mm ø for dried blood spot and 20µL for plasma)[27]. As identification of the metabolites by DI-HRMS is only based on m/z, this technique is less specific than targeted metabolomics. Targeted analysis therefore remains important to validate results from untargeted analyses.

GLUTAMATE METABOLISM

The current era, in which both state of the art *in vitro* and *in vivo* genetic techniques and analytical chemical technologies are progressing rapidly, offers great opportunities to detect new IEMs and to explore their downstream metabolic consequences. This thesis focuses on inborn errors in enzymes of glutamate metabolism.

Glutamate is an amino acid involved in many metabolic pathways (Figure II)[31,32]. It is best known for its role as the most abundant excitatory neurotransmitter in the central nerve system[32,33]. As such, glutamate is important for signal transduction, induction of axon myelination, synaptic plasticity and regulation of respiratory volume, frequency and rhythm in the respiratory center of the brain[32,34]. It is furthermore the precursor of GABA, a major inhibitory neurotransmitter[31,32]. In addition to its function as a neurotransmitter, glutamate fulfills several functions as both substrate and product of various metabolic reactions (Figure II). It plays an important role in energy metabolism, as it fuels the mitochondrial citric acid (TCA) cycle through α-ketoglutarate[31,35]. By conversion of glutamate into α-ketoglutarate via aminotransferases (mediating the transfer of amino nitrogen to and from glutamate), other amino acids are produced. These have their own biological functions and are used as building blocks for protein and nucleotide synthesis[36]. Glutamate is also the precursor of the anti-oxidant glutathione, synthesized via the ɣ-glutamyl cycle, but paradoxically induces oxidative stress when present in excess[37,38]. It thereby plays an important role in redox

capacity. Glutamate can be converted into glutamine. Glutamine and glutamate together are key players in ammonia detoxification. By capturing ammonia and forming glutamine, glutamate serves as a nontoxic inter-organ carrier towards the liver. In the liver, glutamate provides the urea cycle with intermediates to detoxify ammonia[39]. Glutamine is acquired for NAD^+ synthesis, which is important for electron transfer to maintain redox homeostasis[40]. In addition, glutamine is a source of other amino acids, proteins and nucleotides[36,41,42].

Disturbed glutamate-glutamine homeostasis is known to be detrimental. Glutamate excitotoxicity is associated with neurodegenerative and psychiatric disorders and epilepsy[37,43]. Glutamate excitotoxicity is the process in which excessive activation of glutamate receptors leads to oxidative stress, causing cell toxicity and cell death and decreased plasticity[37]. The excessive activation of glutamate receptors is either caused by increased glutamate release (by injury, ischemia, hypoglycemia or inflammation), by decreased glutamate uptake by defective transporters, or by glutamate receptor defects leading to ongoing activation[37,44]. The extensive metabolic consequences of glutamate excess are intensively studied in the field of oncology, in which GLS overexpression causes glutamate excess. However, many other cellular processes are changed in cancer cells, impeding the study of the metabolic consequences of isolated glutamate excess[45].

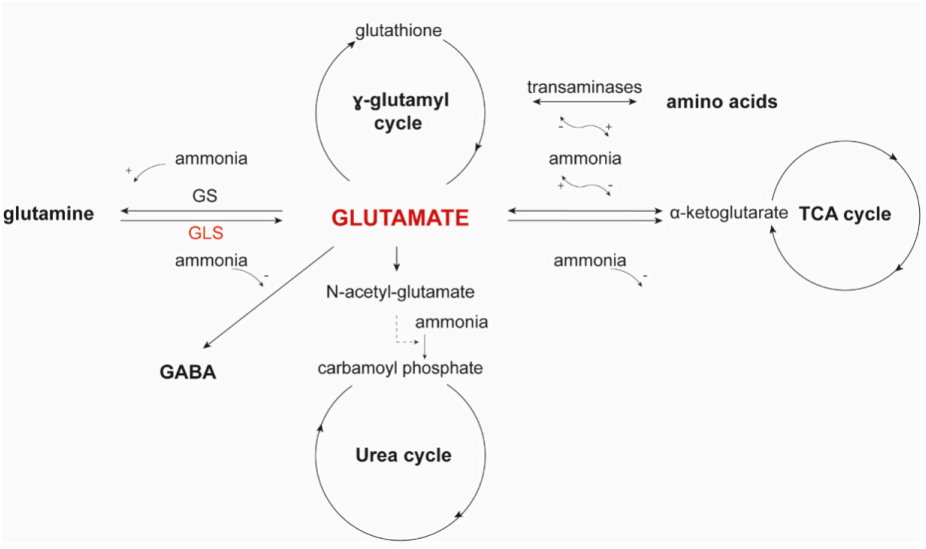

FIGURE II: glutamate is involved in a variety of metabolic pathways, including GABA metabolism, the TCA cycle, amino acid synthesis, the γ-glutamyl and -urea cycle and the interconversion with glutamine by the enzymes glutamine synthetase (GS) and glutaminase (GLS).

Glutamate deficiency has not been described in a human condition and its effects are unknown. Glutamine excess has been associated with cerebral edema and subsequent encephalopathy, but only in the context of hyperammonemia[46]. The isolated consequences of glutamine excess are therefore more difficult to predict.

Several enzymes are involved in glutamine-glutamate homeostasis, but two enzymes play pivotal roles: glutamine synthetase (GS) and glutaminase (GLS) (Figure II). GS converts glutamate into glutamine and is ubiquitously expressed[47]. GLS catalyzes the deamination of glutamine into glutamate and ammonia and exists in two isoforms: GLS which is present in two splice variants KGA and GAC and is mainly expressed in kidney and brain; and GLS2, ubiquitously expressed with the highest expression in the liver[22,48]. In the brain, glutamate homeostasis is regulated by the glutamine-glutamate shuttle, providing glutamate recycling. Glutamate is excreted by neurons into synapses, where it plays its role as a neurotransmitter by binding to glutamate receptors on the post synaptic cell. It is then actively taken up again by glutamate transporters into astrocytes, where it is converted into glutamine by glutamine synthetase (GS). Subsequently, it is transported to neurons and converted into glutamate by glutaminase (GLS) to repeat the cycle[49].

Despite the important roles of GS and GLS for securing glutamate and glutamine homeostasis, relatively little is known about the clinical and metabolic consequences of errors in these enzymes. As both glutamine and glutamate are involved in a variety of metabolic pathways, disturbed homeostasis is expected to have extensive –but hard to predict- downstream metabolic consequences. GS deficiency has been described in 3 patients with lethal neonatal epilepsy[50]. It is postulated that GS deficiency, leading to glutamine deficiency, both results in hyperammonemia and defective NAD^+ synthesis, disturbing redox homeostasis[51]. Further studies show that decreased GS enzyme activity provokes increased GS protein expression as a compensatory mechanism, providing the information that GS protein expression is regulated by its own kinetics[52]. Defects of GLS have not been identified in human conditions, however GLS knockout mice show reduced neuronal glutamate release, reduced respiration and early death[53]. The early death might play a contributing role to the fact that GLS defects have not yet been identified. The clinical and extensive metabolic consequences of GLS defects -either loss-of-function and hyperactivity- therefore remain unknown. Inborn errors of other enzymes in glutamate metabolism are described and cause a wide variety of biochemical and clinical phenotypes, depending on the function of the affected pathway downstream from the defect.

SCOPE OF THIS THESIS

The research presented in this thesis describes the identification two novel inborn errors of glutamate metabolism, caused by opposing defects in GLS. It focuses on the pathophysiology of these novel IEMs from genetic defect, metabolic alterations to clinical phenotypes. In addition, other enzymatic defects of glutamate metabolism are reviewed. This research comprises novel knowledge about the regulation of glutamate metabolism and provides starting points for improvement of disease identification in the era of metabolomics and genomics.

In **Chapter 2** we describe the identification of a novel IEM, caused by autosomal recessive GLS loss-of-function variants in two families with neonatal epilepsy, respiratory insufficiency and death. This was achieved through a "genome first approach", in which WES identified the variants in the GLS gene, which co-segregated within the family, and targeted metabolic analyses confirmed loss-of-function. In **Chapter 3** we describe the identification and pathology of a *de novo* GLS hyperactivity variant in a patient with infantile cataract and profound developmental delay. This variant was identified by trio WES, allowing identification of a *de novo* heterozygous variant followed by clinical and metabolic analyses which revealed a hypermorphic nature of the genetic defect. The pathophysiology was furthermore studied by analyses of oxidative stress parameters and of cataract in a zebrafish model. In **Chapter 4** we further elucidate the downstream consequences of GLS hyperactivity on the metabolome by untargeted metabolomics with DI-HRMS. We thereby create additional insight into the pathophysiology of GLS hyperactivity and illustrate the great possibility of this state of the art technique to provide an overview of the broad metabolic consequences of a single genetic alteration. In **Chapter 5** we review all reported inborn errors of enzymes of glutamate metabolism and provide an overview of their clinical and biochemical characteristics. By drawing phenotypic and biochemical parallels, we attempt to create insight into the clinical effect of disturbed glutamate metabolism. In **Chapter 6** we describe the newly developed microscopic method used in chapter 3 to accurately visualize the zebrafish lens. We improve and extend the experimental tools to study the effects of genetic defects on the lens. In **Chapter 7** we discuss the novel knowledge that can be extracted from the research described in this thesis, with the focus on the (patho)physiology of glutamate metabolism and the bench-to-bed side translation towards diagnostics and treatment.

REFERENCES

1. Garrod AE. The incidence of alkaptonuria: a study in chemical individuality. 1902 [classical article]. *Yale J Biol Med.* 2002;75(4):221-231.
2. Muller H. Further studies on the nature and causes of gene mutations. Proceedings of the Sixth International Congress of Genetics. *Ithaca, New York.* 1932;1:213-255.
3. Saudubray JM, Baumgartner MR. *Inborn Metabolic Diseases, diagnosis and treatment.* Berlin: Springer; 2016.
4. Weiner D. *Metabolic emergencies. In: Textbook of pediatric emergency medicine.* 5th ed. Philadelphia2006.
5. Chandler RJ, Venditti CP. Gene Therapy for Metabolic Diseases. *Transl Sci Rare Dis.* 2016;1(1):73-89.
6. Alfadhel M, Al-Thihli K, Moubayed H, Eyaid W, Al-Jeraisy M. Drug treatment of inborn errors of metabolism: a systematic review. *Arch Dis Child.* 2013;98(6):454-461.
7. Zschocke J. Dominant versus recessive: molecular mechanisms in metabolic disease. *J Inherit Metab Dis.* 2008;31(5):599-618.
8. Palladino AA, Stanley CA. The hyperinsulinism/hyperammonemia syndrome. *Rev Endocr Metab Disord.* 2010;11(3):171-178.
9. Vissers LE, de Ligt J, Gilissen C, et al. A de novo paradigm for mental retardation. *Nat Genet.* 2010;42(12):1109-1112.
10. Crow JF. The origins, patterns and implications of human spontaneous mutation. *Nat Rev Genet.* 2000;1(1):40-47.
11. Veltman JA, Brunner HG. De novo mutations in human genetic disease. *Nat Rev Genet.* 2012;13(8):565-575.
12. Yubero D, Brandi N, Ormazabal A, et al. Targeted Next Generation Sequencing in Patients with Inborn Errors of Metabolism. *PLoS One.* 2016;11(5):e0156359.
13. Ait-El-Mkadem S, Dayem-Quere M, Gusic M, et al. Mutations in MDH2, Encoding a Krebs Cycle Enzyme, Cause Early-Onset Severe Encephalopathy. *Am J Hum Genet.* 2017;100(1):151-159.
14. Ramos RJJK, C; Tarailo-Graovac, M; Skrypnyk, C; Lee van der, R; Drogemoller, B.I; Koster, J; Campeau, P; Ruiter, J; Ciapate, J; Kluijtmans, L.A.J; Jans, J.J.M; Ross, C.J; Wintjes, L.T; Rodenburg, R.J; Waterham, H.R; Wasserman, W.W; Wanders, R.J.A; Verhoeven-Duif, N.M; Wevers, R.A GOT2 deficiency: a novel disorder of the malate aspartate shuttle resulting in serine deficiency. *JIMD abstracts SSIEM 2018.* 2018.
15. van Hasselt PM, Ferdinandusse S, Monroe GR, et al. Monocarboxylate transporter 1 deficiency and ketone utilization. *N Engl J Med.* 2014;371(20):1900-1907.
16. Tarailo-Graovac M, Shyr C, Ross CJ, et al. Exome Sequencing and the Management of Neurometabolic Disorders. *N Engl J Med.* 2016;374(23):2246-2255.
17. Sanger F, Nicklen S, Coulson AR. DNA sequencing with chain-terminating inhibitors. *Proc Natl Acad Sci U S A.* 1977;74(12):5463-5467.
18. Venter JC, Adams MD, Myers EW, et al. The sequence of the human genome. *Science.* 2001;291(5507):1304-1351.
19. Shendure J, Ji H. Next-generation DNA sequencing. *Nat Biotechnol.* 2008;26(10):1135-1145.
20. Bamshad MJ, Ng SB, Bigham AW, et al. Exome sequencing as a tool for Mendelian disease gene discovery.

Nat Rev Genet. 2011;12(11):745-755.

21. Ng SB, Buckingham KJ, Lee C, et al. Exome sequencing identifies the cause of a mendelian disorder. *Nat Genet.* 2010;42(1):30-35.
22. Aledo JC, Gomez-Fabre PM, Olalla L, Marquez J. Identification of two human glutaminase loci and tissue-specific expression of the two related genes. *Mamm Genome.* 2000;11(12):1107-1110.
23. Chan WK, Lorenzi PL, Anishkin A, et al. The glutaminase activity of L-asparaginase is not required for anticancer activity against ASNS-negative cells. *Blood.* 2014;123(23):3596-3606.
24. Genome of the Netherlands C. Whole-genome sequence variation, population structure and demographic history of the Dutch population. *Nat Genet.* 2014;46(8):818-825.
25. Lek M, Karczewski KJ, Minikel EV, et al. Analysis of protein-coding genetic variation in 60,706 humans. *Nature.* 2016;536(7616):285-291.
26. Lek M KK, Minikel EV. Analysis of protein-coding genetic variation in 60,706 humans http://gnomad.broadinstitute.org (last access 8th of March 2018). Accessed March 20, 2018.
27. Haijes H.A, Willemse M, van der Ham M, Gerrits J, Pras-Raves M.L, Prinsen H.C.M.T, van Hasselt P.M, de Sain-van der Velden M.G.M, Verhoeven-Duif N.M, Jans J.J.M. Direct infusion based metabolomics identifies metabolic disease in patients' dried blood spots and plasma. *Metabolites.* 2019, accepted.
28. Miller MJ, Kennedy AD, Eckhart AD, et al. Untargeted metabolomic analysis for the clinical screening of inborn errors of metabolism. *J Inherit Metab Dis.* 2015;38(6):1029-1039.
29. Coene KLM, Kluijtmans LAJ, van der Heeft E, et al. Next-generation metabolic screening: targeted and untargeted metabolomics for the diagnosis of inborn errors of metabolism in individual patients. *J Inherit Metab Dis.* 2018;41(3):337-353.
30. Johnson CH, Ivanisevic J, Siuzdak G. Metabolomics: beyond biomarkers and towards mechanisms. *Nat Rev Mol Cell Biol.* 2016;17(7):451-459.
31. Yelamanchi SD, Jayaram S, Thomas JK, et al. A pathway map of glutamate metabolism. *J Cell Commun Signal.* 2016;10(1):69-75.
32. Nedergaard M, Takano T, Hansen AJ. Beyond the role of glutamate as a neurotransmitter. *Nat Rev Neurosci.* 2002;3(9):748-755.
33. Curtis DR, Phillis JW, Watkins JC. The chemical excitation of spinal neurones by certain acidic amino acids. *J Physiol.* 1960;150:656-682.
34. Mount CW, Monje M. Wrapped to Adapt: Experience-Dependent Myelination. *Neuron.* 2017;95(4):743-756.
35. Eelen G, Dubois C, Cantelmo AR, et al. Role of glutamine synthetase in angiogenesis beyond glutamine synthesis. *Nature.* 2018;561(7721):63-69.
36. Cory JG, Cory AH. Critical roles of glutamine as nitrogen donors in purine and pyrimidine nucleotide synthesis: Asparaginase treatment in childhood acute lymphoblastic leukemia. *In Vivo.* 2006;20(5):587-589.
37. Dong XX, Wang Y, Qin ZH. Molecular mechanisms of excitotoxicity and their relevance to pathogenesis of neurodegenerative diseases. *Acta Pharmacol Sin.* 2009;30(4):379-387.

38. Lu SC. Regulation of glutathione synthesis. *Mol Aspects Med.* 2009;30(1-2):42-59.
39. Hakvoort TB, He Y, Kulik W, et al. Pivotal role of glutamine synthetase in ammonia detoxification. *Hepatology.* 2017;65(1):281-293.
40. LaRonde-LeBlanc N, Resto M, Gerratana B. Regulation of active site coupling in glutamine-dependent NAD(+) synthetase. *Nat Struct Mol Biol.* 2009;16(4):421-429.
41. Altman BJ, Stine ZE, Dang CV. From Krebs to clinic: glutamine metabolism to cancer therapy. *Nat Rev Cancer.* 2016;16(10):619-634.
42. Zhang J, Pavlova NN, Thompson CB. Cancer cell metabolism: the essential role of the nonessential amino acid, glutamine. *EMBO J.* 2017;36(10):1302-1315.
43. O'Donovan SM, Sullivan CR, McCullumsmith RE. The role of glutamate transporters in the pathophysiology of neuropsychiatric disorders. *NPJ Schizophr.* 2017;3(1):32.
44. Lewerenz J, Maher P. Chronic Glutamate Toxicity in Neurodegenerative Diseases-What is the Evidence? *Front Neurosci.* 2015;9:469.
45. Miller DM, Thomas SD, Islam A, Muench D, Sedoris K. c-Myc and cancer metabolism. *Clin Cancer Res.* 2012;18(20):5546-5553.
46. Butterworth RF. Pathophysiology of brain dysfunction in hyperammonemic syndromes: The many faces of glutamine. *Mol Genet Metab.* 2014;113(1-2):113-117.
47. Meister A. Glutamine synthetase from mammalian tissues. *Methods Enzymol.* 1985;113:185-199.
48. Curthoys NP, Watford M. Regulation of glutaminase activity and glutamine metabolism. *Annu Rev Nutr.* 1995;15:133-159.
49. Bak LK, Schousboe A, Waagepetersen HS. The glutamate/GABA-glutamine cycle: aspects of transport, neurotransmitter homeostasis and ammonia transfer. *J Neurochem.* 2006;98(3):641-653.
50. Spodenkiewicz M, Diez-Fernandez C, Rufenacht V, Gemperle-Britschgi C, Haberle J. Minireview on Glutamine Synthetase Deficiency, an Ultra-Rare Inborn Error of Amino Acid Biosynthesis. *Biology (Basel).* 2016;5(4).
51. Hu L, Ibrahim K, Stucki M, et al. Secondary NAD+ deficiency in the inherited defect of glutamine synthetase. *J Inherit Metab Dis.* 2015;38(6):1075-1083.
52. Haberle J, Gorg B, Rutsch F, et al. Congenital glutamine deficiency with glutamine synthetase mutations. *N Engl J Med.* 2005;353(18):1926-1933.
53. Masson J, Darmon M, Conjard A, et al. Mice lacking brain/kidney phosphate-activated glutaminase have impaired glutamatergic synaptic transmission, altered breathing, disorganized goal-directed behavior and die shortly after birth. *J Neurosci.* 2006;26(17):4660-4671.

Chapter 2

Identification of a Loss-of-Function Mutation in the Context of Glutaminase Deficiency and Neonatal Epileptic Encephalopathy

JAMA Neurol. (2018) doi:10.1001/jamaneurol.2018.2941

Lynne Rumping^, Benjamin Büttner^, Oliver Maier, Holger Rehmann, Maarten Lequin, Jan-Ulrich Schlump, Bernhard Schmitt, Birgit Schiebergen-Bronkhorst, Hubertus C.M.T. Prinsen, Michele Losa, Ralph Fingerhut, Johannes R. Lemke, Fried J.T. Zwartkruis, Roderick H.J. Houwen, Judith J.M. Jans, Nanda M. Verhoeven-Duif, Peter M. van Hasselt*, Rami Jamra*.

^both authors share first authorship *both authors share last authorship

ABSTRACT

QUESTION

What is the consequence of glutaminase deficiency?

FINDINGS

This study of 2 families with 4 affected children used exome sequencing followed by functional analysis to show that biallelic loss-of-function pathogenic variants in the glutaminase gene *GLS* lead to early neonatal refractory seizures, respiratory failure, structural brain abnormalities and cerebral edema, and death within weeks after birth.

MEANING

Based on these results, it is hypothesized that glutaminase deficiency disturbs glutamine-glutamate homeostasis and leads to neonatal lethal epileptic encephalopathy and respiratory insufficiency; this emphasizes its importance for respiratory regulation, neurotransmission, and survival.

This study uses exome sequencing and genetic evaluation to explain the shared condition of 4 children from 2 unrelated families who were affected by refractory epileptic seizures, respiratory failure, brain abnormalities, and death in the neonatal period.

IMPORTANCE

The identification and understanding of the monogenic causes of neurodevelopmental disorders are of high importance for personalized treatment and genetic counseling.

OBJECTIVE

To identify and characterize novel genes for a specific neurodevelopmental disorder characterized by refractory seizures, respiratory failure, brain abnormalities, and death in the neonatal period; describe the outcome of glutaminase deficiency in humans; and understand the underlying pathological mechanisms.

DESIGN, SETTING, AND PARTICIPANTS

We performed exome sequencing of cases of neurodevelopmental disorders without a clear genetic diagnosis, followed by genetic and bioinformatic evaluation of candidate variants and genes. Establishing pathogenicity of the variants was achieved by measuring metabolites in dried blood spots by a hydrophilic interaction liquid chromatography method coupled with tandem mass spectrometry. The participants are 2 families with a total of 4 children who each had lethal, therapy-refractory early neonatal seizures with status epilepticus and suppression bursts, respiratory insufficiency, simplified gyral structures,

diffuse volume loss of the brain, and cerebral edema. Data analysis occurred from October 2017 to June 2018.

MAIN OUTCOMES AND MEASURES

Early neonatal epileptic encephalopathy with glutaminase deficiency and lethal outcome.

RESULTS

A total of 4 infants from 2 unrelated families, each of whom died less than 40 days after birth, were included. We identified a homozygous frameshift variant p.(Asp232Glufs*2) in GLS in the first family, as well as compound heterozygous variants p.(Gln81*) and p.(Arg272Lys) in GLS in the second family. The *GLS* gene encodes glutaminase (Enzyme Commission 3.5.1.2), which plays a major role in the conversion of glutamine into glutamate, the main excitatory neurotransmitter of the central nervous system. All 3 variants probably lead to a loss of function and thus glutaminase deficiency. Indeed, glutamine was increased in affected children (available *z* scores, 3.2 and 11.7). We theorize that the potential reduction of glutamate and the excess of glutamine were a probable cause of the described physiological and structural abnormalities of the central nervous system.

CONCLUSIONS AND RELEVANCE

We identified a novel autosomal recessive neurometabolic disorder of loss of function of glutaminase that leads to lethal early neonatal encephalopathy. This inborn error of metabolism underlines the importance of GLS for appropriate glutamine homeostasis and respiratory regulation, signal transduction, and survival.

INTRODUCTION

Epileptic encephalopathies are a large and heterogeneous group of disorders. Genetic factors are assumed to be causative in most cases.[1-4] In outbred populations, frequent causes of severe epileptic encephalopathy are de novo heterozygous genetic variants.[5-7] However, autosomal recessive inheritance is common, especially for metabolic disorders.[8] Identification and characterization of genetic causes of neurodevelopmental disorders is essential to enable counselling of relatives regarding prognosis and recurrence risk. Understanding the pathological mechanisms is an essential basic knowledge for developing and enabling personalized and specific treatment.

In this study, we describe pathogenic alterations in the K-type mitochondrial glutaminase (GLS; Enzyme Commission 3.5.1.2) encoded by *GLS* that is ubiquitously expressed, with a particularly high expression in the brain.[9] Glutaminase plays a pivotal role in the production of glutamate, the main excitatory neurotransmitter in the central nervous system, including the brain stem respiratory center.[10-12] In the respiratory center, respiratory volume, frequency, and rhythm are regulated by information from chemoreceptors and mechanoreceptors mediated by glutamatergic signal transduction.[13] In addition, glutamate induces myelination of axons. It furthermore fuels the mitochondrial citric acid (tricarboxylic acid) cycle through α-ketoglutarate, thereby regulating energy metabolism, which is important for the high energy demands of the brain.[14,15] Glutamate is produced by GLS from glutamine, an important ammonia detoxifier and a building block of proteins, and a source of other amino acids, purines, and pyrimidines. Here, we describe 4 individuals from 2 families with biallelic *GLS* loss-of-function variants, who clinically presented with neonatal respiratory failure, status epilepticus with suppression bursts, and early death.

METHODS

ETHICAL APPROVAL

All analyses were performed in concordance to the provisions of the German Gene Diagnostic Act (Gendiagnostikgesetz) and the General Data Protection Act (Bundesdatenschutzgesetz). The testing was done as part of routine clinical care. The project was approved by the ethics committee of the University of Leipzig, Germany in accordance with the Declaration of Helsinki.[16] Written informed consent of all examined individuals or their legal representatives was obtained after advice and information about the risks and benefits of the study was given.

EXOME SEQUENCING

We performed 2x100bp exome sequencing on a HiSeq4000 platform (Illumina) after library preparation with SureSelectXT (Agilent Genomics) and enrichment with SureSelect All Human Version 6 (60Mb; Agilent Genomics). In one family, we performed single-exome sequencing of 1 affected child (coverage of ×10 at 98.7% of the targeted sequences). In the other family, we performed trio-exome sequencing; coverage of ×10 was achieved in 98.8% of targeted sequences in the affected infant: 98.7% in 1 parent and 99.1% in the other parent. Validation of the findings and segregation of the variants were performed with Sanger sequencing for all available family members.

VARIANT PRIORITIZATION

Analysis of the raw data was performed using the software Varfeed (Limbus Medical Technologies) and the variants were annotated and prioritized using the software Varvis (Limbus Medical Technologies). To identify previously described variants, we compared our findings with the Human Gene Mutation Database and ClinVar.[17,18] Candidate variants were prioritized based on phenotype, family history, inheritance, minor allele frequency, effect on protein function, in silico prediction tools, gene and variant attributes, and the published literature.

BLOOD SPOT ANALYSES AND METABOLIC MEASUREMENTS

Glutamine and glutamate concentrations were measured in dried blood spots by a hydrophilic interaction liquid chromatography method coupled with tandem mass spectrometry (Xevo TQ; Waters). This method is based on a previously described method for amino acid analysis in plasma, with slight modifications.[19]

STATISTICAL ANALYSIS

To correct for spontaneous in vitro conversion of glutamine into glutamate, concentrations were converted to *z* scores based on 10 control blood spots obtained on the same day and stored under the same circumstances. *z* Scores greater than 2 were considered significant. Data analysis occurred from October 2017 to June 2018.

RESULTS

FAMILY 1

One affected infant (Figure 1A) was a child of consanguineous, healthy parents. The infant was born by cesarean section. Apgar scores were 6, 5, and 7 at 1, 5, and 10 minutes, respectively, with limited spontaneous respiration and marked muscular hypotonia. The infant initially improved with short-term ventilation via facemask and oxygen supplementation. However, shortly after birth, respiration became insufficient. In addition, myoclonic jerks were noted. The infant was transferred to the neonatal intensive care unit and sedated, incubated, and artificially ventilated. Within the next few hours, focal seizures intensified and spread and eventually also included tonic-clonic seizures of all limbs. The infant was cardiorespiratory stable on the ventilator. Seizures were refractory to lorazepam, levetiracetam, sodium benzoate, valproic acid, pulse steroid therapy, and a trial of dextromethorphan given on suspicion of nonketotic hyperglycinemia. Temporary remission of seizures was achieved when starting phenobarbital and initiating a 3-day thiopental-induced coma. However, after discontinuation, seizures reoccurred within 1 day. Similarly, a continuous infusion of ketamine was started and led to a seizure-free interval of 2 days, but this medication then lost its effect even after the dose was increased to 5 mg/kg/h. Physical examinations revealed an inadequate reaction to external stimuli, muscular hypotonia, absence of sucking reflex, and uncoordinated movements. There were no dysmorphic features. Results of the metabolic newborn screening were unremarkable. Repeated attempts to wean the infant from the ventilator were unsuccessful. Electroencephalography revealed long-lasting suppressed activity that was interrupted by short, high-amplitude Θ activity, meeting the criteria of persistent burst-suppression patterns. Magnetic resonance imaging (MRI) showed a simplified frontal gyral pattern with an anterior-to-posterior gradient and deep and subcortical white matter involvement (Figure 1A). A follow-up MRI later showed gliosis, especially in the frontal deep white matter, caused by brain parenchymal destruction, as well as marked volume loss of the initially normal-appearing basal ganglia, corpus callosum, thalami, brainstem, and vermis, all possibly because of direct destruction and secondary network injury (Figure 1B-E). On a diffusion-weighted magnetic resonance image, extensive vasogenic cerebral edema was seen, especially in the deep white matter and corpus callosum, which was interpreted as being caused by the seizure activity. Therapy was discontinued in agreement with the parents, and the infant died. At that time, the diagnosis remained unknown. Another infant of the family had died after a similar disease course. A summary of the phenotype is given in the Table.

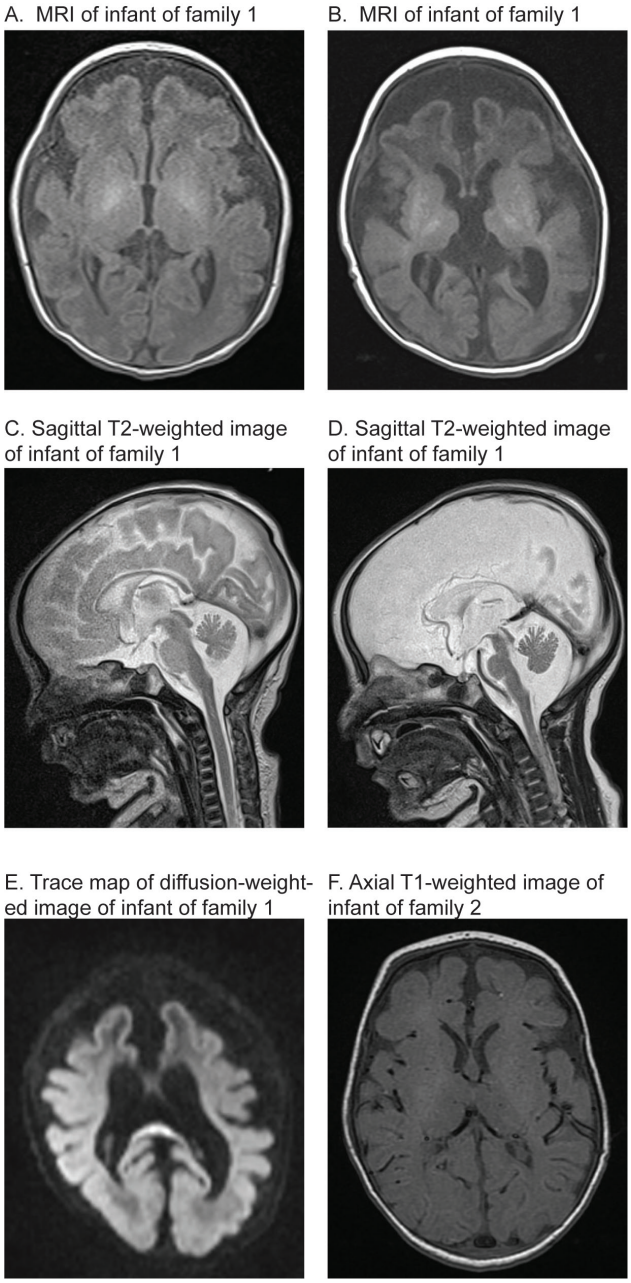

FIGURE 1. Magnetic Resonance Images of Affected Children. A, A magnetic resonance image (MRI) shows simplified gyral patterns and destruction over time in axial T1 weighted image of the affected infant in family 1, including an anterior-to-posterior gradient and deep and subcortical white matter involvement on day 1. **B,** Gliosis and volume loss of the basal ganglia and thalami, as well as a

pronounced white matter involvement. **C** and **D,** Sagittal T2-weighted images shortly after birth and later, with reduction of an initially normally constructed brainstem, vermis, and corpus callosum, with a prominent cisterna magna also depicted. **E,** A trace map of a diffusion-weighted image with a high signal at the splenium, pointing to vasogenic edema. **F,** An axial T1-weighted image of an affected child of family 2, with a simplified gyral pattern of the frontal lobes and white matter involvement of the corticospinal tracts at the level of the posterior limb of the internal capsule.

FAMILY 2

An affected infant of this family (Figure 1B) was a child of nonconsanguineous, healthy parents. Pregnancy had been largely uneventful until the last month. During delivery at full term, pethidine was administered, and meconium-stained amniotic fluid and a pathological cardiotocography were noticed. Apgar scores were 2, 7, and 7 at 1, 5, and 10 minutes, respectively, with limited spontaneous respiration and marked muscular hypotonia. The infant improved with respiratory support. However, when respiratory support was withheld, the infant exhibited Cheyne-Stokes respiration and was therefore transferred to the intensive care unit. There, the infant was sedated, incubated, and artificially ventilated. Low arterial blood pressure was treated with catecholamine, dopamine, and adrenaline. Additionally, diabetes insipidus was suspected because of high diuresis, for which a trial of desmopressin was administered. At day 2, the infant developed focal seizures, with variably combined asymmetric tonic movements, irregular eye movement, clonus of the eyelid and the upper and the lower extremities, and myoclonic jerks. Electroencephalography revealed long-lasting suppressed activity that was interrupted by short, high-amplitude Θ activity, a pattern consistent with suppression bursts. Seizures were refractory to phenobarbital, phenytoin, pyridoxine, midazolam, and topiramate. A physical examination revealed muscular hypotonia with absence of movements against gravity and absence of reflexes. There were no dysmorphic features. An MRI of the brain revealed a simplified gyral pattern of the frontal lobes and white matter involvement (Figure 1F), similar to that of the other affected infants. Treatment was stopped, and the infant died. The diagnosis remained unknown.

Another infant in the family showed a similar clinical presentation of neonatal respiratory failure and status epilepticus with suppression bursts. On delivery, the infant had no spontaneous respiration, and Apgar scores were 4, 5, and 7 at 1, 5, and 10 minutes. Respiratory support improved circulation, but hypoventilation and apnea persisted. Within hours, myoclonic seizures were noted with a burst-suppression pattern on electroencephalography, which failed to respond to various antiepileptic drugs. An MRI of

the brain revealed a simplified gyral pattern, particularly in the frontal lobes. The infant died after treatment was discontinued. The Table presents a summary of the phenotype.

TABLE. Genetic and Clinical Descriptions of Affected Offspring

	Family 1		Family 2	
Characteristic	**1**	**2**	**1**	**2**
Genomic position (hg19)	Not tested	chr2:191765378	chr2:191766752 and chr2:191746051	chr2:191766752 and chr2:191746051
Human Genome Variation Society DNA reference[a]	Not tested	c.695dup	c.815G>A/c.241C>T	c.815G>A/c.241C>T
Protein alteration	Not tested	p.(Asp232Glufs*2)	p.(Arg272Lys)/p.(Gln81*)	p.(Arg272Lys)/p.(Gln81*)
Zygosity	Not tested	Homozygous	Compound heterozygous	Compound heterozygous
Length at birth[20]				
Length, cm	Unknown	49	47	47
Percentile	Unknown	25th	1st	1st
Weight at birth[20]				
Weight, g	Unknown	3040	2990	3000
Percentile	Unknown	43rd	8th	11th
Head circumference at birth[20]				
Circumference, cm	Unknown	36.5	Unknown	32
Percentile	Unknown	90th	Unknown	1st
Apgar scores				
1 min	Unknown	6	2	4
5 min	Unknown	5	7	5
10 min	Unknown	7	7	7
Respiratory dysfunction	Respiratory insufficiency	Respiratory insufficiency and ventilation support	Respiratory insufficiency, ventilation support, and Cheyne-Stokes respirations when support was withheld	Respiratory insufficiency, hypoventilation, apnea, and ventilation support
Seizures				
Description	Similar course to affected sibling	Focal cerebral seizures within 10 min after birth	Focal seizures at day 2, followed by variably combined asymmetric tonic movements, irregular eye movement, clonus of the eyelid and the upper and the lower extremities, and single myoclonic jerks	Myoclonic seizures of the mouth at day 1
Response to therapy	Similar to affected sibling	Refractory	Refractory	Refractory
Muscular tonus	Unknown	Muscular hypotonia	Muscular hypotonia	Muscular hypotonia

TABLE CONTINUED. Genetic and Clinical Descriptions of Affected Offspring

	Family 1		Family 2	
Characteristic	**1**	**2**	**1**	**2**
Electroencephalographic results	Unknown	Burst-suppression patterns	Burst-suppression patterns, ictal pattern: variable focal onset and variable morphologic features, often superimposed by rhythmic α/β activity	Burst-suppression patterns with generalized rhythmical discharges
Brain magnetic resonance imaging				
Time of examination, days postbirth	Unknown	0 and 30	3	3
Results	Unknown	At birth, simplified frontal gyral pattern with an anterior to posterior gradient and deep and subcortical white matter involvement; on follow-up, gliosis, volume loss of the initially normal appearing basal ganglia, corpus callosum, thalami, brain stem and vermis, and vasogenic cerebral edema	Simplified gyral pattern of the frontal lobes and white matter involvement	Severe demyelination; calcium spots and recess of the fibers in the subcortical white matter
Dysmorphic features	Unknown	No	No	No
Medications administered	Unknown	Sterofundin, hydrocortisone, ampicillin, cefotaxim, tobramycin, aciclovir, lorazepam, levetiracetame, phenobarbital, thiopental, vitamin B-6, pyridoxal 5 phosphate, calciumfolinate, ketamine, vigabatrin, steroid, lacosamid, and valproic acid	Clamoxyl, garamycin, dopamine, adrenaline, desmopressin, phenobarbital, phenytoin, pyridoxine, midazolam, and topiramate	Levetiracetam, phenobarbital, vigabatrin, vitamin B-6, and phenytoin

Abbreviations: EEG, electroencephalogram; MRI, magnetic resonance imaging.a NM_001256310.1

GENETIC RESULTS

Whole-exome sequencing (WES) revealed in 1 infant in family 1 a homozygous frameshift variant in *GLS* (NM_001256310.1; chr2:191765378, c.695dup, p.[Asp232Glufs*2]). Sanger sequencing confirmed the variant, and both parents are heterozygous. There was no material available from the other affected infant.

In family 2, trio WES revealed compound heterozygous variants in *GLS*: NM_001256310.1; chr2:191746051, c.241C>T, and p.(Gln81*) inherited from 1 parent and chr2:191766752, c.815G>A, and p.(Arg272Lys) from the other parent. Sanger sequencing confirmed the variants, and each parent was found to be heterozygous for 1 of the variants. Also, we found that 3 of 4 healthy children in the family were heterozygous for 1 variant, while a fourth was homozygous for the wild type.

All 3 variants were absent from all publicly available databases, including GnomAD (last accessed March 8, 2018).[21] The truncating variants probably lead to RNA nonsense-mediated decay.[22] In any case, translation would not result in a catalytically competent protein; Arg272 is conserved across evolution from lampreys to vertebrates (Figure 2A), and in silico prediction tools like MutationTaster (MutationTaster probability value, 0.999 on a scale of 0 to 1), PolyPhen-2 (score, 0.995 on a scale of 0 to 1), and Combined Annotation Dependent Depletion (raw Phil's Read Editor [PHRED] score [University of Washington Genome Center], 34 on a scale of 1 to 40) suggest a pathogenic outcome of the variant.[25-27] Available structural information[28] suggests that Arg272 plays a role in stabilization of the protein fold and may thereby reduce the amount of active *GLS* (Figure 2B and Figure 2C).

METABOLIC ASSAY

To confirm loss of function of GLS as a consequence of the genetic variants, a mass spectrometry–based method was developed to measure glutamine and glutamate in stored Guthrie cards from the newborn period of all of the children of family 2, parallel to segregation analyses. Spontaneous in vitro conversion of glutamine into glutamate during storage was observed and corrected by comparing with control blood spots obtained on the same day and stored under the same conditions. Glutamine levels were significantly increased in the affected individuals (*z* scores = 3.2 and 11.7) compared with healthy control neonates (*z* scores of siblings in family 2: 0.5, 0.4, 2.0, and 0.2), underlining *GLS* loss of function (Figure 2D and Figure 2E). Notably, glutamine was borderline elevated in 1 sibling in family 2 (*z* = 2.0), but not in the other siblings, including a sibling sharing the same genotype. Glutamate levels, which remained relatively stable during storage, did not differ between the affected individuals and control participants (*z* scores = 0.7 and −0.8; Figure 2F and Figure 2G); *z* scores of siblings in family 2 were −0.7, −0.5, −1.9, and −0.6.

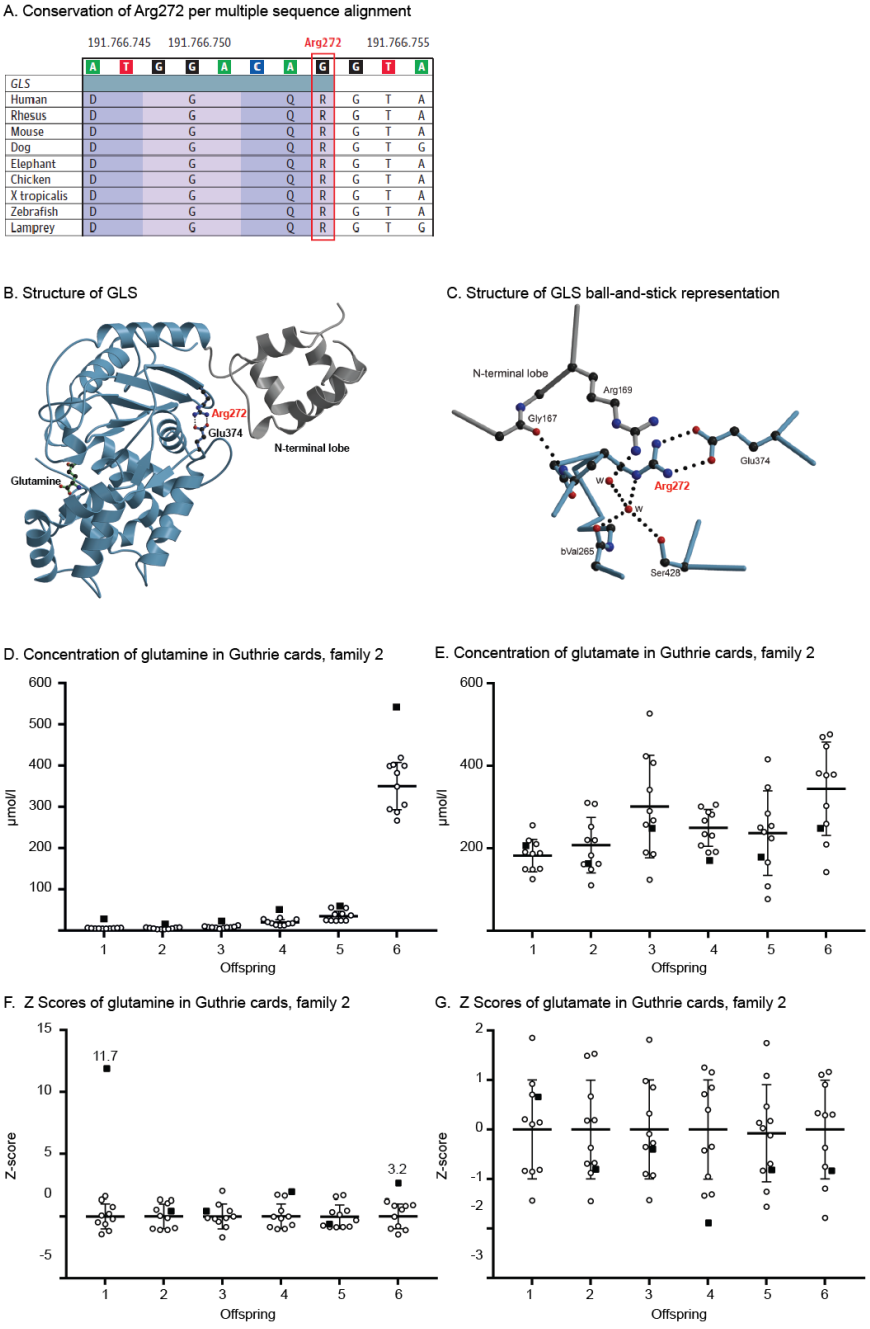

FIGURE 2. Molecular Modeling of Missense Variant in *GLS* and Glutamine and Glutamate Analyses in Guthrie Cards of Family 2. A, Multiple sequence alignment reveals conservation of Arg272 (marked red) throughout evolution across several species (https://genome.ucsc.edu; human

hg19 [Genome Reference Consortium human build 37]). **B**, Structure of GLS, including the N-terminal loop (gray), based on pdb entry 3ss3. **C**, Glutamate (green) taken from pdb entry 3ss5 to indicate the location of the active site, with Arg272 and Glu374 shown and a detailed view of the environment of Arg272. The backbone amid Arg272 is engaged in a hydrogen bond with Gly167 and oriented parallel to the side chain of Arg169, both localized in the N-terminal lobe with water. Parts B and C were generated with moscript and raster 3D.[23,24] Concentration of glutamine **D** and glutamate **E** in Guthrie cards and *z* scores of glutamine **F** and glutamate **G** in Guthrie cards of the children of family 2 (black squares), calculated from the mean and standard deviation of 10 control participants for each measurement obtained at the same day and stored under the same conditions (white dots) and expressed as *z* scores.

DISCUSSION

We describe 4 children in 2 unrelated families with overlapping phenotypes of lethal neonatal-onset respiratory failure and refractory suppression-burst epileptic encephalopathy. While there were no obvious malformations or organic anomalies, brain MRIs within days of birth showed a simplified gyral pattern with an anterior-to-posterior gradient and deep and subcortical white matter involvement. Genetic analyses revealed a homozygous truncating variant of *GLS* in family 1; in family 2, there were 2 compound heterozygous variants, a truncating and a missense variant, in *GLS*. Molecular modeling suggests that the missense variant influences GLS enzyme stability and results in a loss of function. In support of this concept, metabolic analysis on dried blood spots obtained from the newborn screening revealed increased glutamine levels in both affected children of family 2. The increase of glutamine levels in a healthy sibling was borderline (*z* score = 2) and thus much less than 2 affected siblings (*z* scores = 11.7 and 3.2, respectively). This mild elevation of glutamine may be because of technical artifacts or to a minor influence of the mutation on the biochemical values but not on the clinical presentation. Similar phenomena are observed in other metabolic disorders, such as phenylketonuria.[29]

The highly overlapping phenotype of the affected children in both families, as well as the comparable genetic findings, implicate a biallelic loss-of-function variants in *GLS* that leads to a novel metabolic disorder of early neonatal, refractory, and lethal epileptic encephalopathy.

The *GLS* loss of function seems to have profound consequences for both construction and maintenance of brain structures. Although the glutamate levels in the dried blood spots were normal, this does not exclude decreased glutamate levels in the brain, as has been

shown in knockout mouse model.[30] The *GLS* gene is highly expressed in the brain and has a pivotal role in creating glutamate abundance in the brain, contrary to the systemic circulation, in which glutamine is the most abundant amino acid.[31,32]

Brain MRIs of the affected children of both families showed simplified gyral patterns. An affected child of family 1 was followed up after 1 month, revealing cerebral vasogenic edema and destruction of initially normal appearing basal ganglia, corpus callosum, thalami, brain stem and vermis. Cerebral edema might be because of glutamine accumulation, which is associated with cerebral osmotic, thus cellular edema.[33,34] However, the observed vasogenic (rather than cellular) edema in the white matter is also a known consequence of ongoing epileptic activity.[35] Subsequent damage of the white matter tracts results in gliosis formation, which was seen in this infant in the follow-up MRI.[36]

Decreased glutamate levels may also contribute to the pathogenic brain morphology. As glutamate induces myelin synthesis, decreased glutamate levels are likely to result in white matter involvement, probably explaining the unmyelinated corticospinal tract at the level of the thalami seen in the affected children.[37]

The normal glutamate levels in dried blood spots might be explained by uptake from the diet and the numerous enzymes that metabolize glutamate.[36] These enzymes might have corrected the glutamate deficiency created by *GLS* loss of function, pointing to the importance of maintained glutamate levels.

The *GLS* loss of function has severe consequences on brain physiology. Glutamate facilitates signal transduction in the brainstem respiratory center, where respiratory volume, frequency, and rhythm are regulated immediately after birth.[13] Respiratory dysfunction in the affected children is therefore likely a consequence of *GLS* loss of function. A *GLS* knockout mouse model supports this observation, because these mice also develop respiratory dysfunction.[30] This mouse model shows that GLS deficiency leads to reduced neuronal glutamate release, reduced chemosensitivity to carbon dioxide, hypoventilation, and a decreased tidal volume. This is in line with the respiratory phenotype of the affected children, which is characterized by hypoventilation, apnea, and Cheyne-Stokes respiration. It cannot be fully excluded that respiratory dysfunction is secondary to epilepsy. However, in the knockout mouse model, respiratory dysfunction was observed, and the authors did not report seizures.[30]

The observed refractory epilepsy of the affected children may be the consequence of glutamate deficiency caused by *GLS* loss of function. Disturbed glutamine-glutamate

shuttling is a known cause of epilepsy.[38,39] Another known mechanism of epilepsy is mitochondrial dysfunction via energy depletion.[40] Glutamate deficiency likely leads to a decreased tricarboxylic acid cycle flux because there is less α-ketoglutarate supply, and it might therefore lead to mitochondrial dysfunction. Interestingly, another inborn error of glutamate metabolism with mitochondrial dysfunction has been associated with neonatal epileptic encephalopathy and suppression bursts. This defect is caused by biallelic variants in mitochondrial glutamate carrier 1 (GC1, encoded by *SLC25A22*), which lead to reduced mitochondrial glutamate transport and oxidation.[41,42]

Interestingly, patients with different defects in the glutamate-metabolizing pathway show clinical parallels and differences. Patients with a *SLC25A22* defect present similarly with very early neonatal severe intractable myoclonic seizures, muscular hypotonia, and epileptic encephalopathy.[41,42] There is no known effective treatment, and children with this condition either die within 1 to 2 years after birth or survive in a persistent vegetative state. Deficiency of glutamine synthetase (Enzyme Commission 6.3.1.2), which performs the reverse reaction of *GLS*, has been reported in 3 individuals. As expected, these patients presented biochemically with decreased glutamine concentrations, rather than increased concentrations, in the brain, plasma, and urine.[39,43] Additionally, they exhibited hyperammonemia, which was absent in our patients. Nevertheless, despite the contrasting biochemical phenotype, these patients also exhibited neonatal encephalopathy, seizures, respiratory failure, and early death. However, glutamine synthetase–deficient individuals did not show suppression bursts on electroencephalographic examination.

Interestingly, in all described disorders affecting glutamate metabolism, disturbed glutamate homeostasis leads to a severe neurological phenotype. Under physiological circumstances, homeostasis of glutamine and glutamate in the brain is strictly regulated by the glutamine-glutamate shuttle. Glutamate is excreted by neurons into the synaptic cleft as a neurotransmitter and absorbed by astrocytes, where it is converted into glutamine by glutamine synthetase. Glutamine is then transported toward neurons and again converted into glutamate by glutaminase to restart signal transduction.[38,44] It is therefore not surprising that disturbed glutamate homeostasis, either by defective synthesis in both directions or by defective transport, is detrimental for neurological functioning.

This inborn error of metabolism underlines the importance of *GLS* for appropriate glutamine-glutamate homeostasis and respiratory regulation, neurotransmission, and survival. It is quite possible that different variants in *GLS* may lead to milder phenotypes (e.g. ones caused by hypomorphic mutations). Independent reporting of additional affected individuals would delineate the phenotype and its correlation with the genotype.

LIMITATIONS

This study describes the findings of 2 families and 4 affected individuals. Further cases are necessary to further delineate the phenotype and describe its full spectrum. The functional analyses in this study were limited to dry blood spots. Analyses in cell lines may lead to deviating findings and are necessary to better understand the pathological mechanisms and suggest therapeutic approaches.

CONCLUSIONS

In conclusion, we describe a novel autosomal recessive cause of lethal neonatal-onset respiratory failure and epileptic encephalopathy caused by biallelic loss-of-function variants in *GLS*. We describe a novel autosomal recessive disorder of lethal neonatal-onset respiratory failure and epileptic encephalopathy caused by biallelic loss-of-function variants in *GLS*.

REFERENCES

1. Lemke JR, Riesch E, Scheurenbrand T, et al. Targeted next generation sequencing as a diagnostic tool in epileptic disorders. Epilepsia. 2012;53(8):1387-1398. doi:10.1111/j.1528-1167.2012.03516.
2. McTague A, Howell KB, Cross JH, Kurian MA, Scheffer IE. The genetic landscape of the epileptic encephalopathies of infancy and childhood. Lancet Neurol. 2016;15(3):304-316. doi:10.1016/S1474-4422(15)00250-1
3. von Deimling M, Helbig I, Marsh ED. Epileptic encephalopathies-clinical syndromes and pathophysiological concepts. Curr Neurol Neurosci Rep. 2017;17(2):10. doi:10.1007/s11910-017-0720-7
4. Olson HE, Kelly M, LaCoursiere CM, et al. Genetics and genotype-phenotype correlations in early onset epileptic encephalopathy with burst suppression. Ann Neurol. 2017;81(3):419-429. doi:10.1002/ana.24883
5. Rauch A, Wieczorek D, Graf E, et al. Range of genetic mutations associated with severe non-syndromic sporadic intellectual disability: an exome sequencing study. Lancet. 2012;380(9854):1674-1682.doi:10.1016/S0140-6736(12)61480-9
6. de Ligt J, Willemsen MH, van Bon BWM, et al. Diagnostic exome sequencing in persons with severe intellectual disability. N Engl J Med. 2012;367(20):1921-1929. doi:10.1056/NEJMoa1206524
7. Heyne HO, Singh T, Stamberger H, et al; EuroEPINOMICS RES Consortium. De novo variants in neurodevelopmental disorders with epilepsy. Nat Genet. 2018;50(7):1048-1053. doi:10.1038/s41588-018-0143-7
8. van Karnebeek CDM, Houben RFA, Lafek M, Giannasi W, Stockler S. The treatable intellectual disability APP www.treatable-id.org: a digital tool to enhance diagnosis & care for rare diseases. Orphanet J Rare Dis. 2012;7:47. doi:10.1186/1750-1172-7-47
9. The Broad Institute of MIT and Harvard. GTEx Portal. https://www.gtexportal.org. Accessed March 20, 2018.
10. Curthoys NP, Watford M. Regulation of glutaminase activity and glutamine metabolism. Annu Rev Nutr. 1995;15:133-159. doi:10.1146/annurev.nu.15.070195.001025
11. Curtis DR, Phillis JW, Watkins JC. The chemical excitation of spinal neurones by certain acidic amino acids. J Physiol. 1960;150(3):656-682. doi:10.1113/jphysiol.1960.sp006410
12. Rowley NM, Madsen KK, Schousboe A, Steve White H. Glutamate and GABA synthesis, release, transport and metabolism as targets for seizure control. Neurochem Int. 2012;61(4):546-558. doi:10.1016/j.neuint.2012.02.013
13. Kolesnikova EÉ. Role of glutamate and GABA in mechanisms underlying respiratory control. Neurophysiology. 2011;42(4):349-360. doi:10.1007/s11062-011-9162-z
14. Mount CW, Monje M. Wrapped to adapt: experience-dependent myelination. Neuron. 2017;95(4):743-756. doi:10.1016/j.neuron.2017.07.009
15. Nedergaard M, Takano T, Hansen AJ. Beyond the role of glutamate as a neurotransmitter. Nat Rev Neurosci. 2002;3(9):748-755. doi:10.1038/nrn916
16. World Medical Association. World Medical Association Declaration of Helsinki: ethical principles for medical research involving human subjects. JAMA. 2013;310(20):2191-2194. doi:10.1001/jama.2013.281053
17. Stenson PD, Ball EV, Mort M, et al. Human gene mutation database (HGMD): 2003 update. https://portal.biobase-international.com/hgmd. Published 2003. Accessed March 20, 2018.
18. Landrum MJ, Lee JM, Riley GR, et al. ClinVar: public archive of relationships among sequence variation and

human phenotype. Nucleic Acids Res. 2014;42(database issue):D980-D985. doi:10.1093/nar/gkt1113

19. Prinsen HCMT, Schiebergen-Bronkhorst BGM, Roeleveld MW, et al. Rapid quantification of underivatized amino acids in plasma by hydrophilic interaction liquid chromatography (HILIC) coupled with tandem mass-spectrometry. J Inherit Metab Dis. 2016;39(5):651-660. doi:10.1007/s10545-016-9935-z
20. Voigt M, Fusch C, Olbertz D, et al. Analyse des Neugeborenenkollektivs der Bundesrepublik Deutschland. Geburtshilfe Frauenheilkd. 2006;66(10):956-970. doi:10.1055/s-2006-924458
21. Lek M, Karczewski KJ, Minikel EV, et al; Exome Aggregation Consortium. Analysis of protein-coding genetic variation in 60,706 humans. Nature. 2016;536(7616):285-291. doi:10.1038/nature19057
22. Lykke-Andersen S, Jensen TH. Nonsense-mediated mRNA decay: an intricate machinery that shapes transcriptomes. Nat Rev Mol Cell Biol. 2015;16(11):665-677. doi:10.1038/nrm4063
23. Kraulis PJ. MOLSCRIPT: a program to produce both detailed and schematic plots of protein structures. J Appl Cryst. 1991;24:946-950. Journal of Applied Crystallography. doi:10.1107/S0021889891004399
24. Merritt EA, Murphy ME. Raster3D version 2.0: a program for photorealistic molecular graphics. Acta Crystallogr D Biol Crystallogr. 1994;50(pt 6):869-873. doi:10.1107/S0907444994006396
25. Schwarz JM, Cooper DN, Schuelke M, Seelow D. MutationTaster2: mutation prediction for the deep-sequencing age. Nat Methods. 2014;11(4):361-362. doi:10.1038/nmeth.2890
26. Adzhubei IA, Schmidt S, Peshkin L, et al. A method and server for predicting damaging missense mutations. Nat Methods. 2010;7(4):248-249. doi:10.1038/nmeth0410-248
27. Kircher M, Witten DM, Jain P, O'Roak BJ, Cooper GM, Shendure J. A general framework for estimating the relative pathogenicity of human genetic variants. Nat Genet. 2014;46(3):310-315. doi:10.1038/ng.2892
28. Cassago A, Ferreira APS, Ferreira IM, et al. Mitochondrial localization and structure-based phosphate activation mechanism of glutaminase C with implications for cancer metabolism. Proc Natl Acad Sci U S A. 2012;109(4):1092-1097. doi:10.1073/pnas.1112495109
29. Blitzer MG, Bailey-Wilson JE, Shapira E. Discrimination of heterozygotes for phenylketonuria, persistent hyperphenylalaninemia and controls by phenylalanine loading. Clin Chim Acta. 1986;161(3):347-352. doi:10.1016/0009-8981(86)90020-3
30. Masson J, Darmon M, Conjard A, et al. Mice lacking brain/kidney phosphate-activated glutaminase have impaired glutamatergic synaptic transmission, altered breathing, disorganized goal-directed behavior and die shortly after birth. J Neurosci. 2006;26(17):4660-4671. doi:10.1523/JNEUROSCI.4241-05.2006
31. Newsholme P, Procopio J, Lima MMR, Pithon-Curi TC, Curi R. Glutamine and glutamate—their central role in cell metabolism and function. Cell Biochem Funct. 2003;21(1):1-9. doi:10.1002/cbf.1003
32. Bode BP. Recent molecular advances in mammalian glutamine transport. J Nutr. 2001;131(9)(suppl):2475S-2485S. doi:10.1093/jn/131.9.2475S
33. Takahashi H, Koehler RC, Brusilow SW, Traystman RJ. Inhibition of brain glutamine accumulation prevents cerebral edema in hyperammonemic rats. Am J Physiol. 1991;261(3 pt 2):H825-H829.
34. Butterworth RF. Pathophysiology of brain dysfunction in hyperammonemic syndromes: the many faces of

glutamine. Mol Genet Metab. 2014;113(1-2):113-117. doi:10.1016/j.ymgme.2014.06.003

35. Hong K-S, Cho Y-J, Lee SK, Jeong S-W, Kim WK, Oh EJ. Diffusion changes suggesting predominant vasogenic oedema during partial status epilepticus. Seizure. 2004;13(5):317-321. doi:10.1016/j.seizure.2003.08.004
36. Yelamanchi SD, Jayaram S, Thomas JK, et al. A pathway map of glutamate metabolism. J Cell Commun Signal. 2016;10(1):69-75. doi:10.1007/s12079-015-0315-5
37. Lundgaard I, Luzhynskaya A, Stockley JH, et al; Charles Ffrench-Constant. Neuregulin and BDNF induce a switch to NMDA receptor-dependent myelination by oligodendrocytes. PLoS Biol. 2013;11(12):e1001743. doi:10.1371/journal.pbio.1001743
38. Barker-Haliski M, White HS. Glutamatergic mechanisms associated with seizures and epilepsy. Cold Spring Harb Perspect Med. 2015;5(8):a022863. doi:10.1101/cshperspect.a022863
39. Spodenkiewicz M, Diez-Fernandez C, Rüfenacht V, Gemperle-Britschgi C, Häberle J. Minireview on glutamine synthetase deficiency, an ultra-rare inborn error of amino acid biosynthesis. Biology (Basel). 2016;5(4):E40.
40. Rahman S. Pathophysiology of mitochondrial disease causing epilepsy and status epilepticus. Epilepsy Behav. 2015;49:71-75. doi:10.1016/j.yebeh.2015.05.003
41. Molinari F, Kaminska A, Fiermonte G, et al. Mutations in the mitochondrial glutamate carrier SLC25A22 in neonatal epileptic encephalopathy with suppression bursts. Clin Genet. 2009;76(2):188-194. doi:10.1111/j.1399-0004.2009.01236.x
42. Molinari F, Raas-Rothschild A, Rio M, et al. Impaired mitochondrial glutamate transport in autosomal recessive neonatal myoclonic epilepsy. Am J Hum Genet. 2005;76(2):334-339. doi:10.1086/427564
43. Häussinger D, Schliess F. Glutamine metabolism and signaling in the liver. Front Biosci. 2007;12:371-391. doi:10.2741/2070
44. Bak LK, Schousboe A, Waagepetersen HS. The glutamate/GABA-glutamine cycle: aspects of transport, neurotransmitter homeostasis and ammonia transfer. J Neurochem. 2006;98(3):641-653. doi:10.1111/j.1471-4159.2006.03913.x

Chapter 3

GLS hyperactivity causes glutamate excess, infantile cataract and profound developmental delay

Human Molecular Genetics, 2018. Doi: 10.1093/hmg/ddy330

Lynne Rumping^, Federico Tessadori^, Petra J.W. Pouwels, Esmee Vringer, Jannie P. Wijnen, Alex A. Bhogal, Sanne M.C. Savelberg' Karen J. Duran, Mark J.G. Bakkers, Rúben J.J. Ramos, Peter A.W. Schellekens, Hester Y. Kroes, Dennis W.J. Klomp, Graeme C.M. Black, Rachel L. Taylor, Jeroen P.W. Bakkers, Hubertus C.M.T. Prinsen, Marjo S. van der Knaap, Tobias B. Dansen, Holger Rehmann, Fried J.T. Zwartkruis, Roderick H.J. Houwen, Gijs van Haaften, Nanda M. Verhoeven-Duif, Judith J.M. Jans* and Peter M. van Hasselt*

^both authors share first authorship *both authors share last authorship

ABSTRACT

Loss-of-function mutations in glutaminase (GLS), the enzyme converting glutamine into glutamate, and the counteracting enzyme glutamine synthetase (GS) cause disturbed glutamate homeostasis and severe neonatal encephalopathy. We report a *de novo* Ser482Cys gain-of-function variant in *GLS* encoding GLS associated with profound developmental delay and infantile cataract. Functional analysis demonstrated that this variant causes hyperactivity and compensatory downregulation of GLS expression combined with upregulation of the counteracting enzyme GS, supporting pathogenicity. Ser482Cys-GLS likely improves the electrostatic environment of the GLS catalytic site, thereby intrinsically inducing hyperactivity. Alignment of +/−12.000 GLS protein sequences from >1000 genera revealed extreme conservation of Ser482 to the same degree as catalytic residues. Together with the hyperactivity, this indicates that Ser482 is evolutionarily preserved to achieve optimal- but submaximal- GLS activity. In line with GLS hyperactivity, increased glutamate and decreased glutamine concentrations were measured in urine and fibroblasts. In the brain (both grey and white matter), glutamate was also extremely high and glutamine was almost undetectable, demonstrated with magnetic resonance spectroscopic imaging at clinical field strength and subsequently supported at ultra-high field strength. Considering the neurotoxicity of glutamate when present in excess, the strikingly high glutamate concentrations measured in the brain provide an explanation for the developmental delay. Cataract, a known consequence of oxidative stress, was evoked in zebrafish expressing the hypermorphic Ser482Cys-GLS and could be alleviated by inhibition of GLS. The capacity to detoxify reactive oxygen species was reduced upon Ser482Cys-GLS expression, providing an explanation for cataract formation. In conclusion, we describe an inborn error of glutamate metabolism caused by a GLS hyperactivity variant, illustrating the importance of balanced GLS activity.

INTRODUCTION

The amino acid glutamate is best known for its role as excitatory neurotransmitter, but also serves as a substrate for other key metabolites including the anti-oxidant glutathione.[1–3] Glutamate homeostasis is mainly warranted by two enzymes: glutamine synthetase (GS; EC 6.3.1.2) and glutaminase (GLS; EC 3.5.1.2). GS converts glutamate into glutamine and is ubiquitously expressed.[4] GLS catalyzes the deamination of glutamine into glutamate and ammonia and exists in the following two isoforms: GLS, which is present in two splice variants kidney-type glutaminase (KGA) and GAC, which is mainly expressed in kidney and brain; and GLS2, which is ubiquitously expressed with the highest expression in the liver.[5,6] Inborn errors of metabolism are usually due to severe loss-of-function of the involved enzymes, hence recessive inheritance. In line, a disturbed equilibrium of glutamate and glutamine was described in patients with GS deficiency, clinically resulting in glutamine deficiency, neonatal epilepsy and early death.[7] Recently, GLS loss of function has been described to cause lethal epileptic encephalopathy and glutamine excess in two families.[8] The description of patients with spastic ataxia and optic atrophy harboring bi-allelic hypomorphic variants in GLS suggests a phenotypic spectrum -presumably depending on the degree of residual activity- that is yet to be uncovered.[9] Theoretically, glutamate homeostasis can also be disturbed by hyperactivity of either enzyme. This option is commonly disregarded as there are only few examples of genetic variants that induce enzyme hyperactivity, glutamate dehydrogenase (GDH) and IDH2 gain of functions.[10,11] These examples indicate that a heterozygous variant is sufficient to induce overall enzyme hyperactivity.

In this study, we characterize a *de novo* hypermorphic heterozygous *GLS* variant found in a patient with infantile onset cataract, skin abnormalities, profound developmental delay and intracerebral glutamate excess. This new inborn error of metabolism illustrates the importance of regulated GLS activity for lens transparency and brain function.

RESULTS

CLINICAL DESCRIPTION

In a female patient, bilateral cataract was diagnosed at the age of 3 months after the parents noticed decreased eye contact and loss of the red light reflex of the pupils on photos (Fig. 1A and Supplementary Material, S1). The proband is the first child of healthy non-consanguineous parents of Dutch descent (Fig. S1A) as indicated by family history

and single nucleotide polymorphism (SNP)-array. Gestation and delivery were uneventful. After lens extraction and replacement, eye contact unexpectedly remained absent. By the age of 8 months, delayed development was noted, along with a relative decrease of the head circumference from 0 standard deviations (SD) to −2 SD. She developed recurrent dermatological abnormalities on her extremities, cheeks and ears without pruritus, characterized as erythematic subcutaneous nodules of ~1 cm (Fig. 1B). Histopathological analysis of these lesions showed deep perivascular and periglandular lymphohistiocytic infiltrates and pronounced leukocytoclasia at the surface of the dermis and focal vacuolar alterations, hyperkeratosis and parakeratosis of the epidermis. A dermatological diagnosis remained inconclusive. Over time, the girl lost the ability to make meaningful sounds and the ability to sit. She developed profound axial hypotonia leading to kyphoscoliosis. Upon arousal she exhibited uncontrolled motoric agitation and self-injurious behavior. Development remained slow paced. At the most recent follow up at the age of 11 years, she was able to use gestures for communication, to understand verbal single component instructions and to steer her own wheelchair.

IDENTIFICATION OF THE SER482CYS-GLS *DE NOVO* VARIANT

Extensive diagnostic workup unexpectedly revealed extremely low glutamine levels and high glutamate levels in both cortex and white matter as detected consistently with quantitative brain proton magnetic resonance spectroscopy (MRS) and magnetic resonance spectroscopic imaging (MRSI) at 1.5Tesla (Fig. 1C and Supplementary Material, S1B) and recently also shown at 7Tesla (Fig. 1D and Supplementary Material, S1C). Interestingly, cerebrospinal fluid and plasma levels were unaffected (Supplementary Material, Table S1). Brain MRI at the age of 16 months showed delayed myelination (Fig. 1E). Analyses of stored urine samples similarly showed low concentrations of glutamine and high concentrations of glutamate (Fig. 1F and Supplementary Material, Table S1). The diagnosis remained enigmatic until trio-based whole-exome sequencing (WES) revealed a heterozygous *de novo GLS* missense variant (NC_000002.11:g.191 795182C > G). Analysis of WES data using recessive filters yielded no rare homozygous damaging variants. The analysis for compound heterozygosity (including correctness of segregation in parents) yielded two genes hit by rare and possibly damaging variants, but based on gene function, absent links with human disease and the high prevalence within the healthy population, these variants were considered as unlikely to contribute to the phenotypes of the patient (supplementary results). The conservative mutation in *GLS* from serine to cysteine at position 482 NP 055720.3:p.(Ser482Cys) was confirmed by Sanger sequencing (Fig. 1G, supplementary results). GLS mediates the conversion of glutamine into glutamate; therefore, this genetic change could only be explained if the encoded protein would be hyperactive.

SER482CYS-GLS LEADS TO GLS HYPERACTIVITY

The effect of the Ser482Cys-*GLS* variant on the activity of the GLS enzyme was assessed in fibroblasts from the patient by quantification of intracellular glutamine and glutamate. The *GLS* variant indeed resulted in an increased intracellular glutamate/glutamine ratio (Fig. 2A and B and Supplementary Material, S2A). To validate enhanced catalytic activity of the GLS variant, a HEK293 cell model with inducible expression of Ser482Cys-*GLS* (KGA, the long splice variant) was generated. Induction of Ser482Cys-*GLS* again strongly increased the glutamate/glutamine ratio while induction of wildtype *GLS* had no effect (Fig. 2C and D and Supplementary Material, S2B). Inhibition of GLS with CB-839 resulted in normalization of glutamate and glutamine concentrations in both fibroblasts and HEK293 cells, providing additional evidence that the Ser482Cys-*GLS* variant leads to GLS hyperactivity.

GLS HYPERACTIVITY LEADS TO METABOLIC COMPENSATORY MECHANISMS

Protein expression of both GLS splice variants KGA and GAC in patient fibroblasts was decreased -rather than increased- compared to controls, ruling out that increased GLS activity was due to increased protein availability. Conversely, the observed downregulation of GLS protein expression suggests it served as a compensatory mechanism aiming at normalizing glutamine and glutamate concentrations (Fig. 2B). In support, introduction of Ser482Cys-*GLS* in HEK293 cells also evoked decreased GAC expression levels (Fig. 2D and Supplementary Material, S2C). Furthermore, CB-839-induced GLS inhibition restored GLS expression. GLS expression could also be restored by normalization of glutamate levels through depletion of extracellular glutamine, pointing to glutamate as a regulator of GLS expression (Fig. 2D). Finally, the observation that protein levels of the reciprocal enzyme GS increased upon expression of Ser482Cys-GLS -an effect that could also be reversed through CB-839-mediated GLS inhibition (Fig. 2B and D)- underlines that cellular efforts were aimed at normalizing glutamine and glutamate concentrations.

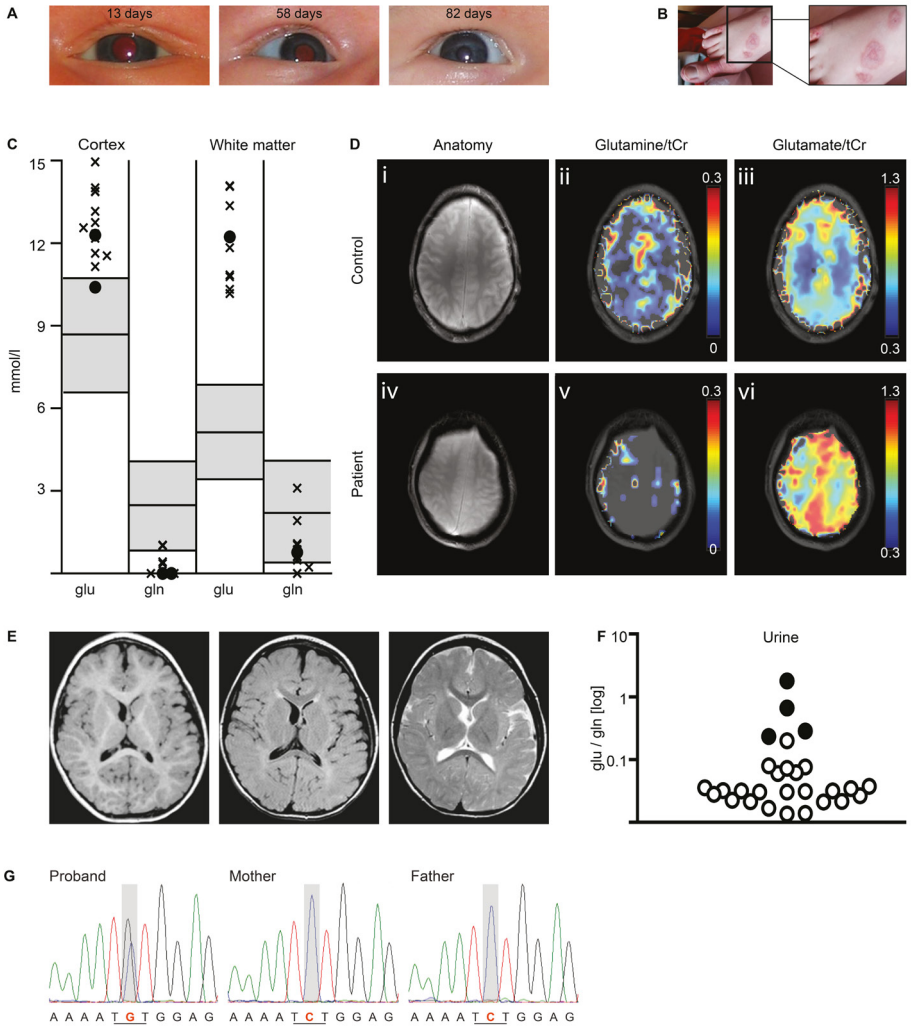

FIGURE 1. Identification of a *GLS de novo* variant in a patient with bilateral infantile cataract. (**A**) Photographs of the eyes of the patient at different ages depict a decrease in light reflex, indicating the formation of cataract before the age of 3 months. (**B**) Dermatological manifestation of erythematic nodules of ~1 cm, here on the dorsum of the foot. (**C**) Glutamine and glutamate concentrations assessed by MRS (1.5 Tesla, both STEAM, TR/TM/TE 6000/30/20 ms and PRESS, TR/TE 3000/30 ms) in the parietal cortex and white matter of the patient at the age of 2 and 3 years. The normal range, +/− 2 SD from mean based on control values of children between 2 and 5 years of age[35] is depicted in grey. Data represent concentrations in single-voxel MRS (o) and in multiple voxels from MRSI (x). (**D**) Maps of glutamine (middle panel) and glutamate (right panel) levels in the brain of the patient at the age of 14 years (lower row) and a control (top row), generated from 2D MRSI acquisitions (7 T, pulse-acquire, matrix 44x44, 0.5x0.5x1.0 cm^3, TR/TE 300/2.5 ms) overlaid on anatomical magnetic

resonance images (left panel). (**E**) Magnetic resonance imaging of the patient at the age of 16 months, revealing delayed myelination. The transverse T1-weighted image (left) shows the myelinated cerebral white matter as white. The FLAIR (middle) and T2-weighted (right) images have a lack of contrast between cerebral hemispheric white matter and cortex, indicating that myelination is incomplete. Better myelinated structures, including corpus callosum and internal capsule, have a lower signal. (**F**) Urinary excretion of glutamate and glutamine, presented as ratios on a logarithmic scale in the urine of the patient (black dots) compared to controls (white dots). (**G**) DNA Sanger sequencing trio analysis shows the Ser482Cys-*GLS de novo* variant in the patient, which is absent in the unaffected parents. The underlined sequence indicates the nucleic acid change causing the substitution of the amino acid serine for cysteine.

SER482 FUNCTIONS AS A HIGHLY CONSERVED INTRINSIC RESTRICTOR OF GLS ACTIVITY

Ser482 is located near the catalytic site of GLS, but does not have an identified role in the catalytic process itself.[12] Alignment of +/− 12.000 GLS protein sequences from >1000 genera revealed that Ser482 is a residue with an extremely high degree of evolutionary conservation (conservation score, >0.98) along with residues directly involved in the catalytic process (Fig. 2E). The Ser482Cys substitution is absent in healthy populations in the databases GoNL[13], gnomAD[14], ClinVar[15] and ExAC[16] and is expected to be tolerated without overall disturbances of the protein fold. Interestingly, substitution by cysteine -containing a sterically more demanding and less polar thiol group than serine- changes the electrostatic environment of Tyr466, one of the catalytic residues that protonates glutamine and thereby accelerates deamination into glutamate. This change is likely to enhance the propensity for proton donation and thereby to increase the speed of the reaction (Fig. 2F and Supplementary Material, S3).

GLS HYPERACTIVITY DECREASES REDOX BUFFER CAPACITY

Oxidative stress is a known consequence of glutamate excess and a common cause of cataract and neuronal injury.[17,18]. In HEK293 cells expressing Ser482Cys-*GLS,* clearance of a sub-lethal pulse of hydrogen peroxide was impaired with normal basal reactive oxygen species (ROS) levels (Fig. 3). This indicates that Ser482Cys-*GLS* results in a lower capacity for ROS scavenging.

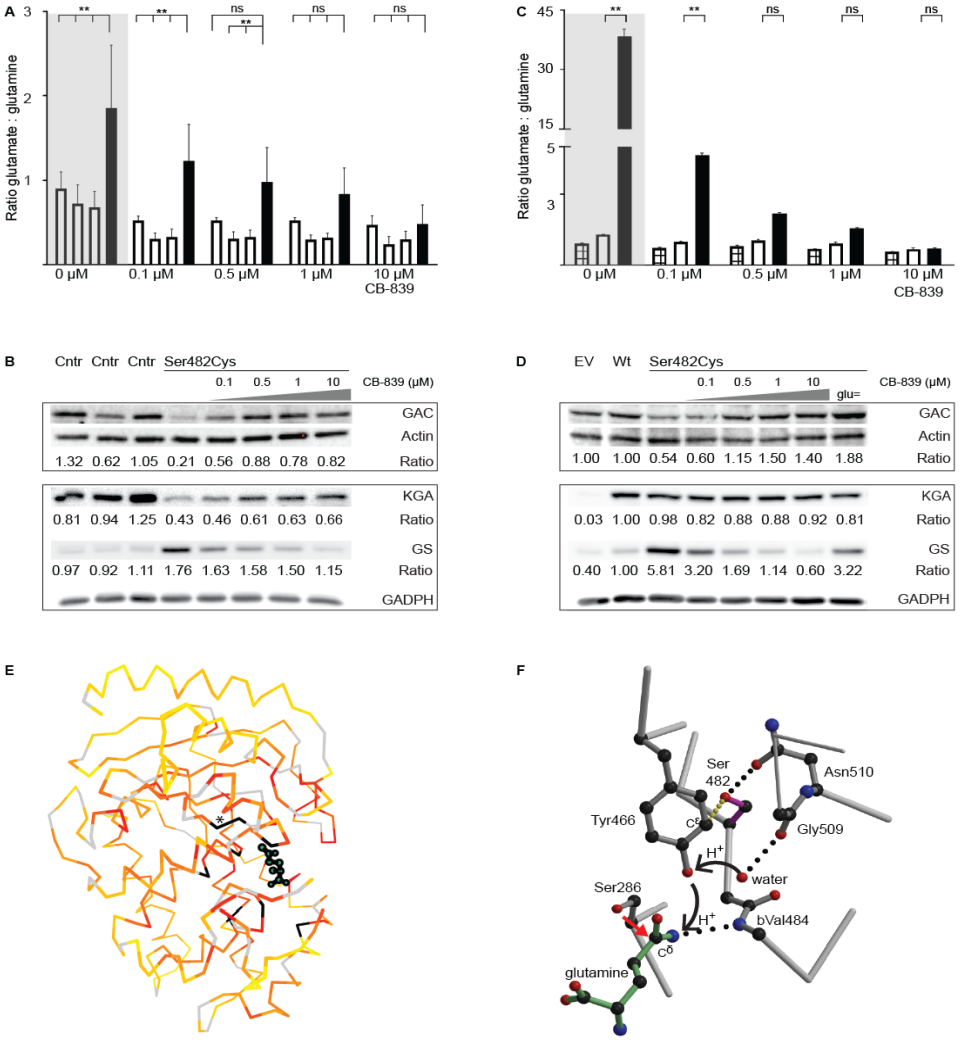

FIGURE 2. Impact of Ser482Cys-GLS on enzyme activity, expression and structure. (**A**–**C**) Glutamate and glutamine values measured with UPLC-MS/MS, expressed as the ratio of glutamate/glutamine in (**A**) fibroblasts of three controls (white) and the proband expressing Ser482Cys-GLS (black) and (**C**) HEK293 cells stably transfected with an EV (checked), wild-type *GLS* (white) or Ser482Cys-*GLS* (black). Cells containing the variant were untreated (highlighted) or treated with 0.1, 0.5, 1 or 10 µM CB-839. Data represent the mean of biological triplicates with standard deviations. **P* < 0.05 (ANOVA, Tukey's test); ***P* < 0.01 (ANOVA, Tukey's test); ns indicates not significant. (**B**–**D**) Western blots of both GLS splice variants -KGA and glutaminase C (GAC)- and GS. (**B**) In fibroblasts of three controls and the patient expressing Ser482Cys-GLS, the latter treated with CB-839 corresponding to panel a. The mean of the expression levels in control fibroblasts is arbitrarily set at 1. (**D**) In HEK293 cells stably transfected with

an EV, wild-type *GLS* (Wt) or Ser482Cys-*GLS* (KGA), the latter treated with CB-839 (corresponding to panel c) or deprived from glutamine to normalize glutamate concentrations (glu=). Expression levels in cells expressing wild-type GLS are arbitrarily set at 1. Results are normalized to actin or glyceraldehyde 3-phosphate dehydrogenase (GADPH). Analyses performed on the same blot are delineated. (**E**) Conservation analysis of GLS, in which residues with conservation scores from 0 to 0.98 are represented by a color gradient from yellow to red and the most conserved residues (>0.98) are represented in black. These residues are clustered around the catalytic site and most of them are directly involved in the catalytic reaction: Ala339 (0.994), Lys481 (0.992), Asn335 (0.991), Lys289 (0.990), Ser286 (0.990), Tyr414 (984), Tyr466 (0.986) and Asn388 (0.983). Among these is Ser482 (0.983), indicated by the asterisk symbol. Glutamine is shown in green ball-and-stick representation. Glycine and proline residues—often conserved for pure structural reasons—were omitted and are shown in light grey. (**F**) Zoom-in on the catalytic site of GLS in complex with glutamine (green) shows that Ser482 (magenta) is located near the catalytic site. The deamination reaction of glutamine is initiated by a nucleophilic attack of Ser286 on C^{δ} of glutamine (red arrow) and is accelerated by Tyr466 via protonation (black arrows indicate proton transfer). The electrostatic environment of Tyr466 is determined by the hydroxyl-group of Ser482 (yellow dotted line). Hydrogen bonds are shown by dotted black lines. Supplementary Material, Fig. S3 provides additional insight into the enzymatic reaction and the possible consequences of the Ser482Cys substitution. Figures are based on pdb entry 3vp0 and were generated with molscript[36] and raster3D[37].

SER482CYS-GLS INDUCES LENS OPACIFICATION

To explore the causal relationship between Ser482Cys-*GLS* expression and cataract, we examined the effect of this variant in developing zebrafish embryos. Lens transparency at 5 days post fertilization (dpf) in zebrafish embryos injected with Ser482Cys-*GLS* cDNA was compared to that in control embryos injected with wild-type *GLS* or uninjected embryos (Supplementary Material, Fig. S4A). Of the embryos expressing the Ser482Cys-GLS variant, 34 (72%) of 47 developed structural opacities in the lens, which were not observed in any of the control embryos (Fig. 4A–C and Supplementary Material, S4B–D). GLS inhibition with CB-839 from 6 h post fertilization (hpf) resulted in profoundly decreased formation of structural opacities in the lens of the Ser482Cys-*GLS* zebrafish embryos (Fig. 4D and Supplementary Material, Fig. S4E).

DISCUSSION

We characterize a *de novo* heterozygous, hyperactive *GLS* variant found in a patient with infantile onset cataract, skin abnormalities, profound developmental delay and intracerebral

glutamate excess. The increased conversion of glutamine into glutamate observed upon introduction of this variant provides a compelling explanation for the strikingly elevated glutamate levels in cerebro and -in view of the central role of glutamate in brain functioning likely explains the developmental delay. Furthermore, zebrafish studies unexpectedly reveal that introducing the hypermorphic GLS variant induces lens opacities. Together with the observations that the lens opacities are amenable to GLS inhibition, this supports a role for GLS activity in cataract formation.

Inborn errors of metabolism are usually due to bi-allelic or mono-allelic loss-of-function variants with few exceptions. Of these, hyperinsulinism-hyperammonemia syndrome is caused by increased sensitivity of the enzyme GDH to allosteric activation and D-2-hydroxyglutaric aciduria is caused by a neomorphic function of the enzyme IDH2[19,20]. The variant described here truly increases enzymatic activity (Supplemental discussion) likely due to an improved electrostatic environment of the GLS catalytic site. To the best of our knowledge, this nature of hypermorphic gain of function in which activity is intrinsically increased by improvement of the catalytic machinery has not been described before. Although rare by nature, it is possible that the current paradigm- heterozygous variants in enzyme encoding genes are usually harmless- hampers identification of comparable disease causing hypermorphic variants in enzyme encoding genes.

The cellular efforts, aimed at counteracting the effects of the hyperactive enzyme by decreasing GLS protein availability while increasing the reciprocal enzyme GS, underline that increased GLS activity is detrimental. Our data underline the observation by Krebs in 1935 that glutamate acts as a sensor for GLS regulation and reveal that glutamate not only affects GLS enzyme kinetics but also its expression. The extremely high degree of conservation of the hypermorphic residue across >1000 genera -comparable only to residues directly involved in the enzymatic conversion of glutamine into glutamate- suggests that the serine residue serves as a built-in restrictor, ensuring submaximal activity rather than maximal enzyme activity of GLS.

A point of interest is the observation that the ratio between glutamate and glutamine was increased in brain and urine, while it remained unaltered in CSF and plasma. We postulate that this discrepancy is explained by the degree to which glutamine and glutamate levels are controlled by GLS. Tissues with abundant expression of GLS -neurons and kidney- are mainly under GLS control.[6] The relative importance of GLS within the brain is illustrated by a high glutamate/glutamine ratio (2:1) in normal population.[21]. GLS overactivity may be masked in other tissues in which GLS is only one of several players- including GS- that together regulate glutamine and glutamate levels. The reduced importance of GLS in

plasma is reflected by the significantly lower ratio of glutamate/glutamine (1:15).[22] Further supporting this hypothesis, the ratio is even lower (~1:100) in CSF, which is produced by choroid plexus from plasma by glial cells that are known to have high GS expression.[4,22]. The striking contrast between CSF and brain could be regarded as a cautionary note: CSF should not be readily regarded as a proxy for the brain.

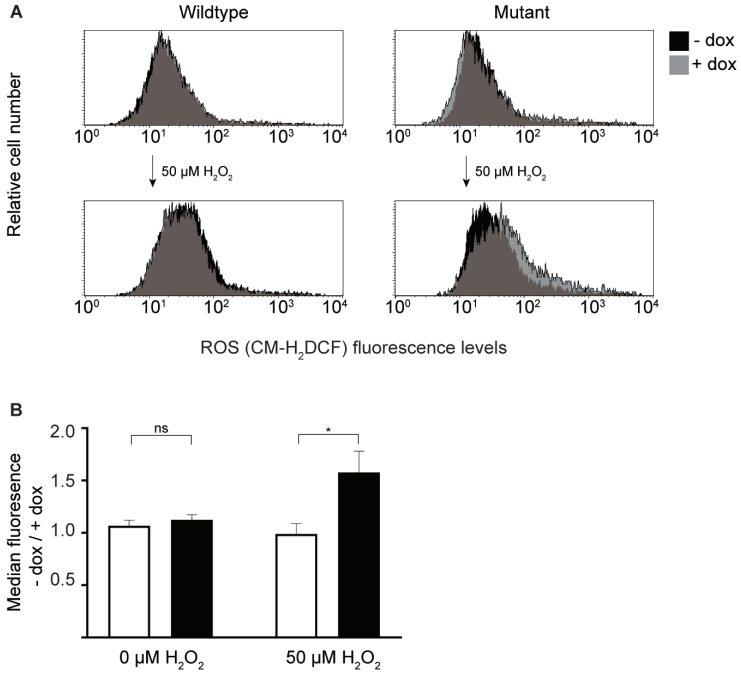

FIGURE 3. ROS levels and redox buffering capacity. HEK293 cells were transfected with wild-type *GLS* or Ser482Cys-*GLS*, with and without exposure to H_2O_2, measured with flow cytometry, using CM-H_2DCF-DA. (**A**) Histograms of non-induced (−dox, black) and induced (+dox, grey) cells, showing the shift in CM-H_2DCF fluorescence intensity after induction with doxycycline and exposure to 50 μM H_2O_2, Data are normalized to total cell counts and are representative for biological triplicates. (**B**) Ratio of the median CM-H_2DCF fluorescence intensities of cells induced with doxycycline over uninduced cells. Data present the mean of biological triplicates with standard errors of the mean. *P < 0.05 (ANOVA, Tukey's test); ns indicates not significant.

Under physiological conditions, glutamate is important for redox homeostasis as it is the precursor of the anti-oxidant glutathione.[2]. Glutamate excess, however, is associated with oxidative stress, a common cause of cataract and neuronal damage.[17,18] We show

that GLS hyperactivity indeed leads to decreased capacity for redox buffering, which can result in oxidative stress. We therefore postulate that glutamate excess contributes to the ophthalmologic phenotype of our patient. In the aqueous humor -nourishing the lens- glutamate concentrations are strictly regulated and even kept low by metabolism and transport.[23] Exposure to glutamate causes cataract in chick and rat embryos.[17,24,25] In line with the phenotype of the affected patient, zebrafish expressing Ser482Cys-GLS develop lens opacities, which could be largely prevented by GLS inhibition. Interestingly, neurons and lens cells are both of ectodermal origin, as is the skin, and share similarities in expression and regulation of glutamate receptors, supporting the notion that disturbed glutamate homeostasis not only affects the brain, but also skin and lens.[26] Glutamate excitotoxicity has been associated with epilepsy, numerous neurodegenerative diseases, self-injury and agitated behavior.[18,27] The measured glutamate excess in the brain of our patient might therefore provide a plausible explanation for the self-injury behavior and developmental delay of our patient.

Interestingly, other defects affecting glutamate homeostasis lead to neurological phenotypes as well. Under physiological circumstances, homeostasis of glutamine and glutamate in the brain is strictly regulated by neuronal GLS and astrocytic GS via the glutamine–glutamate shuttle.[4] GLS loss-of-function variants lead to a phenotypic spectrum. The first description was of a late-childhood onset disease, including optic atrophy and spastic ataxia.[9] Recently, bi-allelic loss-of-function variants in *GLS* were described to cause lethal, neonatal onset encephalopathy characterized by respiratory failure, status epilepticus and early death within weeks after birth.[8] These patients had simplified gyral patterns and showed destructions of initially normal-appearing brain structures. Both the reported hiccups during pregnancy and the simplified gyral patterns on imaging suggest the damage has its onset prenatally. Given the truncating mutations present in the latter phenotype, it is tempting to speculate a dose effect relationship explaining the phenotypic spectrum. This inborn error -together with GLS hyperactivity- illustrates the importance of proper GLS activity for both brain physiology and morphology.

Deficiency of GS -performing the reversed reaction of GLS- results in decreased glutamine levels but normal glutamate levels and hyperammonemia. This has been reported in three individuals who exhibited neonatal encephalopathy, seizures and respiratory failure and early death.[28]. The absence of epilepsy in our patient with GLS hyperactivity despite increased glutamate levels on brain MRSI is unexpected as glutamate excitotoxicity is considered a critical factor in the initiation of epileptic seizures.[29] Seizures can be provoked by either increased glutamate release into the synaptic cleft or decreased reuptake or recycling from the synaptic cleft, which implies that glutamate levels in the

synaptic cleft of our patient are unaffected despite overall brain glutamate abundance. The phenotypic neurological spectrum of these patients shows the importance of strictly regulated glutamate homeostasis for neurological functioning.

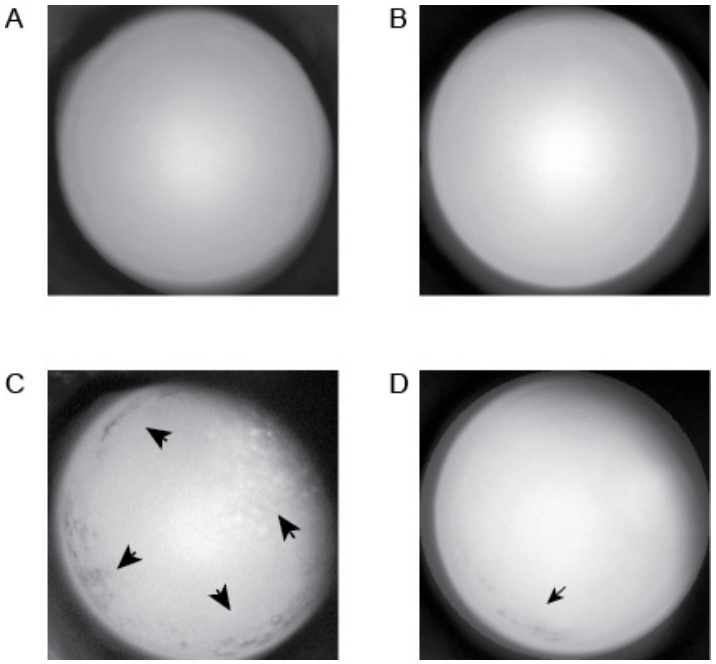

FIGURE 4. Lens opacity of zebrafish expressing Ser482Cys-*GLS*. Representative images of the lenses of 5 dpf zebrafish embryos of **(A)** uninjected (*n*=30) or injected with vectors containing **(B)** wild-type *GLS* cDNA (*n*=28) or **(C)** Ser482Cys-*GLS* cDNA KGA isoform (*n*=47). **(D)** Zebrafish embryos expressing Ser482Cys-*GLS* were treated with 10 µM CB-839 from 6 hpf (*n*=10). Opacities in the lens are indicated with arrows. See Supplementary Material, Fig. S4 for all images. Images were obtained with a fluorescence microscope. Linear image editing was performed.

A limitation of our study is that only a single patient with a hyperactive variant in GLS could be identified. Hyperactive variants are extremely uncommon, especially in a well-conserved catalytic area like in GLS. Intolerance to loss of function in GLS is likely high, meaning that mutations will likely be lethal. These factors contribute to a limited patient pool. While definite pathogenic conclusions are considered difficult based on evidence from unique subjects, when adequately studied, these cases can be regarded as experiments of nature and provide invaluable insights. Such is the case here, were we provide strong evidence that GLS hyperactivity causes a new metabolic disorder of

glutamate metabolism. Our study furthermore provides insight into the regulation of GLS activity and illustrates the importance of appropriate GLS activity for human brain function, skin and lens transparency.

MATERIALS AND METHODS

CLINICAL PHENOTYPING, DIAGNOSTICS AND EXOME SEQUENCING

Clinical phenotyping was performed and diagnostic tests were requested by metabolic pediatricians, clinical geneticists, ophthalmologist, neurologists and dermatologist. Amino acids analyses in urine were performed on a Biochrom30 analyzer. In the brain, these were determined with quantitative MRS and MRSI at 1.5Tesla at the age of 2 and 3 years and with MRSI at 7Tesla at the age of 14 years. Genetic analysis was performed by trio-based whole-exome sequencing and Sanger sequencing. See supplementary methods for details.

GLS ACTIVITY

GLS activity was determined in patient fibroblasts and in human embryonic kidney 293 (HEK293) cells stably transfected with either wild-type or Ser482Cys-*GLS* (KGA isoform) or an empty vector (EV), in absence or presence of different concentrations of the allosteric GLS inhibitor CB-839.[30] GLS activity was defined as the formation of glutamate from glutamine, quantified by ultra-performance liquid chromatography tandem mass spectrometry.[31] Protein expression was assessed by Western Blot.

CONSERVATION ANALYSIS

Sequences homologous to human GLS from the non-redundant protein collection at National Center for Biotechnology Information were aligned in SeaView.[32] Obvious partial sequences as well as all protein data bank (pdb) sequences were removed, which resulted in about 12.000 sequences. The consensus were determined in JalView[33] and fraction of the modal residue in a column were used for generating a color gradients, which was mapped onto the GLS structure as a measure of conservation (consensus score).

REACTIVE OXYGEN SPECIES

ROS-levels were quantified by flow cytometry (BD FACSCalibur™) as previously described in wild-type *GLS* or Ser482Cys-*GLS* transfected HEK293 cells[34].

ANIMAL MODEL

Zebrafish *(Danio rerio)* embryos were microinjected at the 1-cell stage with DNA constructs coding for wild-type or Ser482Cys-GLS (KGA isoform). Uninjected zebrafish embryos were

used as controls. The embryos were kept under standard laboratory conditions, either in the absence or in the presence of the GLS inhibitor CB-839, prior to assessment of glutamine and glutamate concentrations and lens opacity at 5 dpf.

STATISTICS

Statistical analyses were performed by ANOVA, post-hoc Tukey's test using International Business Machines Statistical Package for the Social Sciences (IBM SPSS) statistics 21.

STUDY APPROVAL

The proband's parents provided written informed consent for all aspects of the study. Zebrafish experiments were carried out in accordance with the guidelines of the Animal Experimentation Committee of the Royal Netherlands Academy of Arts and Sciences.
For more detailed information, see supplementary materials and methods.

ACKNOWLEDGEMENTS

We are grateful for the contribution of the patient's family to this study. We would like to thank Willem Hoefakker, Birgit Schiebergen-Bronkhorst, Ans Geboers, Mirjam van Aalderen, Annique Claringbould, Elise Meijer and Lida Lughthart for their great technical assistance. We also thank Sahar Nassirpour and Paul Chang for providing assistance in reconstructing the 7Tesla MRSI data. This work was funded by ODAS (2014-1) stichting and Erfelijke Stofwisselingsziekten Nederlands taalgebied.

SUPPLEMENTARY METHODS

CLINICAL PHENOTYPING, DIAGNOSTICS AND EXOME SEQUENCING

Clinical phenotyping was performed and diagnostic tests were requested by metabolic pediatricians, ophthalmologists, neurologists and clinical geneticists.

Amino acid analyses in urine of the patient were performed on a Biochrom30 (Cambridge, UK) amino acid analyzer at age 10 and 11 year. These were compared to reference values and values of control urines which were stored for the same amount of time.

Amino acid analyses in fibroblasts were performed by UPLC-MS/MS (Waters, Manchester, UK) using stable isotope-labeled internal standards as described by Prinsen et al.[36]

Brain metabolites in cerebral white and grey matter were measured with single voxel proton

magnetic resonance spectroscopy[38] at a field strength of 1.5 Tesla (Vision and Sonata, Siemens, Erlangen) at the age of 2 and 3 years (STEAM localization, repetition time (TR) 6000ms, mixing time (TM) 30ms, echo time (TE 20ms)), and with proton magnetic resonance spectroscopic imaging[39] at the age of 3 years (PRESS localization, voxels: 10x10x15 m^3 TR/TE 3000/30ms). Concentrations were quantified with LCModel, and compared with control values of children between 2 and 5 years of age.[35,40]

Glutamate and glutamine in 2 slices in the brain were again determined at the age of 14 years by MRSI. High resolution MRSI data of the brain was acquired at a 7 Tesla MR scanner (Philips) using a crusher coil (MR Coils) inserted into a 32 channel head coil (Nova).[41] We performed a pulse-acquire MRSI experiment using the crusher coil for lipid suppression at the skull, and a CHESS water suppression sequence in which the three water-selective pulses were replaced by subject specific spectral spatial RF pulses.[42] MRSI data was acquired using a 44x44 matrix (voxels: 5x5x10 mm^3, TR/TE 300/2.5 ms, acquisition time: 7:36 minutes). These data were processed using a custom data processing tool (FIDGET). An over-discretized SENSE reconstruction and B_0 correction was used to reduce extra-cranial lipid signal contamination and to improve the SNR and metabolite line-shape.[43, 44] Furthermore, eddy current and zero-order phase correction using low resolution water reference data was performed.[45] Post-processing steps included prediction of the missing FID information (between excitation and signal readout) using a backward linear prediction autoregressive algorithm and residual water peak removal using Hankel Lanczos (HLSVD) method.[46, 47] After post-processing, data was fit using LCModel. Patient results were compared to those taken from a healthy control subject (27yrs old, male).

Exome sequencing and bioinformatic analyses for the proband, siblings and both parents were performed as described previously.[48] Trio-based whole-exome sequencing to an average of 116x, 117x and 98x-fold depth coverage on the target region for index, father and mother was performed in order to identify the causal mutation. A de novo model was considered the most likely because of unrelated healthy parents. The *de novo GLS1* variant was confirmed by Sanger sequencing. The proband's parents provided written informed consent for all aspects of the study.

CELL CULTURE AND STABLE CELL TRANSFECTION

Stably transfected cell lines were generated by transfecting HEK293 T-REx Flp-in host cell lines with plasmids containing wildtype KGA (the long splice variant of *GLS1*), Ser482Cys-KGA, or an empty vector (mCherry) according to the manufacturer's instructions (Invitrogen, Carlsbad, California). For plasmid preparation, the Ser482Cys cDNA sequence was obtained by site-specific mutagenesis (QuikChange II XL, Agilent, Santa Clara, CA, USA)

of the wildtype KGA sequence in pcDNA5/FRT/TO TOPO containing a hybrid CMV/TetO_2 promoter for regulated expression (Life Technologies, Waltham, MA, USA). Cells were cultured at 37°C in 5% CO_2. Fibroblasts were cultured in HAM nutrient mixture F12 with HEPES and HEK293 cells in DMEM-GlutaMax high glucose with pyruvate supplemented with 200 µg/ml hygromycine (Roche, Mannheim, Germany). Medium was supplemented with 10% heat-inactivated fetal bovine serum, 100 U/ml penicillin, 0.1 mg/ml streptomycin and 2 mM L-glutamine (obtained from Gibco by Life Technologies, Waltham, MA, USA, unless stated otherwise). GLS vectors in HEK293 cells were induced with 2 µg/ml doxycycline. Cells were frequently tested for mycoplasma.

GLS ACTIVITY ASSAY

GLS activity was assessed as the formation of glutamate from glutamine in HEK293 cells transfected with Ser482Cys-*GLS1* and compared to control cell lines containing wildtype *GLS1* or mCherry. Cells were incubated with 0 µM, 0.1 µM, 0.5 µM, 1 µM and 10 µM CB-839[30] (Selleckchem, Houston, USA) for 15 hours and collected in methanol (Sigma-Aldrich, Steinheim, Germany). To establish normalization of intracellular glutamate concentrations in a separate assay, HEK293 cells were cultured in glutamine-free medium for 15 hours (Sigma-Aldrich, Steinheim, Germany). Supernatants were evaporated with nitrogen and reconstituted in 1 ml of methanol. Glutamine and glutamate concentrations were determined by UPLC-MS/MS using stable isotope-labeled internal standards as described by Prinsen et al.[31] TargetLynx application manager was used for quantification of the amino acids. Two separate assays were performed in biological triplicates. The data was corrected for total protein. Protein quantification was performed in lysis buffer containing 1% Triton X-100 (Sigma-Aldrich, Steinheim, Germany), 50 mM Tris (Roche, Mannheim, Germany), 150 mM NaCl and protease inhibitor (Roche, Mannheim, Germany), by the use of Pierce BSA assay kit (Thermo Fisher Scientific, Waltham, MA, USA) in biological and analytical triplicates. Statistical analyses were performed by ANOVA, post-hoc Tukey's test using IBM SPSS statistics 21.

CONSERVATION ANALYSIS

Sequences homologous to human GLS from the non-redundant protein collection at NCBI were aligned in SeaView.[32] Obvious partial sequences as well as all pdb sequences were removed which resulted in about 12.000 sequences. The consensus were determined in JalView[33] and fraction of the modal residue in a column were used for generating a color gradients which was mapped onto the GLS structure as a measure of conservation (consensus score).

WESTERN BLOTTING

Proteins were separated by a 4-12% Bis-Tris gel (Thermo Fisher Scientific, Waltham, MA, USA) and transferred to a PVDF membrane (Merck, Darmstadt, Germany). For detection of GLS isoforms, a rabbit monoclonal antibody against KGA (Thermo Fisher Scientific, Waltham, MA, USA, 5H6L15s) in a 1:2500 dilution and a rabbit polyclonal antibody against GAC (Proteintech, Manchester, United Kingdom ,19958-1-AP) in a 1:500 dilution were used. For detection of GLS, a mouse monoclonal antibody (Biosciences, United Kingdom, 610518) in a 1:5000 dilution was used. For loading controls, antibodies against GAPDH (Merck, Darmstadt, Germany, MaB374) or actin (Sigma-Aldrich, Steinheim, Germany, A5060) were used. Blots were developed in ECL prime blocking reagent (GE Healthcare Life Sciences) by the ImageQuant Las400 or Odyssey Imaging System (Li-cor Biosciences) and quantified with ImageJ.

ROS MEASUREMENTS

ROS-levels were quantified by flow cytometry (BD FACSCalibur™) as previously described.[34] Wildtype *GLS1* or Ser482Cys-*GLS1* transfected HEK293 cells (induced and uninduced with doxycycline for 15 hours) were loaded for 10 minutes with 5 µM CM-H_2DCFDA (Thermo Fisher Scientific, Waltham, MA, USA). Part of these cells was challenged with 50 µM H_2O_2. Propidium iodide (PI) (Life Technologies, Waltham, MA, USA) was used to detect dead cells which were discarded from analyses (<5% in all samples) performed by BD CellQuest Pro Software Analysis™. CM-H_2DCF fluorescence was measured in the FL-1 channel on a logarithmic scale. Ten thousand cells per condition were measured and the median CM-H_2DCF fluorescence was used to quantify ROS levels.

ZEBRAFISH HUSBANDRY, DNA INJECTIONS AND PHENOTYPE ASSESSMENT

Tübingen Longfin (TL) zebrafish (*Danio rerio*) were maintained in standard laboratory conditions. Embryos were microinjected at the 1-cell stage with approximately 10 pg circular plasmid DNA of the *GLS1* (KGA) constructs in presence of 25ng/ml Tol2 transposase mRNA. For the constructs, the Ser482Cys-*GLS1* (KGA) cDNA sequence was obtained by site-specific mutagenesis (QuickChange II XL, Agilent, Santa Clara, CA, USA) of the wildtype *GLS1* sequence in pCR8/GW/TOPO (Life Technologies, Waltham, MA, USA). The middle entry vectors were then used in a multi-site Gateway reaction (ThermoFisher Scientific, Waltham, MA, USA) together with pE5'-ubi, p3E-IRES-EGFPpA and as destination vector pDestTol2pA3 to obtain expression constructs. Zebrafish were kept under either standard conditions or in water supplemented with 100 µM CB-839. At 5 days post fertilization (dpf), approximately ten 5 dpf zebrafish larvae per condition were anaesthetized in a solution of 16 mg/ml Tricaine (MS22) in E3 medium and mounted in 0.25% agarose (w/v) prepared in E3 to image the lens. Images were acquired using a Leica AF7000 fluorescence microscope equipped with a Leica DFC365FX camera, 20x NA 0.4 objective, Leica EL6000 External

light source and a Leica A4 filter cube (BP340-380/400/BP450-490) (Leica Microsystems, Wetzlar, Germany). The Leica LAS-AF software was used to capture the images. The acquired images were linearly edited with ImageJ 1.47v and Adobe Photoshop CS6 version 13. Amino acid measurements were performed in biological triplicates, each sample containing six 5 dpf zebrafish larvae, as previously described.[31] Experiments were carried out in accordance with the guidelines of the Animal Experimentation Committee of the Royal Netherlands Academy of Arts and Sciences (KNAW).

STUDY APPROVAL

The proband's parents provided written informed consent for all aspects of the study. Zebrafish experiments were carried out in accordance with the guidelines of the Animal Experimentation Committee of the Royal Netherlands Academy of Arts and Sciences (KNAW).

SUPPLEMENTARY RESULTS

BIOCHEMICAL AND INFECTIOUS WORKUP

Serological analyses were negative for known causes of intrauterine infections (TORCHES). Electrolytes, glucose, C-reactive protein, erythrocyte sedimentation rate, alkaline phosphatase, gamma glutamyltransferase, ASAT, ALAT and arterial blood gas analyses were normal. Hematological analyses were normal. In fibroblasts, respiratory chain complex activities were normal at age 3 years 4 months.

METABOLIC DIAGNOSTIC WORKUP

Metabolic analyses in plasma revealed mild elevations of ammonia (44-92 µmol/L, ref. <35 µmol/L) and lactate (2.6-3.5 mmol/L, ref. <2.2 mmol/L), which were more pronounced during an oral glucose tolerance test, as well as low to low-normal glutamine levels (301-377 µmol/L, ref. 333-857 µmol/L) (table S1). In plasma, acylcarnitine profile, amino acids, transferrin iso-electric focusing, very long chain fatty acids, phytanic acid, pristanic acid and cholesterol intermediates were all normal. These measurements were regularly performed from age 4 months until present.

In urine, organic acids, creatine, guanidinoacetic acid, oligosaccharides, glycosaminoglycans, bile salts and alcohols, sialic acid, purines and pyrimidines were normal. Polyol levels were initially increased, however without a consistent pattern and normalizing over time. Amino acids -except for glutamine and glutamate concentrations (Supplementary Table 1)- were normal.

TABLE S1. Glutamine and glutamate concentrations in plasma, urine and cerebrospinal fluid (CSF) of the patient expressing the Ser482Cys-GLS1 variant.

	7 months	1 year	1.5 years	3 years	10 years	11 years
			GLUTAMINE			
Urine (µmol/mmol creatinine)			33 (62-165)↓		9 (20-112)↓	9 (20-112) ↓ 35 (20-112) 30 (20-112)
Plasma (µmol/l)	301 (402-776)↓		358 (457-857)↓	377 (457-857)↓	339 (333-809)	
CSF (µmol/l)		385 (333-358)				
			GLUTAMATE			
Urine (µmol/mmol creatinine)					32 (0-9)↑	6 (0-9) 10 (0-9) 8 (0-9)
Plasma (µmol/l)	76 (17-69)↑		44 (17-69)	34 (17-69)	37 (17-69)	
CSF (µmol/l)		3 (<8.3)				

The arrows indicate values below (↓) and above (↑) the age-related reference values.[22, 49]

Cerebrospinal fluid analysis at age 2 years revealed normal levels of amino acids, oligosaccharides, polyols, 5-methyltetrahydrofolate, homovanillic acid, 5-hydroxy-indoleacetic acid, 3-O-methyldopa, free and total GABA and amino acids including glutamine and glutamate.

MRS revealed -additional to the deviant glutamine and glutamate concentrations- reduction of N-acetylaspartate (NAA) and relative elevation of alanine and lactate (Figure S1c).

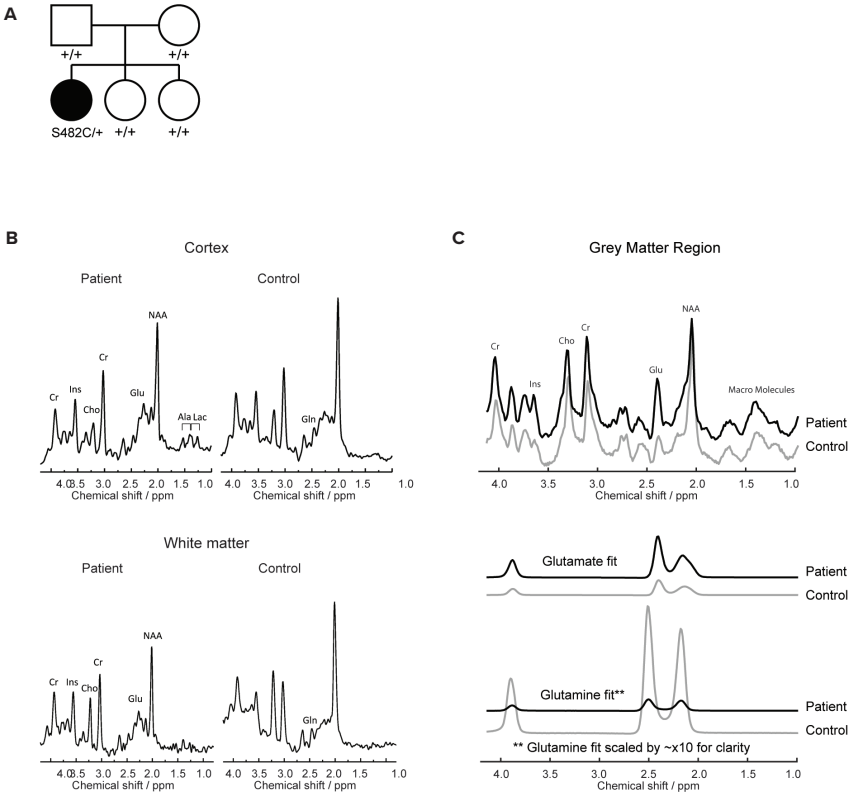

FIGURE S1. Diagnostics in the patient with a *de novo* Ser482Cys-*GLS1* variant. (**A**) The pedigree of the family of the proband (Ser482Cys). Squares and circles indicate males and females respectively. + wildtype allele. Both parents and the two sisters of the proband are clinically healthy. (**B**) MRSI (1.5T, PRESS, TR/TE 3000/30 ms. Spectra are from an individual voxel of 1.5 cm^3) of parietal cortex (upper panel) and parietal white matter (lower panel) of the patient (age 3 years, left) and a control subject (age 7 years, right). Glutamate is elevated and glutamine nearly absent in both cortex and white matter of the patient. NAA was slightly reduced in both tissues. In cortical spectra doublets of alanine (centered at 1.47 ppm) and lactate (centered at 1.33 ppm) are clearly visible in the patient. Ins=myo-inositol Cho=choline; Cr=creatine; Gln=glutamine; Glu=glutamate; NAA=N-acetylaspartate; Ala=alanine; Lac=lactate. (**C**) MRSI (7T, pulse-acquire, 44x44 matrix, 0.5x0.5x1 cm^3, TR/TE 300/2.5 ms) of the grey matter of the patient (age 14 years, black) and a control subject (age 27 years, grey) acquired in the transverse plane. Spectra -located in a volume of approximately 9.5 cm^3 located within the longitudinal fissure- were averaged. Elevated glutamate levels are evident in patient spectrum at 2.3 ppm (upper panel), which is confirmed via fitted concentration values derived with LCModel (middle panel). In accordance with S1-c, glutamine levels were nearly absent in patient versus control according to the LCModel glutamine fit (lower panel).

GENETIC WORKUP

Karyotyping showed normal female 46XX and CGH array showed no abnormalities. FISH del7q11 was normal and no defective variants were found in the RAB3GAP-1 gene and the 15q11-q13 genetic region, rendering Williams syndrome, Warburg microsyndrome and Angelman syndrome unlikely. WES detected 10050 SNPs. A *de novo* model was considered the most likely because of unrelated healthy parents. Biological parenthood was confirmed. Using a *de novo* inheritance model, 8 putative *de novo* mutations were tested by Sanger sequencing, of which one could be validated. This mutation at NC_000002.11:g.191795182C>G [hg19] results in the cDNA change NM_014905.4:c.1445C>G in the *GLS* gene. The consequence is a missense change of a serine to a cysteine at position 482 (NP_055720.3:p.(Ser482Cys). Non-consanguinity of the parents was indicated by family history and SNP-array. Analysis of WES data using recessive filters yielded no rare homozygous damaging variants. The analysis for compound heterozygosity (including correctness of segregation in parents) yielded two genes hit by rare and (possibly) damaging variants, namely DNAH7 (rs370625854 and rs144112024, both missense variants predicted as possibly damaging by Polyphen) and MMP20 (rs61753770 and rs140213840, probably damaging missense (Polyphen) and essential splice, respectively). DNAH7, Dynein axonemal Heavy Chain 7, has not been linked to human disease. MMP20 is associated with autosomal recessive enamel defects. For both genes one of the two variants has been observed homozygously in apparently health people (Exac database). Together, we considered these variants as unlikely to contribute to the phenotypes of the patient.

SUPPLEMENTARY DISCUSSION

Our study shows that the Ser482Cys-*GLS1* variant leads to increased catalytic activity of the GLS enzyme. This can be further explained by available structural information of the GLS enzyme.[12] The Ser482Cys substitution could impinge catalysis in several ways. As cysteine is sterically more demanding than serine, the protein has to adapt to the mutation by small rearrangements. These rearrangements might affect the 1) exact position of Gly509 –which contributes to the coordination of a water molecule required for re-protonation of Tyr466; 2) the exact position of Val484 –which is part of the oxyanion hole; 3) the relative orientation of Tyr466 towards glutamine (Figure S2B, S2C). Each of these effects might improve catalysis, but more evident for the substitution to improve the catalytic activity of GLS is the direct influence of the Ser482Cys substitution on the electrostatic environment of C^{ε} of Tyr466 and thereby the acidity of Tyr466. The side chain of Ser482 is expected to be oriented towards the C^{ε} of Tyr466 with a negatively charged free electron pair of

OH-group (Figure S2C). Ser482 thus reduces the acidity of Tyr466 and thereby reduces the catalytic activity. This effect is likely to be less pronounced if Ser482 is replaced by a cysteine, thereby explaining enhanced activity as a consequence of the Ser482Cys variant.

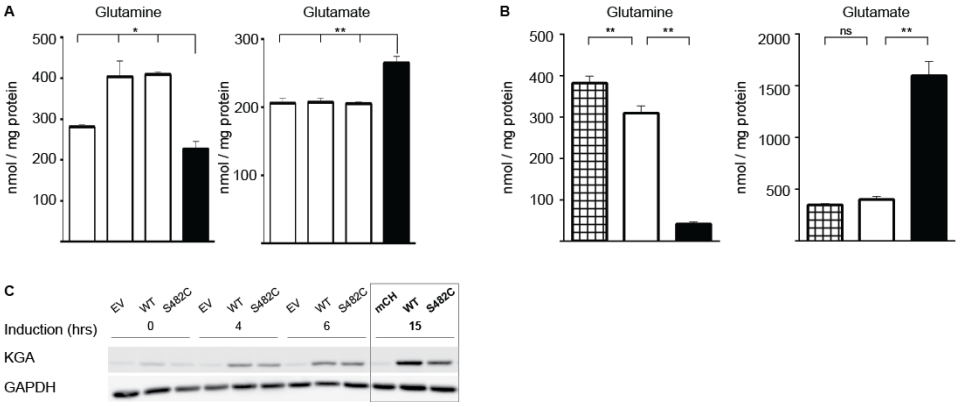

Figure S2. GLS activity and expression (**A**) Intracellular glutamine and glutamate levels of 3 control fibroblasts cell lines (white) and fibroblasts of the proband expressing Ser482Cys-GLS (black) corrected for total protein. Results represent the mean with standard deviations of biological triplicates. (**B**) Intracellular glutamine and glutamate levels of HEK293 cells after 15 hours of induction with doxycycline, harboring an empty vector (checked), wildtype-*GLS1* (white) or Ser482Cys-*GLS1* (black) corrected for total protein. Results represent the mean with standard deviations of biological triplicates. (**C**) Western blot of the GLS-isoform KGA in HEK293 cells expressing an empty vector (EV), wildtype-*GLS1* KGA isoform (WT) or Ser482Cys-*GLS1* KGA isoform induced for 0, 4, 6 and 15 hours with doxycycline. Increased expression of the 66 kD product, corresponding to the KGA isoform cleaved after mitochondrial import,[50] was observed from 4 hours post induction till 15 hours post induction. The latter condition (framed) was used for all amino-acid and protein expression experiments. GAPDH served as a loading control. Images were linearly edited.

A

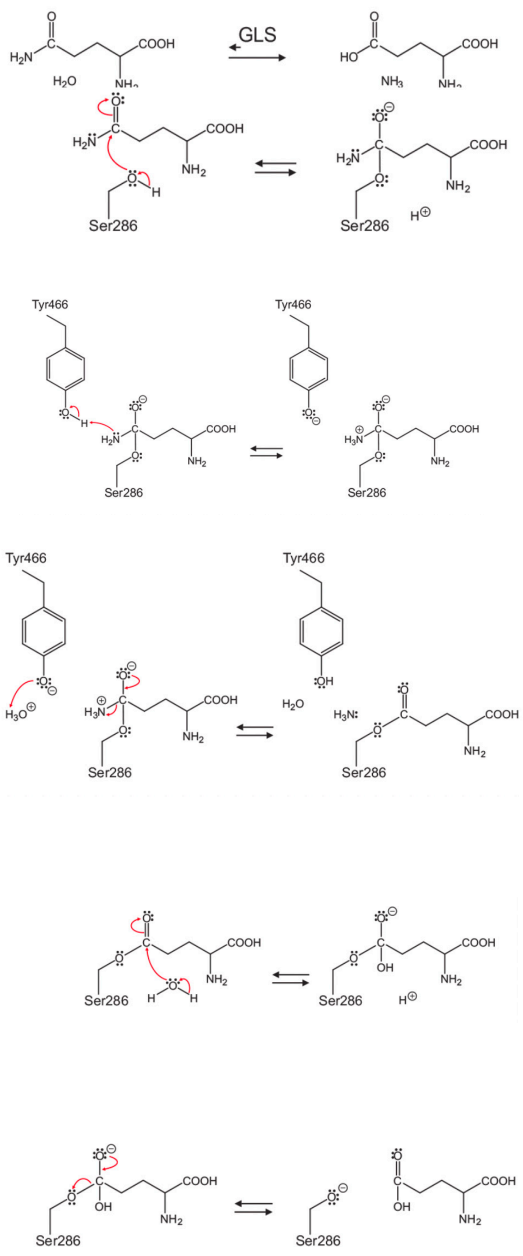

A.1 The deamination of glutamine into glutamate by GLS is initiated by the nucleophilic attack of Ser286 on Cδ of glutamine (left). In consequence, glutamine becomes covalently attached to GLS via Ser286 (right). The oxygen in glutamine now carries a negative charge, as it became single instead of double bonded. To stabilize this intermediate state, GLS provides a binding environment for the negative charged oxygen, **the oxyanion hole**.

A.2 The deamination reaction is accelerated by Tyr466 protonating the amine group of glutamine (left). As a consequence, Tyr466 becomes negatively charged (right). The efficiency of this step (the propensity to donate the proton) depends on the **acidity** of Cε of Tyr466 which is influenced by the electrostatic character of its environment.

A.3 The amine-group is released from glutamine as the Cδ–NH3 bond of glutamine breaks as a consequence of the electron rearrangement (red arrows, left). The oxygen has lost its negative charge and is double bonded to Cδ again. Tyr466 becomes **re-protonated** (the proton is provided by the solvent i.e. an H¬2O or H-3O+ ¬molecule) and is thereby "compensated for its loss" and ready for the next round of catalysis (right).

A.4 The de-aminated "glutamine" is still attached to GLS (left). A nucleophilic attack by a water molecule on the Cδ results in the attachment of a new OH-group (the former water) to Cδ. The originally double bounded oxygen becomes single bonded again with a negative charge (right). As before, GLS provides a binding environment for the negative charged oxygen, **the oxyanion hole**.

A.5 The bond between the Cδ of glutamate and Ser286 breaks as the electrons rearrange immediately (left). The oxygen has lost its negative charge and is double bonded to Cδ again. Hereby, glutamate is obtained as the product of the reaction which is no longer covalently attached to GLS (right).

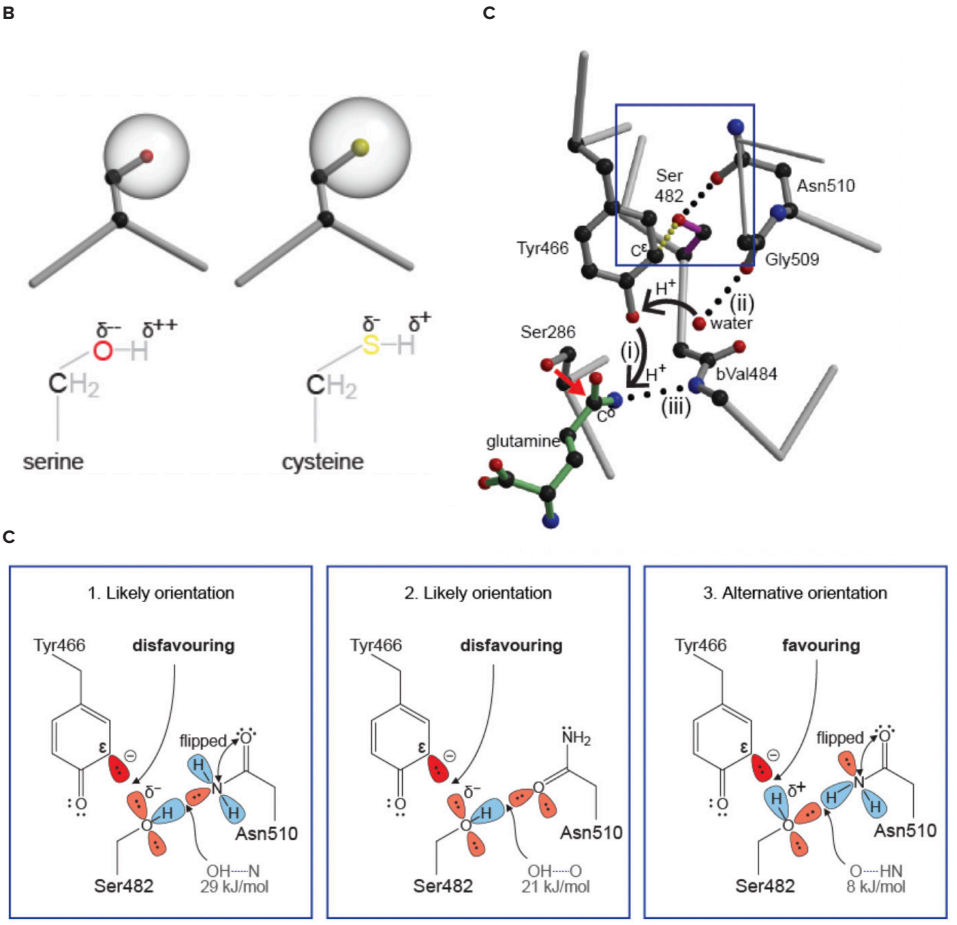

FIGURE S3. The catalytic mechanism of GLS and the role of Ser482. (**A**) The catalytic mechanism of GLS-mediated deamination of glutamine into glutamate.[12] Red arrows indicate electron transfer. (**B**) The different electrostatic and steric properties of the amino acids serine and cysteine. Serine contains a hydroxyl (OH) –group and cysteine contains a thiol (SH)-group. Cysteine is sterically more demanding than serine. Since the atom radius of sulphur (yellow) is bigger than that of oxygen (red), the S-H bond (0.181 nm) is longer compared to the O-H bond (0.143 nm). The S-H bond of cysteine is less polar than the O-H bond, meaning that in the OH-group the oxygen accumulates a stronger negative charge than the sulphur of the thiol-group. Likewise, the positive charge of the hydrogen in the OH-group is stronger and therefore hydrogen bonds formed by serine are stronger than those formed by cysteine. (**C**) The environment of Ser482 (magenta). Residues of the catalytic site of GLS are shown in complex with glutamine (green). Hydrogen bonds are shown by dotted black lines. Black arrows indicate the proton transfer. The OH-group of Ser482 forms a hydrogen bond with Asn510. The Ser482Cys substitution might impinge the catalytic activity in several ways: (i) **Acidity of Tyr466**: A slight repositioning of Tyr466 might result in a changed geometric orientation between

the proton donor and acceptor, impinging the efficiency of proton transfer and thereby the acidity and propensity of Tyr466 to protonate glutamine. In the de-protonated state of Tyr466, the negative charge is partially localized at C^{ε} (the Figure shows the resonance structure with the free electron pair at C^{ε}). The acidity of Tyr466 is determined by the electrostatic property of the sidechain of the amino acid at position 482. In the case of a serine, it is likely that the OH-group of Ser482 is orientated with the negatively charged oxygen towards C^{ε} of Tyr466, reducing the acidity of Tyr466 (framed Figure 1 and 2). The OH-group of Ser482 could also be orientated with the partially positively charged hydrogen (blue) towards C^{ε} of Tyr466, as the amide-group of asparagine residues can flip "freely" although the OH-group of Ser482 is engaged in a hydrogen bond with Asn510 which determines the orientation of the OH-group (framed Figure 3). However, the binding energies of the different possible hydrogen bonds between Ser482 and Asn510 suggest that in the majority of GLS molecules the OH-group of Ser482 is orientated with the negatively charged oxygen towards C^{ε} of Tyr466. In case of a Ser482Cys substitution, the SH-group is likely to create a les negative environment of Tyr466. (ii) **Re-protonation:** Asn510 and in consequence Gly509 might be shifted slightly, which would influence the ability of Gly509 to position the water molecule that re-protonates Tyr466. (iii) **Oxyanion hole**: A slight backbone shift might extend to Val484 and thereby alters the interaction of the negative charged oxygen with the amide of Val484. The Figure is based on pdb entry 3vp0 and was generated with molscript[36] and raster3D[37].

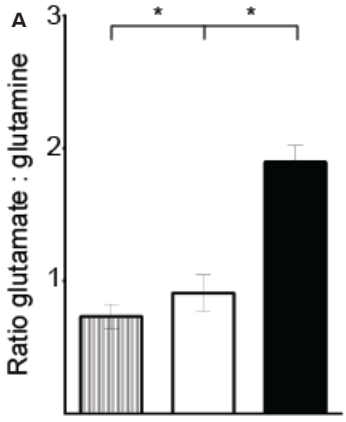

B

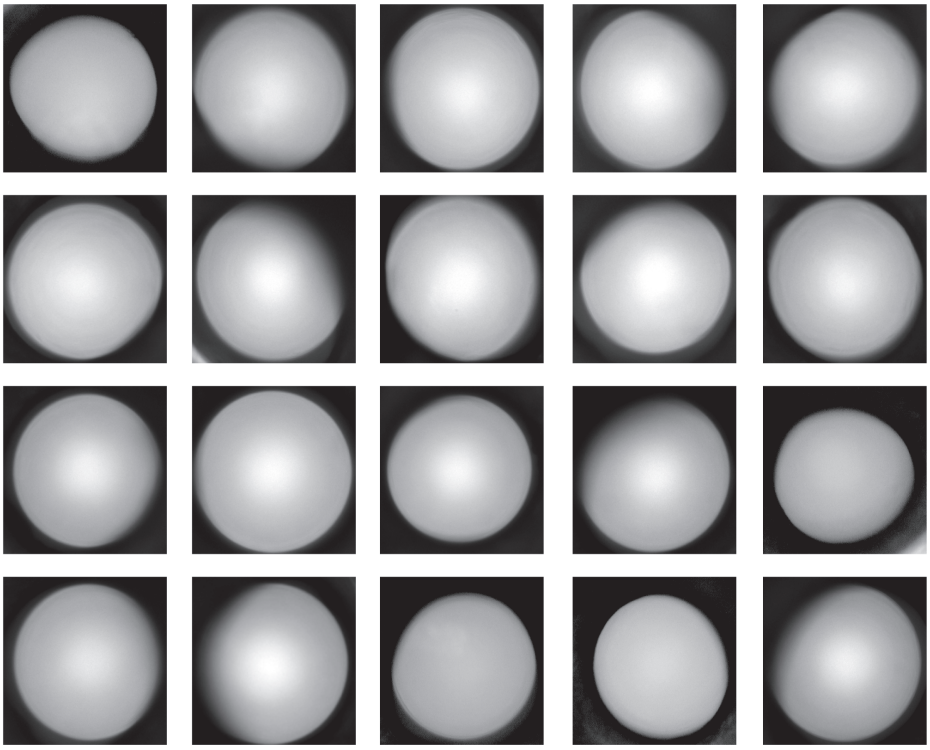

C

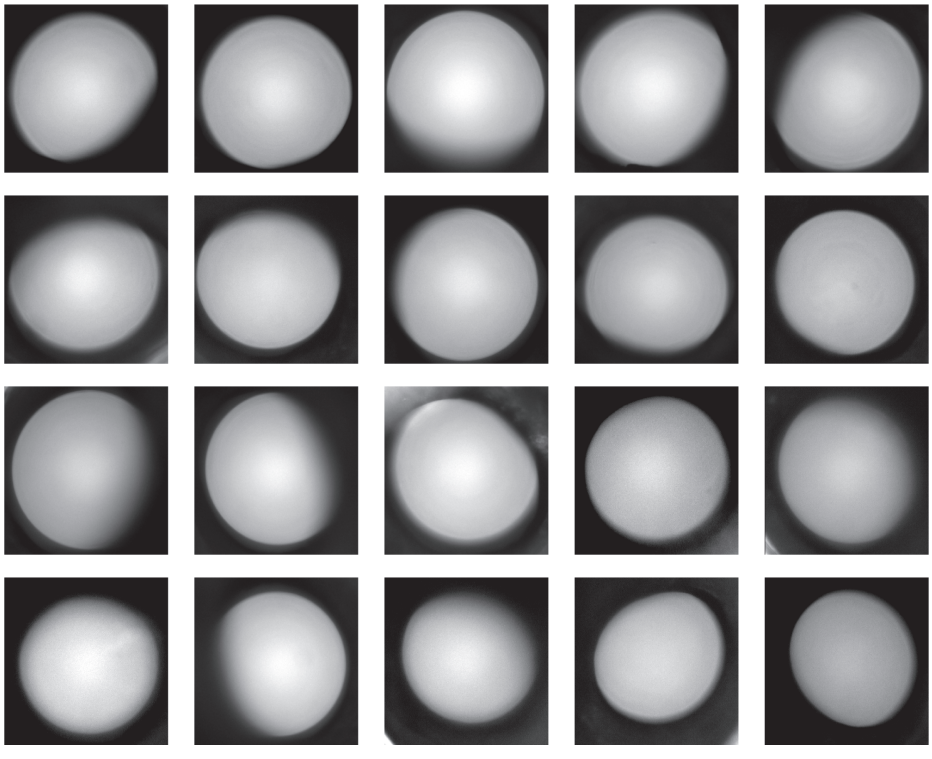

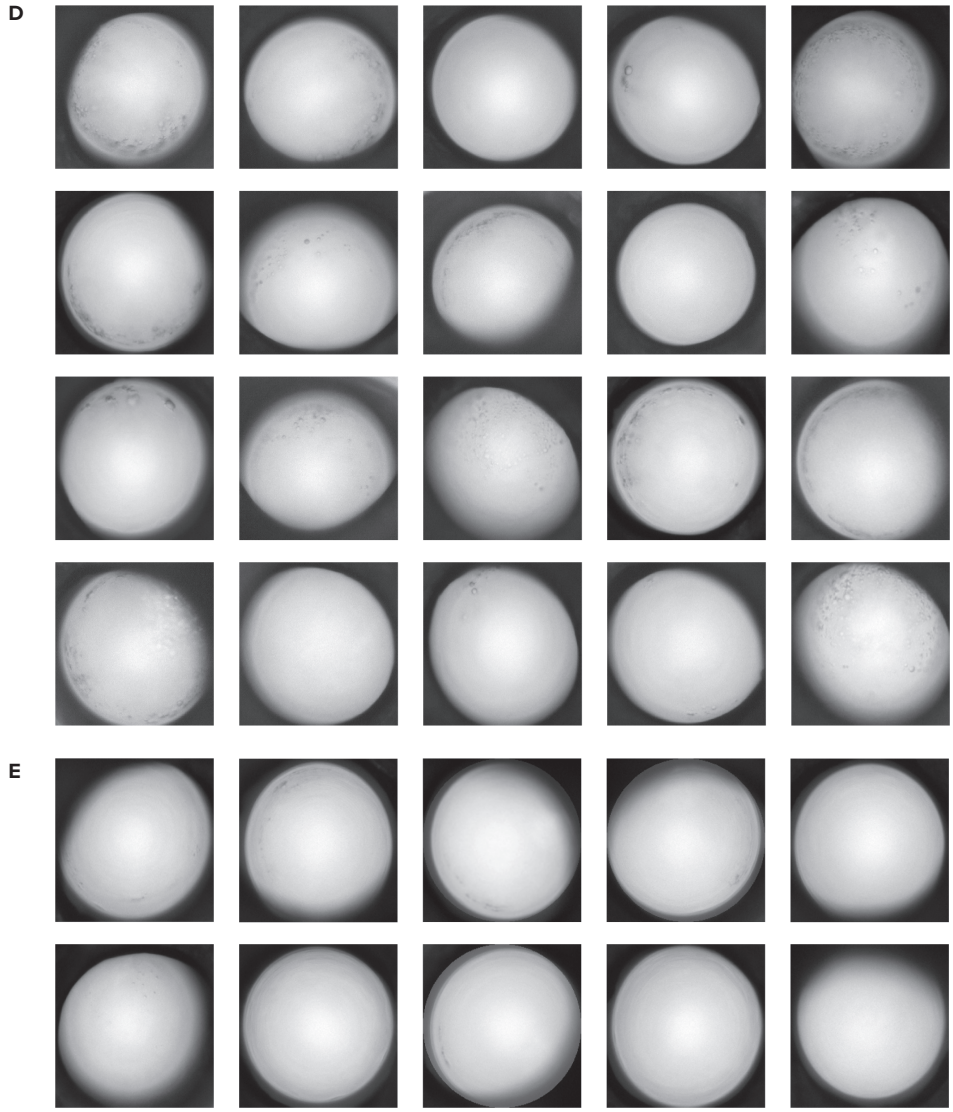

FIGURE S4. Ser482Cys-*GLS1* leads to lens opacity in zebrafish. (**A**) The glutamate:glutamine ratios in uninjected zebrafish (striped) and zebrafish injected with expression constructs containing wildtype *GLS1* cDNA (white) or Ser482Cys-*GLS1* cDNA (black). Results represent mean +/- SD of biological triplicates of 6 embryos at 5 dpf per sample. *p<0.05 (ANOVA, Tukey test). (**B**) Representative microscopic images of the lens of uninjected zebrafish embryos (n=30); (**c**) of the lens of zebrafish embryos injected with expression constructs containing wildtype *GLS1* cDNA (n=28); (**D**) of the lens of zebrafish embryos injected with expression constructs containing Ser482Cys-*GLS1* cDNA (n=47); (**E**) of the lens of zebrafish embryos injected with vectors containing Ser482Cys-*GLS1* cDNA, treated with 10 μM CB-839 from 6 hpf (n=10). Images were linearly edited.

REFERENCES

1. Curtis, D.R., Phillis, J.W. and Watkins, J.C. (1960) The chemical excitation of spinal neurones by certain acidic amino acids. *J. Physiol.*, **150**, 656–682.
2. Lu, S.C. (2009) Regulation of glutathione synthesis. *Mol. Aspects Med.*, **30**, 42–59.
3. Nedergaard, M., Takano, T. and Hansen, A.J. (2002) Beyond the role of glutamate as a neurotransmitter. *Nat. Rev. Neurosci.*, **3**, 748–755.
4. Bak, L.K., Schousboe, A. and Waagepetersen, H.S. (2006) The glutamate/GABA-glutamine cycle: aspects of transport, neurotransmitter homeostasis and ammonia transfer. *J. Neurochem.*, **98**, 641–653.
5. Curthoys, N.P. and Watford, M. (1995) Regulation of glutaminase activity and glutamine metabolism. *Annu. Rev. Nutr.*, **15**, 133–159.
6. Aledo, J.C., Gomez-Fabre, P.M., Olalla, L. and Marquez, J. (2000) Identification of two human glutaminase loci and tissue-specific expression of the two related genes. *Mamm. Genome*, **11**, 1107–1110.
7. Spodenkiewicz, M., Diez-Fernandez, C., Rufenacht, V., Gemperle-Britschgi, C. and Haberle, J. (2016) Minireview on glutamine synthetase deficiency, an ultra-rare inborn error of amino acid biosynthesis. *Biology (Basel)*, **5**, 40–57.
8. Rumping L, Buttner B, Maier O, et al. Identification of a Loss-of-Function Mutation in the Context of Glutaminase Deficiency and Neonatal Epileptic Encephalopathy. *JAMA Neurol.* 2018.
9. Lynch, D.S., Chelban, V., Vandrovcova, J., Pittman, A., Wood, N.W. and Houlden, H. (2018) GLS loss of function causes autosomal recessive spastic ataxia and optic atrophy. *Ann. Clin. Transl. Neurol.*, **5**, 216–221.
10. Kapoor, R.R., Flanagan, S.E., Fulton, P., Chakrapani, A., Chadefaux, B., Ben-Omran, T., Banerjee, I., Shield, J.P., Ellard, S. and Hussain, K. (2009) Hyperinsulinism-hyperammonaemia syndrome: novel mutations in the GLUD1 gene and genotype-phenotype correlations. *Eur. J. Endocrinol.*, **161**, 731–735.
11. Yang, H., Ye, D., Guan, K.L. and Xiong, Y. (2012) IDH1 and IDH2 mutations in tumorigenesis: mechanistic insights and clinical perspectives. *Clin. Cancer Res.*, **18**, 5562–5571.
12. Brown, G., Singer, A., Proudfoot, M., Skarina, T., Kim, Y., Chang, C., Dementieva, I., Kuznetsova, E., Gonzalez, C.F., Joachimiak, A. *et al.* (2008) Functional and structural characterization of four glutaminases from Escherichia coli and Bacillus subtilis. *Biochemistry*, **47**, 5724–5735.
13. Genome of the Netherlands Consortium (2014) Whole genome sequence variation, population structure and demographic history of the Dutch population. *Nat. Genet.*, **46**, 818–825.
14. Lek, M., Karczewski, K.J., Minikel, E.V., Samocha, K.E., Banks, E., Fennell, T., O'Donnell-Luria, A.H., Ware, J.S., Hill, A.J., Cummings, B.B., *et al.* (2016) Analysis of proteincoding genetic variation in 60,706 humans http://gnomad. broadinstitute.org (last access 8th of March 2018). *Nature*, **536**, 285–291.
15. Landrum, M.J., Lee, J.M., Benson, M., Brown, G.R., Chao, C., Chitipiralla, S., Gu, B., Hart, J., Hoffman, D., Jang, W. *et al.* (2018) ClinVar: improving access to variant interpretations and supporting evidence. *Nucleic Acids Res.*, **46**, D1062–D1067.
16. Lek, M., Karczewski, K.J., Minikel, E.V., Samocha, K.E., Banks, E., Fennell, T., O'Donnell-Luria, A.H., Ware, J.S., Hill, A.J., Cummings, B.B. *et al.* (2016) Analysis of protein-coding genetic variation in 60,706 humans. *Nature*,

536, 285–291.

17. Spector, A. (1995) Oxidative stress-induced cataract: mechanism of action. *FASEB J*, **9**, 1173–1182.
18. Dong, X.X., Wang, Y. and Qin, Z.H. (2009) Molecular mechanisms of excitotoxicity and their relevance to pathogenesis of neurodegenerative diseases. *Acta Pharmacol. Sin.*, **30**, 379–387.
19. Grimaldi, M., Karaca, M., Latini, L., Brioudes, E., Schalch, T. and Maechler, P. (2017) Identification of the molecular dysfunction caused by glutamate dehydrogenase S445L mutation responsible for hyperinsulinism/hyperammonemia. *Hum. Mol. Genet.*, **26**, 3453–3465.
20. Kranendijk, M., Salomons, G.S., Gibson, K.M., Van Schaftingen, E., Jakobs, C. and Struys, E.A. (2011) A lymphoblast model for IDH2 gain-of-function activity in d-2-hydroxyglutaric aciduria type II: novel avenues for biochemical and therapeutic studies. *Biochim. Biophys. Acta*, **1812**, 1380–1384.
21. van de, B.L., Emir, U.E., Boer, V.O., Asten van, J.J.A., Maas, M.C., Wijnen, J.P. and Kan, H.E. (2015) Multi-center reproducibility of neurochemical profiles in the human brain at 7 Tesla. *NMR Biomed*, **28**, 306–316.
22. Blau, N., Duran, M. and Gibson, K.M. (2008) *Laboratory Guide to the Methods in Biochemical Genetics*. Springer, Heidelberg Berlin.
23. Hu, R.G., Lim, J.C., Kalloniatis, M. and Donaldson, P.J. (2011) Cellular localization of glutamate and glutamine metabolism and transport pathways in the rat ciliary epithelium. *Invest. Ophthalmol. Vis. Sci.*, **52**, 3345–3353.
24. Kawamura, M. and Azuma, N. (1992) Morphological studies on cataract and small lens formation in neonatal rats treated with monosodium-L-glutamate. *Ophthalmic Res.*, **24**, 289–297.
25. Laszczyk, W.A. (1975) Development of cataract as the effect of glutamic acid administration to chick embryo. *Ophthalmic Res.*, **7**, 432–439.
26. Farooq, M., Kaswala, R.H., Kleiman, N.J., Kasinathan, C. and Frederikse, P.H. (2012) GluA2 AMPA glutamate receptor subunit exhibits codon 607 Q/R RNA editing in the lens. *Biochem. Biophys. Res. Commun.*, **418**, 273–277.
27. Brodie, M.J., Besag, F., Ettinger, A.B., Mula, M., Gobbi, G., Comai, S., Aldenkamp, A.P. and Steinhoff, B.J. (2016) Epilepsy, antiepileptic drugs, and aggression: an evidence-based review. *Pharmacol. Rev.*, **68**, 563–602.
28. Haberle, J., Gorg, B., Rutsch, F., Schmidt, E., Toutain, A., Benoist, J.F., Gelot, A., Suc, A.L., Hohne, W., Schliess, F. *et al.* (2005) Congenital glutamine deficiency with glutamine synthetase mutations. *N. Engl. J. Med.*, **353**, 1926–1933.
29. Barker-Haliski, M. and White, H.S. (2015) Glutamatergic mechanisms associated with seizures and epilepsy. *Cold Spring Harb. Perspect. Med.*, **5**, a022863.
30. Gross, M.I., Demo, S.D., Dennison, J.B., Chen, L., Chernov-Rogan, T., Goyal, B., Janes, J.R., Laidig, G.J., Lewis, E.R., Li, J. *et al.* (2014) Antitumor activity of the glutaminase inhibitor CB-839 in triple-negative breast cancer. *Mol. Cancer Ther.*, **13**, 890–901.
31. Prinsen, H.C.M.T., Schiebergen-Bronkhorst, B.G.M., Roeleveld, M.W., Jans, J.J.M., de Sain-van der Velden, M.G.M., Visser, G., van Hasselt, P.M. and Verhoeven-Duif, N.M. (2016) Rapid quantification of underivatized amino acids in plasma by hydrophilic interaction liquid chromatography (HILIC) coupled with tandem mass-

spectrometry. *J Inherit. Metab. Dis.*, **39**, 651–660.

32. Gouy, M., Guindon, S. and Gascuel, O. (2010) SeaView version 4: a multiplatform graphical user interface for sequence alignment and phylogenetic tree building. *Mol. Biol. Evol.*, **27**, 221–224.
33. Waterhouse, A.M., Procter, J.B., Martin, D.M., Clamp, M. and Barton, G.J. (2009) Jalview Version 2–a multiple sequence alignment editor and analysis workbench. *Bioinformatics*, **25**, 1189–1191.
34. Jelluma, N., Yang, X., Stokoe, D., Evan, G.I., Dansen, T.B. and Haas-Kogan, D.A. (2006) Glucose withdrawal induces oxidative stress followed by apoptosis in glioblastoma cells but not in normal human astrocytes. *Mol. Cancer Res.*, **4**, 319–330.
35. Pouwels, P.J., Brockmann, K., Kruse, B., Wilken, B., Wick, M., Hanefeld, F. and Frahm, J. (1999) Regional age dependence of human brain metabolites from infancy to adulthood as detected by quantitative localized proton MRS. *Pediatr. Res.*, **46**, 474–485.
36. Kraulis, P.J. (1991) Molscript a program to produce both detailed and schematic plots of protein structures. *J. Appl. Cryst.*, **24**, 946–950.
37. Merritt, E.A. and Murphy, M.E. (1994) Raster3D Version 2.0. A program for photorealistic molecular graphics. *Acta. Crystallogr. D Biol. Crystallogr.*, **50**, 869–873.
38. van der Voorn JP, Pouwels PJ, Hart AA, et al. Childhood white matter disorders: quantitative MR imaging and spectroscopy. Radiology. 2006;241(2):510-517.
39. Steenweg ME, Pouwels PJ, Wolf NI, van Wieringen WN, Barkhof F, van der Knaap MS. Leucoencephalopathy with brainstem and spinal cord involvement and high lactate: quantitative magnetic resonance imaging. Brain. 2011;134(Pt 11):3333-3341.
40. Provencher SW. Estimation of metabolite concentrations from localized in vivo proton NMR spectra. Magn Reson Med. 1993;30(6):672-679.
41. Boer VO, van de Lindt T, Luijten PR, Klomp DW. Lipid suppression for brain MRI and MRSI by means of a dedicated crusher coil. Magn Reson Med. 2015;73(6):2062-2068.
42. Ma J, Wismans C, Cao Z, Klomp DWJ, Wijnen JP, Grissom WA. Tailored spiral in-out spectral-spatial water suppression pulses for magnetic resonance spectroscopic imaging. Magn Reson Med. 2018;79(1):31-40.
43. Kirchner T, Fillmer A, Henning A. Mechanisms of SNR and line shape improvement by B0 correction in overdiscrete MRSI reconstruction. Magn Reson Med. 2017;77(1):44-56.
44. Kirchner T, Fillmer A, Tsao J, Pruessmann KP, Henning A. Reduction of voxel bleeding in highly accelerated parallel (1) H MRSI by direct control of the spatial response function. Magn Reson Med. 2015;73(2):469-480.
45. Klose U. In vivo proton spectroscopy in presence of eddy currents. Magn Reson Med. 1990;14(1):26-30.
46. Cabanes E, Confort-Gouny S, Le Fur Y, Simond G, Cozzone PJ. Optimization of residual water signal removal by HLSVD on simulated short echo time proton MR spectra of the human brain. J Magn Reson. 2001;150(2):116-125.
47. Kay SM. Modern Spectral Estimation: theory and Application. Englewood Cliffs, NJ: Precentic-Hall; 1998.
48. Harakalova M, van Harssel JJ, Terhal PA, et al. Dominant missense mutations in ABCC9 cause Cantu syndrome. Nat Genet. 2012;44(7):793-796.

49. Hagenfeldt L, Larsson A, Andersson R. The gamma-glutamyl cycle and amino acid transport. Studies of free amino acids, gamma-glutamyl-cysteine and glutathione in erythrocytes from patients with 5-oxoprolinuria (glutathione synthetase deficiency). N Engl J Med. 1978;299(11):587-590.
50. Srinivasan M, Kalousek F, Curthoys NP. In-Vitro Characterization of the Mitochondrial Processing and the Potential Function of the 68-Kda Subunit of Renal Glutaminase. Journal of Biological Chemistry. 1995;270(3):1185-1190.

Chapter 4

Metabolic fingerprinting reveals extensive consequences of GLS hyperactivity

Submitted

Lynne Rumping, Mia L Pras-Raves, Johan Gerrits, Yuen Fung Tang, Marcel A Willemsen, Roderick HJ Houwen, Gijs van Haaften, Peter M van Hasselt, Nanda M Verhoeven-Duif, Judith JM Jans

ABSTRACT

High glutaminase (GLS) activity is an important pathophysiological phenomenon in tumorigenesis and metabolic disease. Insight into the metabolic consequences of high GLS activity contributes to the understanding of the pathophysiology of both oncogenic pathways and inborn errors of glutamate metabolism. Glutaminase (GLS; l-glutaminase; EC3.5.1.2) catalyzes the conversion of glutamine into glutamate, thereby interconnecting many metabolic pathways. We developed a cell model that enables tuning of GLS activity by combining the expression of a hypermorphic *GLS* variant with incremental GLS inhibition. The metabolic consequences of increasing GLS activity were studied by metabolic profiling using Direct-Infusion High-Resolution Mass-Spectrometry (DI-HRMS). Of 12437 detected features [m/z], 109 features corresponding to endogenously relevant metabolites were significantly affected by high GLS activity. As expected, these included strongly decreased glutamine and increased glutamate levels. Additionally, increased levels of tricarboxylic acid (TCA) intermediates with a truncation of the TCA cycle at the level of citrate were detected as well as increased metabolites of transamination reactions, proline and ornithine synthesis and GABA metabolism. Levels of asparagine and nucleotide metabolites showed the same dependence on GLS activity as glutamine. Of the nucleotides, especially metabolites of the pyrimidine thymine metabolism were negatively impacted by high GLS activity, which is remarkable since their synthesis depend both on aspartate (product of glutamate) and glutamine levels. Metabolites of the glutathione synthesizing γ-glutamyl-cycle were either decreased or unaffected, rather than increased, pointing to co-dependency on additional enzyme induction for glutathione synthesis. By providing a metabolic fingerprint of increasing GLS activity, this study shows the large impact of high glutaminase activity on the cellular metabolome.

INTRODUCTION

Inborn errors of metabolism and oncogenic pathways are often the consequence of disturbed enzyme activity secondary to genetic alterations. Insight into the effect of the genetic alteration on enzyme activity can be generated by determination of substrate and product levels and closely related metabolites. The study to the extensive downstream metabolic consequences of disturbed enzyme activity might create additional insight into the pathophysiological mechanism of disease. Direct-Infusion High-Resolution Mass Spectrometry (DI-HRMS) provides a metabolic fingerprint, enabling the investigation of extensive metabolic consequences of pathogenic stimuli and genetic alterations.

Altered glutaminase (GLS; l-glutaminase, EC 3.5.1.2) activity is an important patho-physiological phenomenon in tumorigenesis and metabolic disease. GLS catalyzes the conversion of glutamine into glutamate, two amino acids at the center of a multitude of metabolic pathways[1]. Glutamate can be converted into the TCA-cycle intermediate α-ketoglutarate by transamination, with concomitant production of amino acids which are used for protein and nucleotide synthesis[2]. In parallel, glutamate is the precursor of the neurotransmitter GABA, glutamic-γ-semialdehyde -for proline and ornithine synthesis- and of the anti-oxidant glutathione. Glutamine on the other hand is important for asparagine synthesis as well as for nucleotide synthesis[2-4]. GLS is strictly regulated under physiological conditions, suggesting that derangements are disadvantageous[5]. Given the divergent roles of both glutamine and glutamate, the consequences of changes in GLS activity on the involved processes cannot easily be predicted. It is therefore difficult to assess which metabolic consequences are responsible for a phenotypic outcome, and therefore to determine a potential therapeutic target. The detrimental consequences of increased GLS activity are illustrated by the recently described inborn error of metabolism in which GLS hyperactivity due to a hypermorphic germline variant leads to glutamate excess in a child with infantile cataract and developmental delay[6]. These phenotypic features are assumed to be the direct consequence of glutamate excess and –more downstream- of oxidative stress. However, other downstream consequences might also contribute to the pathophysiology. In numerous tumor types GLS overexpression appears to favor tumorigenesis or tumor progression. Increased presence of glutamate fuels the TCA cycle and provides the cell with building blocks, such as amino acids and nucleotides as well as the antioxidant glutathione [3,4,7]. Based on these observations, GLS inhibition is currently tested in clinical oncology to halt tumor growth[8]. GLS overexpression in this context, however, is usually due to oncogenic c-Myc, which regulates the expression of GLS together with many other genes, thus precluding a definite conclusion of the role of GLS[9].

In this study, we developed a model that allows the delineation of the cellular consequences of high GLS activity. The model is based on the expression of the recently described hypermorphic *GLS* germline variant followed by incremental GLS inhibition, enabling tuning of GLS activity[6]. DI-HRMS provided an in-depth metabolic fingerprint, capturing the extensive metabolic consequences of increasing GLS activity. This study creates insight into the metabolic consequences of high GLS activity, which might contribute into the understanding of the pathophysiology of both oncogenic pathways and inborn errors of glutamate metabolism.

RESULTS AND DISCUSSION

MODELING HIGH GLS ACTIVITY

To generate a cell model expressing high GLS activity, HEK293 cells were stably transfected with a GLS-hyperactivity variant[6]. This hypermorphic variant causes intrinsically increased GLS activity rather than GLS overexpression. As expected, UPLC-MS/MS amino acid analysis revealed increased intracellular glutamate concentrations and decreased glutamine concentrations compared to cells transfected with an empty vector, indicating successful transfection and high GLS activity. Stepwise inhibition of GLS activity down to normal was obtained by adding CB-839 at increasing concentrations, as evidenced by completely normalized glutamine and glutamate concentrations at the highest concentration used (Figure 1A, Figure S1). This model thus enables tuning of GLS activity and thereby provides a powerful tool to dissect the metabolic consequences of isolated GLS overactivity.

DI-HRMS

DI-HRMS of cellular extracts with varying GLS activity levels led to the detection of 12437 features [m/z]. 109 features with an accurate mass corresponding to endogenous metabolites based on the Human Metabolome Database were significantly altered upon high GLS activity ($p<0.05$ with T-test and $R^2>0.6$ on lineair regression) (Table S2). Among these metabolites were glutamate and glutamine. The intensities of glutamate and glutamine, both the individual and sum of the adducts, obtained by untargeted DI-HRMS corresponded well with the concentrations obtained by targeted UPLC-MS/MS (Figure 1B, Table 1).

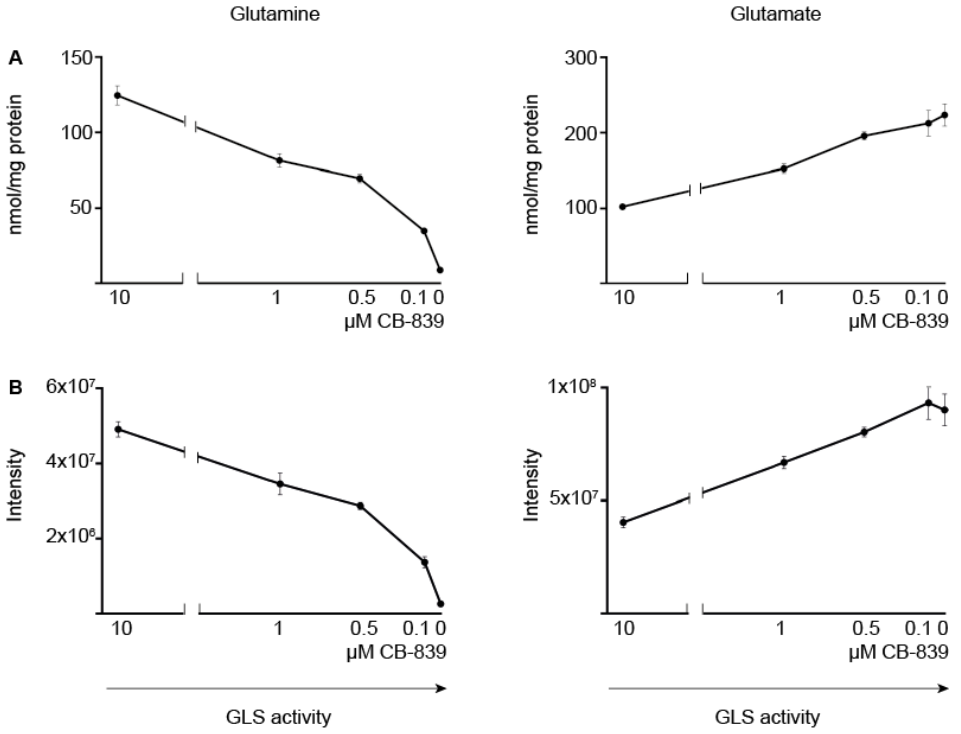

FIGURE 1. Glutamine and glutamate levels in HEK293 cells stably transfected with a hypermorphic GLS variant, in which GLS is stepwise inhibited with CB-839. **A**. Targeted analyses by UPLC-MS/MS show that inhibition of GLS results in increased glutamine and decreased glutamate concentrations. Data represents mean concentrations of biological triplicates corrected for protein (n=3) with standard deviations. **B**. The same pattern of these amino acids was detected by untargeted metabolomics using DI-HRMS. Data represent the mean intensities in biological triplicates of the sum of adducts (positive mode, negative mode, Na^+, K^+, Cl^-) with standard deviations.

TABLE 1. selected metabolites sorted by metabolic pathway.

Pathway	Compound	Adducts	Slope	R2	p-value
GLS reaction	Glutamine$^{\Delta}$	$Na^+ + Cl^- - K^+$	↓	0.99	3.63 E-07
	Glutamate*	$K^+ Na^+ + - Cl^-$	↑	0.88	8.21 E-05
TCA cycle	α-Ketoglutarate	-	↑	0.73	4.38 E-04
	Succinate	Na^+	↑	0.69	2.43 E-02
	Fumarate	$- Cl^-$	↑	0.84	1.00 E-06
	Malate	$Na^+ +$	↑	0.72	4.21 E-05
	Oxaloacetate	Cl^-	↑	0.73	2.01 E-02
	Cis-aconitate	-	↓	0.64	7.53 E-04
	Citrate Iso-citrate	-	↓	0.62	1.07 E-04
	Alanine	+ -	↑	0.84	4.16 E-03
Serine Glycine metabolism	Phosphohydroxypyruvate	Na^+	↑	0.68	8.15 E-03
	Phosphoserine*	$- + Na^+ K^+ Cl^-$	↑	0.88	3.08 E-04
	Serine	K^+	↑	0.74	1.54 E-03
GABA metabolism	GABA°	-	↑	0.85	3.96 E-05
	Succinate-semialdehyde	-	↑	0.66	2.48 E-03
Proline - ornithine metabolism	Glutamic-γ-semialdehyde	K^+	↑	0.63	2.00 E-03
	1-Pyrroline-5-carboxylate	+	↑	0.78	8.08 E-04
	Ornithine	Na^+	↑	0.68	2.37 E-02
	γ-Glutamyl-alanine	$- Na^+ Cl^- K^+$	↓	0.90	1.13 E-05
	γ-Glutamyl-glutamine γ-Glutamyl-analyl-glycine	- +	↓	0.73	3.12 E-07
	5-Oxoproline	+	↓	0.63	6.11 E-03
Asparagine metabolism	Asparagine	Cl^- -	↓	0.84	6.66 E-07
	Aspartate	$- Cl^- K^+ + Na^+$	↑	0.96	2.94 E-06
Nucleotide metabolism	Thymine	-	↓	0.79	4.18 E-03
	Dihydrothymine	$Na^+ - K^+$	↓	0.98	4.65 E-06
	Deoxycytidine	+	↓	0.64	8.94 E-03
	Ureido-isobutyrate$^{\Delta}$	$Na^+ + Cl^- - K^+$	↓	0.99	3.63 E-07
	3-Amino-isobutyrate°	-	↑	0.85	3.96 E-05
	Urate	+	↓	0.89	9.48 E-04
	Dihydrouracil	-	↓	0.82	2.94 E-05
	Xanthosine triphosphate	+	↑	0.64	4.29 E-02
	Deoxyinosine	-	↓	0.63	1.08 E-02

Metabolites without adducts measured in positive (+) or negative (-) mode, or with adducts (Na^+ Cl^- K^+) sorted by metabolic pathways. Metabolites involved in multiple pathways are listed only ones. Per metabolite, all formed adducts are listed ranged from high-low R^2 (left to right). The R^2 and p-value of only the metabolite-adduct with the highest R^2 is shown. ↓ decreased; ↑ increased; = not affected (R^2<0.6 or p>0.05). Metabolites with the same mass are displayed in the same cell or symbolized with Δ * O.

METABOLIC CONSEQUENCES OF HIGH GLS ACTIVITY

Metabolic profiling revealed that high GLS activity indeed increases the concentration of multiple metabolites downstream from glutamate while reducing the concentration of metabolites downstream of glutamine as compared to normal GLS activity (Figure 2, Table 1).

Specifically, high GLS activity led to increased levels of α-ketoglutarate -the direct product of glutamate transamination- as well as the TCA cycle intermediates succinate, fumarate, malate and oxaloacetate. Levels of cis-aconitate, and citrate and/or isocitrate were decreased. This combination of alterations is known as a truncated TCA cycle (Figure 2A, Figure 3, Table 1)[10]. As citrate and isocitrate share the same mass and therefore cannot be distinguished by DI-HRMS, we validated these findings by UPLC-MS/MS and confirmed these results (Figure S2). The truncated TCA cycle as a result of increased glutaminolysis has been described in glutamine-dependent cancer cells. In these cancer cells, GLS expression is upregulated in parallel to other c-Myc induced alterations, supporting tumorigenesis and tumor progression[7,11]. Our results show that high GLS activity solely is sufficient to drive this phenomenon.

Transamination of glutamate into α-ketoglutarate is coupled to the production of amino acids - particularly aspartate, alanine and phosphoserine- from organic acids. The levels of these amino acids increased upon high GLS activity, suggesting that high GLS activity leads to an increased transamination rate and amino acid production (Figure 2B). Serine levels also increased, most likely following from increased phosphoserine levels (Figure 2C). The level of glycine, which is one enzymatic step more distant from GLS, was unaffected by GLS activity. In addition to increased levels of transamination products and GABA -a direct product of glutamate conversion by glutamate decarboxylase- and its breakdown products succinate-semialdehyde and succinate increased with high GLS activity (Figure 2D).

Proline and ornithine are produced from glutamate through glutamic-γ-semialdehyde and pyrroline-carboxylate. Glutamic-γ-semialdehyde, pyrroline-carboxylate and ornithine were increased at high GLS activity (Figure 2E). The level of proline -one step more distant from GLS- was unaffected.

GLS activity is considered the drive for glutathione synthesis. Surprisingly, metabolites of the γ-glutamyl-cycle, rather than increased, were either decreased (γ-glutamyl-alanine, γ-glutamyl-glutamine and/or γ-glutamyl-analyl-glycine and oxoproline) or unaffected (glycine, cysteinylglycine, reduced glutathione). As the γ-glutamyl-cycle produces the anti-oxidant glutathione, this appears to be in contrast with reports of cancer cells with upregulated GLS expression in which glutathione synthesis increases[4]. These

observations are supported by our previous observation that GLS hyperactivity decreases redox buffering capacity, probably secondary to glutamate excitotoxicity[6,12]. Our finding suggests that increased glutathione synthesis in cancer cells may be caused by the induction of additional enzymes, rather than solely GLS. This is supported by the previously demonstrated co-dependency for glutathione synthesis of GLS on γ-glutamylcysteine synthetase[13].

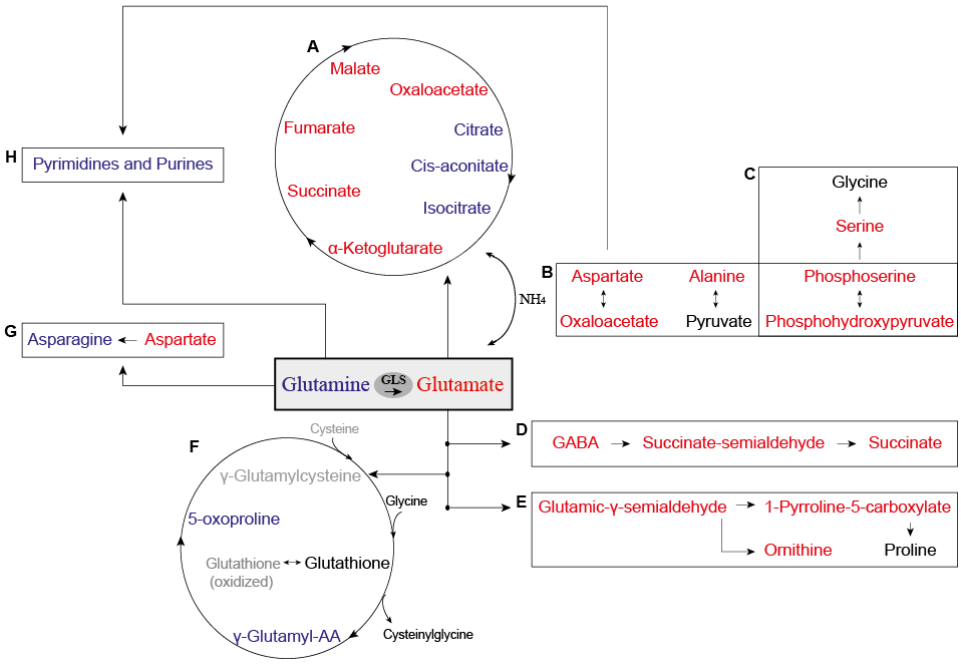

FIGURE 2. Metabolic pathways interconnected by GLS and their response to high GLS activity. DI-HRMS detected increased (red), decreased (blue) or non-affected (black) metabolites upon high GLS activity. Undetected metabolites (non-informative) are marked in grey. **A.** TCA cycle via α-ketoglutarate produced by dehydrogenation or transamination of glutamate. **B.** Transamination reactions coupled to the reversible conversion of glutamate into α-ketoglutarate. **C.** Serine and glycine biosynthesis from phosphoserine, produced by transamination. **D.** GABA, a direct product of glutamate decarboxylation. **E.** Proline and ornithine biosynthesis from glutamic-γ-semialdehyde. **F.** γ-glutamyl cycle metabolizes glutathione from glutamate, glycine and cysteine. **G.** Asparagine synthesis from aspartate, requiring nitrogen from glutamine. **H.** Purine and pyrimidine synthesis, requiring both glutamine and aspartate.

In line with a glutamine decrease, high GLS activity resulted in a decrease of asparagine, which is produced through nitrogen donation from glutamine to aspartate (Figure 2G). Interestingly, the biosynthesis of pyrimidine and purine nucleotides requires both glutamine and aspartate and is therefore linked to both sides of the GLS reaction (Figure 2H)[2]. We show that high GLS activity leads to decreased levels of the pyrimidine thymine and its degradation products dihydrothymine, deoxycytidine and possibly ureido-isobutyrate. Next to thymine metabolism, the purine urate and other related metabolites were affected, but these did not explicitly point towards a single pathway (Table 1). These results indicate that high GLS activity decreases the synthesis of thymine and possibly of nucleotides in general by depriving cells from glutamine, an effect that could be alleviated by GLS inhibition. This notion contrasts previous reports which concluded that GLS upregulation in cancer cells favors nucleotide synthesis -and thereby tumor growth- by providing these cells with glutamate-derived aspartate[3,14]. This disparity underlines the necessity of both glutamine and aspartate availability for nucleotide synthesis. Although this discrepancy may reflect a cell type-specific response to pathophysiological stimuli due to the unique metabolic composition of each cell type, it also suggests that the increased nucleotide synthesis in cancer cells with upregulated GLS activity is not caused by enhanced glutaminolysis, but rather by other c-Myc related changes. This would explain why GLS inhibition has different therapeutic effects in different cancer cells while in all of these cancers GLS expression is upregulated[15]. We show that GLS inhibition restores glutamine levels, which may -undesirably- favor nucleotide synthesis. This implies that GLS inhibition as a therapeutic treatment should be carefully considered per tumor type.

In addition to the pathways directly linked to GLS, 54 other features (m/z) were affected (Table S2). Among these were several increased metabolites of gluconeogenesis or glycolysis (phosphoenolpyruvate, 2-phosphoglycerate and/or 3-phosphoglycerate, fructose-6-phosphate and/or glucose-6-phosphate). Other affected metabolites include the carnitines acetylcarnitine, propionylcarnitine, butyrylcarnitine and/or isobutyrylcarnitine, which decreased with high GLS activity. These metabolites are not evidently or directly related to glutamine or glutamate. They underscore the extensiveness of metabolic changes upon a single enzymatic alteration and have the potential to unveil novel metabolic connections.
This study creates insight into the pathophysiology of the *GLS* germline hyperactivity mutation found in an infant with cataract and profound developmental delay[6]. The clinical features are assumed to be the direct cause of a neurotransmitter imbalance and of oxidative stress secondary to glutamate excess, as increased glutamate was shown to decrease redox buffer capacity. This is supported by our findings of decreased γ-glutamyl-cycle metabolites. Furthermore, both glutamate and GABA levels were increased, unbalancing the neurotransmitters ratio, which might also contribute to the profound

developmental delay. Additionally, defects in purine and pyrimidine regulation are associated with neurodevelopmental defects[16]. These metabolic consequence of GLS hyperactivity are interesting leads that help uncover the pathophysiology of this novel inborn error of metabolism (IEM). Recently, another IEM involving GLS caused by germline *GLS* loss-of-function mutations has been described. These patients have a phenotypic spectrum ranging from optric atrophy to fatal, neonatal encephalopathy, without a clear pathophysiological mechanism[17,18]. Metabolic profiling of the consequences of these *GLS* loss-of-function mutations by DI-HRMS might provide interesting leads towards the pathophysiology.

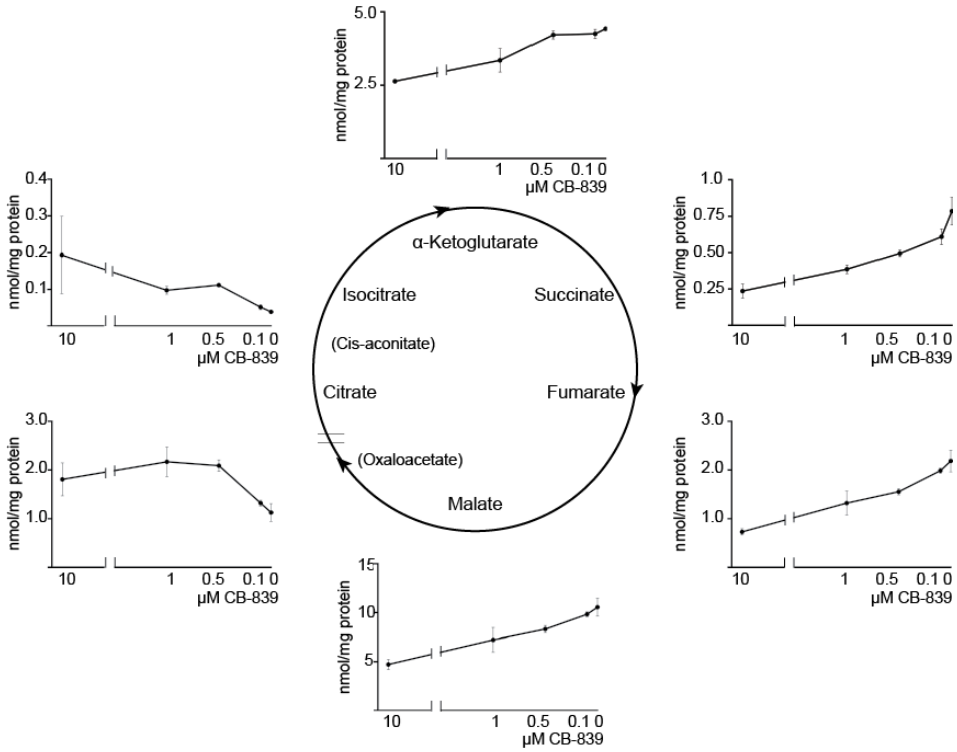

FIGURE 3. High GLS activity leads to a fueled, truncated TCA cycle. DI-HRMS reveals increased adduct ions of α-ketoglutarate, succinate, fumarate, malate and oxaloacetate and decreased cis-aconitate, isocitrate and/or citrate (same m/z, therefore presented only once) levels upon high GLS activity. Affected metabolites were defined based on individual adduct ions (Table 1), Data presented here show the sum of the intensities of all adduct ions (affected and unaffected). Measurements are performed in biological and technical replicates with standard deviations.

Metabolic fingerprinting by DI-HRMS creates an overview of metabolic pathways and their changes upon pathogenic stimuli or genetic alterations. Of importance, DI-HRMS detects masses (m/z) that may not be unique to one metabolite. Since multiple metabolites may share the same molecular mass, the identification of these metabolites is limited using DI-HRMS, requiring validation of findings by targeted analyses to confirm and further explore interesting leads, as was done in this study for the TCA intermediates.

Taken together, by combining a cell model that allows tuning of GLS activity with DI-HRMS, we were able to study the metabolic responses directly related to high GLS activity.

MATERIALS AND METHODS

CELL CULTURE AND SAMPLE PREPARATION

A cell line with GLS hyperactivity was created by stably transfecting HEK293 T-REx Flp-in host cell lines with a plasmid containing KGA (the long splice variant of *GLS*) with the Ser482Cys mutation known to lead GLS hyperactivity, as previously described by Rumping et al[6]. For plasmid preparation, the Ser482Cys cDNA sequence was obtained by site-specific mutagenesis (QuikChange II XL, Agilent, Santa Clara, CA, USA) of the wildtype KGA sequence in pcDNA5/FRT/TO TOPO containing a hybrid CMV/TetO_2 promoter for regulated expression (Life Technologies, Waltham, MA, USA). Cells were cultured at 37°C in 5% CO_2 in DMEM-GlutaMax high glucose with pyruvate. Medium was supplemented with 200 µg/ml hygromycine (Roche, Mannheim, Germany) for selection of plasmid-containing HEK293 cells and with 10% heat-inactivated fetal bovine serum, 100 U/ml penicillin, 0.1 mg/ml streptomycin and 2 mM L-glutamine (obtained from Gibco by Life Technologies, Waltham, MA, USA, unless stated differently). Cells were frequently tested for mycoplasma.

The GLS vector was induced with 0.1 µg/ml tetracycline. Simultaneously, the cells were incubated with 0 µM, 0.1 µM, 0.5 µM, 1 µM and 10 µM CB-839 (Selleckchem, Houston, USA) for 15 hours to obtain different levels of GLS activity[19]. Cells were collected in methanol (Sigma-Aldrich, Steinheim, Germany) -of which supernatants were evaporated with nitrogen and reconstituted in 1 ml of methanol for metabolomics or in lysis buffer for protein quantification. Lysis buffer containing 1% Triton X-100 (Sigma-Aldrich, Steinheim, Germany), 50mM Tris (Roche, Mannheim, Germany), 150mM NaCl and protease inhibitor (Roche, Mannheim, Germany) was used. Protein quantification was performed using the Pierce BSA assay kit (Thermo Fisher Scientific, Waltham, MA, USA) in biological and analytical triplicates.

UNTARGETED METABOLOMICS

Direct-Infusion High-Resolution Mass Spectrometry (DI-HRMS)

Direct infusion was performed on the TriVersa NanoMate (Advion, Ithaca, NY, USA) using chip-based infusion (400 nozzles, nominal internal Ø 5 µm). High-resolution mass spectrometry (140.000 at m/z 200 Da) was performed with a Q-ExactivePlus (Thermo Scientific GmbH, Bremen, Germany) in a scan range of *m/z* 70 to 600 in negative and positive modes[20]. Each sample was measured in technical triplicate to improve the accuracy of observed intensities. To achieve high mass accuracy, mass calibration of the instrument was performed and internal lock masses were used[21].

Pipeline

RAW data files were converted to mzXML format using MSConvert[22]. The data were processed using an in-house developed untargeted metabolomics pipeline written in the R programming language. First, the mzXML files were converted to readable format by the XCMS package[23]. For every sample, peak finding was done by fitting Gaussian-shaped curves over the data on the m/z axis. Peaks with the same m/z (within 2 ppm) were grouped over different samples. Peak groups were identified using all entries in the Human Metabolome DataBase (HMDB) and isotopes, using an accuracy of 3 ppm or better and those with intensities > 5000 in all technical triplicates of at least one biological sample were included[24]. The intensities of the technical replicates were averaged. The statistical analysis was a linear regression of measured intensities on the ordinal concentrations (i.e. 10, 1, 0.5, 0.1 and 0 mM were represented as ordinal values 1 through 5).

Selection of metabolites

A selection of metabolites without adducts or with the adducts Na^+, K^+ or Cl^- of endogenous origin according to the HMDB was made. A linear curve of the average intensity of 9 replicates (technical triplicates for every biological replicate) against several GLS activity levels -achieved by different CB-839 concentrations- was plotted. Statistical analyses were performed by the calculation of the R^2 on a linear regression of the curve and a T-test on the extremities. Those metabolites with $R^2 > 0.6$ and $p < 0.05$ were considered affected and included in further analyses.

TARGETED METABOLOMICS

Glutamine and glutamate

The concentrations of these amino acids were determined by UPLC-MS/MS using stable isotope-labeled internal standards as previously described[25].

TCA cycle intermediates

Chromatographic separation

Sample analysis was performed on a Waters Acquity™ ultraperformance liquid chromatography (UPLC) system Waters Corp., Milford, USA). Chromatographic separation was performed at 30 °C using an Acquity HSS T3 column (100 mm × 2.1 mm i.d., 1.8 µm; Waters Corp., Milford, USA) equipped with an ACQUITY UPLC VanGuard Pre-Column HSS T3 (5 mm × 2.1 mm i.d., 1.8 µm). The following eluents were used: solvent A: H_2O, 0.1% (formic acid) (v/v); solvent B: 100% acetonitrile. The gradient elution was as follows: 0-4.0 min isocratic 1% B, 4.0-4.5 min linear from 1% to 100% B, 4.5-5.0 min isocratic 100% B, and 5.0–5.1 min linear from 100% to 1% B, with 5.1-6.0 min for initial conditions of 1% B for column equilibration. The flow rate remained constant at 0.3 ml/min. 10 µl injection volume was used.

Standard and sample preparation

Calibration standards were prepared with internal standards in the following concentration ranges: glutamine and glutamate 0.05-250 µM; lactate 0.05-500 µM; 2-OH-glutarate 0.1-200 µM, all other metabolites 0.05-100 µM. Internal standards were added to 500 µl of cell extract, evaporated with nitrogen and reconstituted in 50 µl of eluent solvent A. UPLC/MS-grade methanol, formate, citrate, isocitrate, fumarate, pyruvate, succinate, lactate, malate, α-ketoglutarate, 2-OH-glutarate, glutamate and glutamine and the internal standards $^{13}C_2$-succinate and $^{13}C_3$-lactate were obtained from Sigma–Aldrich, Denmark. The internal standards $^{2}H_4$-α-ketoglutarate, $^{13}C_5$, ^{15}N-Glutamate and $^{2}H_{5-}$Glutamine were obtained from Cambridge Isotope Laboratories, Inc., USA. Water was provided by a millipore system.

Metabolite detection

Detection of the metabolites was performed using a Waters Xevo™ triple quadrupole tandem mass spectrometer (Waters Corp, Manchester, UK) with a Z-spray electrospray ionization (ESI) source operating both in the positive and negative ion modes. The mass spectrometer was tuned for each individual metabolite to obtain the maximum intensity for the precursor ions (Table S1). The following parameters were used for ESI-MS analysis in negative ion/positive ion mode: capillary (kV) 2.5/3.0, extractor (V) 3/3, LM1 (low mass) / HM1 (high mass) resolution 3.0/15.0 and LM2/HM2 resolution 3.0/15.0. Desolvation gas at a flow rate of 800 l/h. Desolvation at a temperature of 600°C. The cone and collision gas (argon) flows were set to 20/25 l/h and 0.25/0.25 ml/min, respectively. The source temperature remained at 150 °C.

Data analysis

Chromatographic data were analyzed with Waters MassLynx v4.1 software. Quantification was achieved for each analyte using linear regression analysis of the peak area ratio

analyte/IS (weighed 1/*X*) versus concentration. The assay was performed in biological triplicates. The data was corrected for total protein.

ACKNOWLEDGEMENTS

We thank Fried Zwartkruis and Hanneke Haijes-Siepel (UMC Utrecht) for helpful discussions.

SUPPLEMENTARY FILES

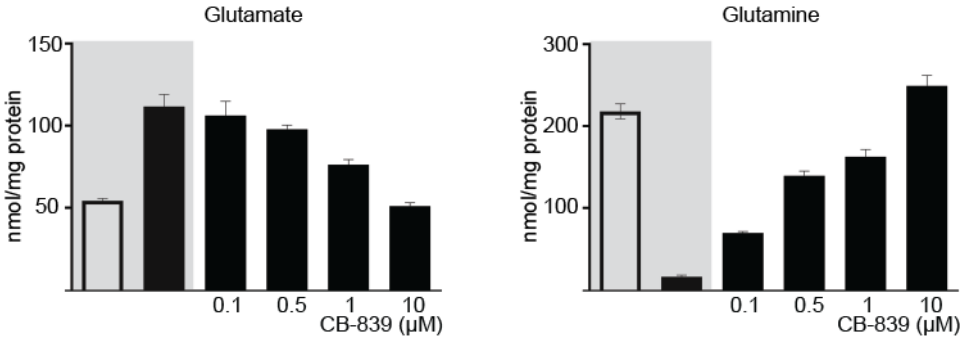

Figure S1. Glutamate and glutamine values in HEK293 cells stably transfected with an empty vector (white) or the GLS superactivity variant Ser482Cys-*GLS1* (black), untreated (highlighted) or treated with 0.1 μM, 0.5 μM, 1 μM or 10 μM CB-839. Glutamine decreased and glutamate increased upon high GLS activity and normalized with GLS inhibition. The data represent the mean of biological triplicates with standard deviations.

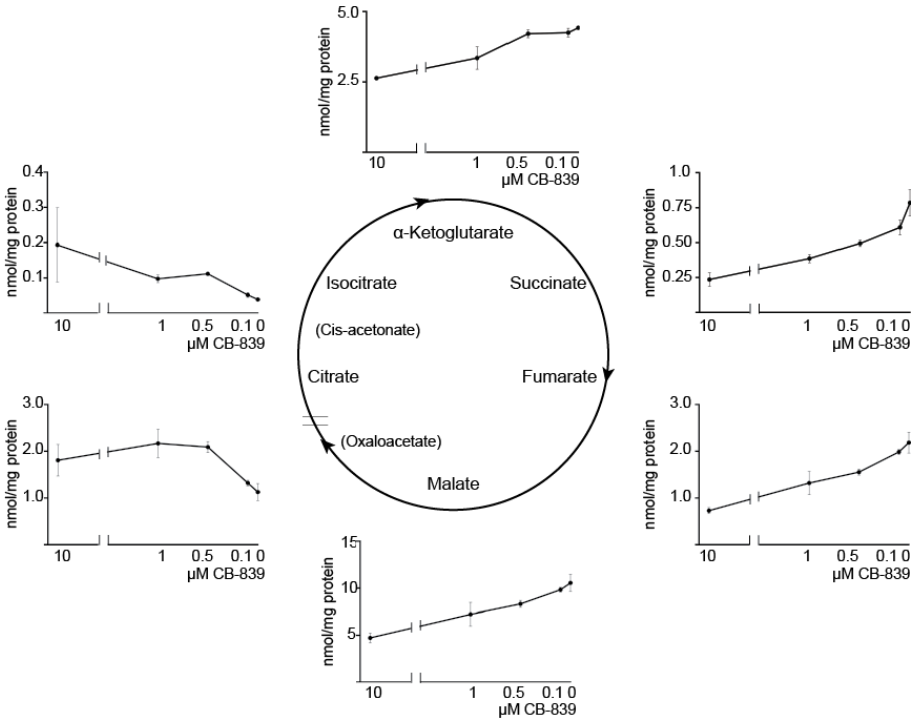

Figure S2. High GLS activity leads to a fueled, truncated TCA cycle. α-ketoglutarate, succinate, fumarate and malate increased and isocitrate and citrate decreased upon the increasing GLS

activity achieved by stepwise GLS inhibition. Oxaloacetate and cis-acetonate were not measured. Measurements are performed by targeted analyzes using UPLC-MS/M. Data is representative for the mean concentration -corrected for protein- of biological triplicates (n=3) with standard deviations.

TABLE S1. Cone voltage and collision energies for the Selected Reaction Monitoring transitions.

Metabolites analyzed using negative ion mode			
Citrate	18/13	191.0 → 110.9	1.97
Isocitrate	18/15	191.0 → 110.9	1.23
Fumarate	18/8	115.0 → 71.0	2.26
Succinate	18/10	117.0 → 73.0	2.53
^{13}C2-Succinate	18/10	119.0 → 75.0	2.53
α-Ketoglutarate	12/12	144.9 → 56.9	1.53
$^{2}H_{4}$-α-Ketoglutarate	14/12	149.0 → 105.0	1.52
Malate	16/10	133.0 → 114.9	1.19
Metabolites analyzed using positive ion mode			
Glutamine	12/14	147.07 → 84.06	0.83
$^{2}H_{5}$-Glutamine	12/14	152.07 → 88.20	0.83
Glutamate	14/14	148.07 → 84.07	0.88
$^{13}C_{5}$, ^{15}N-Glutamate	14/14	154.07 → 89.06	0.86

CV: cone voltage (V); CE: collision energy (eV); SRM: Selected Reaction Monitoring (m/z). RT: retention time (minutes).

REFERENCES

1. Curthoys NP, Watford M. Regulation of glutaminase activity and glutamine metabolism. *Annu Rev Nutr.* 1995;15:133-159.
2. Cory JG, Cory AH. Critical roles of glutamine as nitrogen donors in purine and pyrimidine nucleotide synthesis: Asparaginase treatment in childhood acute lymphoblastic leukemia. *In Vivo.* 2006;20(5):587-589.
3. Altman BJ, Stine ZE, Dang CV. From Krebs to clinic: glutamine metabolism to cancer therapy. *Nat Rev Cancer.* 2016;16(10):619-634.
4. Zhang J, Pavlova NN, Thompson CB. Cancer cell metabolism: the essential role of the nonessential amino acid, glutamine. *EMBO J.* 2017;36(10):1302-1315.
5. Krebs HA. Metabolism of amino-acids: The synthesis of glutamine from glutamic acid and ammonia, and the enzymic hydrolysis of glutamine in animal tissues. *Biochem J.* 1935;29(8):1951-1969.
6. Rumping L, Tessadori F, Pouwels PJW, et al. GLS hyperactivity causes glutamate excess, infantile cataract and profound developmental delay. *Hum Mol Genet.* 2019;28(1):96-104.
7. Xiang Y, Stine ZE, Xia J, et al. Targeted inhibition of tumor-specific glutaminase diminishes cell-autonomous tumorigenesis. *J Clin Invest.* 2015;125(6):2293-2306.
8. Xu X, Meng Y, Li L, et al. Overview of the Development of Glutaminase Inhibitors: Achievements and Future Directions. *J Med Chem.* 2018.
9. Miller DM, Thomas SD, Islam A, Muench D, Sedoris K. c-Myc and cancer metabolism. *Clin Cancer Res.* 2012;18(20):5546-5553.
10. Nain V, Buddham R, Puria R. Role of TCA cycle Truncation in Cancer Cell Energetics. *Current trends in biotechnology and pharmacy.* 2014;8(4):428-438.
11. Bayer E, Bauer B, Eggerer H. Evidence from inhibitor studies for conformational changes of citrate synthase. *Eur J Biochem.* 1981;120(1):155-160.
12. Dong XX, Wang Y, Qin ZH. Molecular mechanisms of excitotoxicity and their relevance to pathogenesis of neurodegenerative diseases. *Acta Pharmacol Sin.* 2009;30(4):379-387.
13. Daemen A, Liu B, Song K, et al. Pan-Cancer Metabolic Signature Predicts Co-Dependency on Glutaminase and De Novo Glutathione Synthesis Linked to a High-Mesenchymal Cell State. *Cell Metab.* 2018;28(3):383-399 e389.
14. Okazaki A, Gameiro PA, Christodoulou D, et al. Glutaminase and poly(ADP-ribose) polymerase inhibitors suppress pyrimidine synthesis and VHL-deficient renal cancers. *J Clin Invest.* 2017;127(5):1631-1645.
15. Davidson SM, Papagiannakopoulos T, Olenchock BA, et al. Environment Impacts the Metabolic Dependencies of Ras-Driven Non-Small Cell Lung Cancer. *Cell Metab.* 2016;23(3):517-528.
16. Fumagalli M, Lecca D, Abbracchio MP, Ceruti S. Pathophysiological Role of Purines and Pyrimidines in Neurodevelopment: Unveiling New Pharmacological Approaches to Congenital Brain Diseases. *Front Pharmacol.* 2017;8:941.
17. Lynch DS, Chelban V, Vandrovcova J, Pittman A, Wood NW, Houlden H. GLS loss of function causes autosomal recessive spastic ataxia and optic atrophy. *Ann Clin Transl Neurol.* 2018;5(2):216-221.

18. Rumping L, Buttner B, Maier O, et al. Identification of a Loss-of-Function Mutation in the Context of Glutaminase Deficiency and Neonatal Epileptic Encephalopathy. *JAMA Neurol.* 2018.
19. Gross MI, Demo SD, Dennison JB, et al. Antitumor activity of the glutaminase inhibitor CB-839 in triple-negative breast cancer. *Mol Cancer Ther.* 2014;13(4):890-901.
20. Birkler RI, Stottrup NB, Hermannson S, et al. A UPLC-MS/MS application for profiling of intermediary energy metabolites in microdialysis samples--a method for high-throughput. *J Pharm Biomed Anal.* 2010;53(4):983-990.
21. de Sain-van der Velden MGM, van der Ham M, Gerrits J, et al. Quantification of metabolites in dried blood spots by direct infusion high resolution mass spectrometry. *Anal Chim Acta.* 2017;979:45-50.
22. Chambers MC, Maclean B, Burke R, et al. A cross-platform toolkit for mass spectrometry and proteomics. *Nat Biotechnol.* 2012;30(10):918-920.
23. Smith CA, Want EJ, O'Maille G, Abagyan R, Siuzdak G. XCMS: processing mass spectrometry data for metabolite profiling using nonlinear peak alignment, matching, and identification. *Anal Chem.* 2006;78(3):779-787.
24. Wishart DS, Jewison T, Guo AC, et al. HMDB 3.0--The Human Metabolome Database in 2013. *Nucleic Acids Res.* 2013;41(Database issue):D801-807.
25. Prinsen HC, Schiebergen-Bronkhorst BG, Roeleveld MW, et al. Rapid quantification of underivatized amino acids in plasma by hydrophilic interaction liquid chromatography (HILIC) coupled with tandem mass-spectrometry. *J Inherit Metab Dis.* 2016;39(5):651-660.

Chapter 5

Inborn errors of glutamate metabolism

Submitted

Lynne Rumping, Peter M van Hasselt, Esmee Vringer, Roderick HJ Houwen, Judith JM Jans, Nanda M Verhoeven-Duif

ABSTRACT

Glutamate is involved in a variety of metabolic pathways. Multiple genes are involved in glutamate metabolism. We reviewed the literature on genetic defects of enzymes that directly metabolize glutamate, leading to inborn errors of glutamate metabolism. Seventeen genetic defects of glutamate metabolizing enzymes have been reported, of which three were only recently identified. These seventeen defects affect amino acid metabolism, the urea cycle- and ammonia metabolism and the γ-glutamyl cycle. We provide an overview of the clinical and biochemical phenotypes of these defects in an effort to ease their recognition and to create insight into the contributing role of deviant glutamate and glutamine levels to the pathophysiology of these diseases. In glutamine synthetase deficiency and glutaminase loss-of-function and hyperactivity, glutamate and glutamine concentrations have been reported as abnormal and postulated to play a pivotal pathophysiologic role. For the other inborn errors of metabolism -with the exception of high glutamine concentrations in urea cycle defects- abnormal glutamate and glutamine concentrations have not been reported. The pathophysiology of these disorders is postulated to be due to disturbed metabolic pathways downstream of the affected enzyme. Nevertheless, tissue-specific abnormalities and pathophysiologic involvement of glutamate and glutamine may still play a role in these inborn errors of glutamate metabolism. To create insight into the clinical consequences of disturbed glutamate metabolism –rather than individual glutamate and glutamine levels- the prevalence of phenotypic abnormalities within the seventeen inborn errors of metabolism was compared to their prevalence within all 10.204 Mendelian disorders notated in the Human Phenotype Ontology database (HPO). For this, a hierarchical database of all phenotypic abnormalities of the seventeen defects in glutamate metabolism based on HPO was created. A neurologic phenotypic spectrum of developmental delay, seizures and hypotonia are common in these inborn errors. Additionally, ophthalmologic and skin abnormalities are often present, suggesting that disturbed glutamate homeostasis affects tissues of ectodermal origin: brain, eye and skin. Reporting glutamate and glutamine concentrations in patients with inborn errors in enzymes of glutamate metabolism would provide additional insight into pathophysiology of these inborn errors in enzymes of glutamate metabolism.

INTRODUCTION

The amino acids glutamate and glutamine are key players in metabolism, functioning as both substrate and product in various enzymatic reactions[1]. Glutamate is the main excitatory neurotransmitter in the central nervous system and triggers responses implicated in neuronal migration and differentiation, synapse remodeling and axon myelination[2,3]. Additionally, glutamate is the precursor of glutathione and the tricarboxylic acid (TCA) cycle intermediates and therefore plays a role in redox state and energy metabolism resp. It is involved in amino acid synthesis and catabolism and as such involved in many metabolic pathways[4]. Together with glutamine, glutamate plays an important role in ammonia detoxification by capturing ammonia -forming glutamine- and providing the urea cycle with intermediates[5]. Glutamine is needed for NAD^+ production, an important metabolite for redox reactions and is also incorporated into proteins, and a source of purines and pyrimidines[6-9].

Excess of glutamate and glutamine is harmful to cells. Glutamate excess in the brain is associated with glutamate excitotoxicity, a cascade of events that eventually leads to oxidative stress, toxicity and cell death[10,11]. Glutamine excess leads to insufficient osmoregulation and subsequent cerebral edema[6,12]. Glutamate and glutamine concentrations are therefore strictly regulated[13]. Defects in glutamate metabolism lead to metabolic diseases.

We performed a literature review of defects in enzymes that directly metabolize glutamate, caused by genetic errors. Seventeen inborn errors of glutamate metabolizing enzymes have been reported, most of which are ultra-rare. We provide an overview of these inborn errors in an effort to ease the recognition and to create insight into the contributing role of glutamine and glutamate to the pathophysiology.

DISORDERS OF GLUTAMINASE AND GLUTAMINE SYNTHETASE

Glutamate and glutamine are interconverted by two enzymes (Figure 1). Glutamine synthetase (GS) catalyzes the conversion of glutamate and ammonia into glutamine. It is ubiquitously expressed and is the only enzyme for glutamine synthesis[14,15]. The reverse reaction is catalyzed by glutaminase (GLS) which hydrolyzes glutamine to yield glutamate and ammonia. GLS exists in two isoforms: GLS, mainly expressed in kidney and brain, and GLS2, primarily expressed in liver[16,17]. Genetic defects in both GS and GLS have been reported (Table 1).

A *de novo* hypermorphic *GLS* variant has recently been reported in a single patient affected with cataract, profound developmental delay, axial hypotonia and agitated, self-injuring behavior[18]. Glutamate and glutamine concentrations in plasma and CSF from the

patient were within the normal range. In urine and in brain, as detected by *in vivo* magnetic resonance spectroscopic imaging (MRSI), glutamate concentrations were increased and glutamine concentrations decreased, in line with the tissue-specific expression of GLS[16]. Glutamate excess is thought to underlie the pathophysiology of the disease by reducing the scavenging capacity for oxygen radicals and making the cell more susceptive for oxidative stress, which is associated with cataract, neurodegenerative disorders and agitated, self-injuring behavior[10,19,20].

GLS loss-of-function variants have been reported recently in unrelated families. In two families, patients clinically presented with neonatal respiratory dysfunction and fatal, refractory status epilepticus[21]. MRI of the brain showed extensive cerebral edema and white matter involvement. The *GLS* variants were discovered by post-mortem exome sequencing. Retrospective amino acid analyses of stored dried bloodspots from neonatal screening revealed increased glutamine values. Increased glutamine is a possible cause of the ongoing epileptic activity secondary to cerebral edema[12,22]. Glutamate values were unaltered in bloodspots. Considering the importance of glutamate in signal transduction and myelin synthesis in the brain, decreased glutamate levels might also have played a contributing pathogenic role in this metabolic disease by causing epilepsy and secondary cerebral edema. Glutamate levels in the brain could however not be determined. In another family, decreased GLS expression was detected in two brothers who initially developed normally, but from the age of 7 years developed progressive optic atrophy, truncal ataxia and hypertonia in the limbs. MRI of the brain showed cerebellar atrophy with normal white matter. Glutamine and glutamate values were not reported[23].

Congenital glutamine synthetase deficiency, caused by bi-allelic mutations is the *GLUL* gene, has been described in four unrelated children. All the patients suffered from seizures which developed either after birth or within few months of life. Two suffered from necrolytic migratory erythema and died within the first month of life from multi-organ failure[24]. These exhibited dysmorphic features including a broad, flat nasal root and low set ears. The third patient developed drug-resistant tonic-clonic seizures and died at six years of age from acute respiratory decompensation. The fourth patient was recently described and mainly suffers from seizures. Glutamine concentrations in these patients were either strongly or borderline decreased in plasma, urine, CSF and in brain (as detected by MRS), in line with the ubiquitous expression of GS. Plasma ammonia levels were increased. Glutamine supplementation in the third patient normalized glutamine concentrations in plasma, improved EEG and even reduced seizure attacks[25]. In the fourth patient, glutamine supplementation also normalized glutamine levels and decreased ammonia levels, however follow-up is still performed to study the clinical effect.[26] Hyperammonemia

and NAD^+ deficiency secondary to glutamine deficiency are likely the pathogenic factors causing the phenotype. Hyperammonemia is highly toxic for the brain and associated with encephalopathy and seizures, and NAD^+ is important for numerous redox reactions in the cell[6,27]. Recently a new biological function of GS for motility and migration of endothelial cells has been revealed, which contributes to the formation of new vessels in development and disease[28]. Whether this plays a contributing role to the clinical phenotype of GS deficiency has not been elucidated yet.

In conclusion, defects in enzymes interconverting glutamate and glutamine lead to different, mainly neurological, phenotypes. They result in disturbed levels of glutamate and glutamine in several body fluids and tissues which plays an important pathophysiologic role.

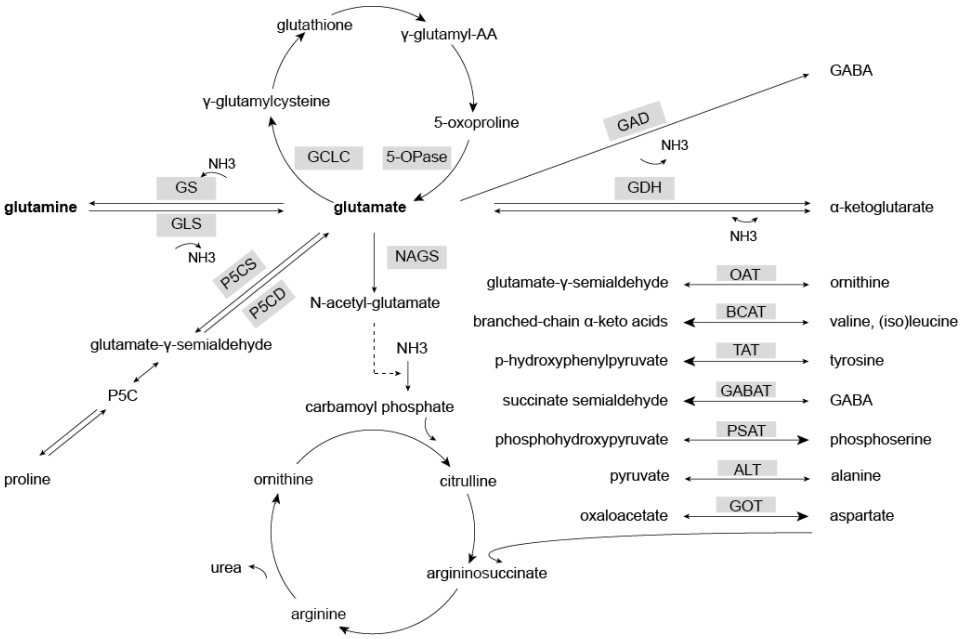

FIGURE 1. Metabolic pathways of glutamate metabolism in which genetic defects lead to metabolic disease. Clockwise from the top: γ-glutamyl cycle, GABA synthesis, α-ketoglutarate synthesis or transamination with concomitant production or catabolism of amino acids, urea cycle, proline synthesis and catabolism, glutamine synthesis and catabolism. All enzymes are marked grey. bi-directional reaction with preferred direction in bold; - - - cofactor of reaction.

DISORDERS OF AMINO ACID METABOLISM

Glutamate functions as a substrate for amino acid synthesis and as a product of amino

acid catabolism (Figure 1). Defects in these enzymes of amino acid metabolism, including several transaminases, lead to deviant amino acid levels and to a broad spectrum of clinical phenotypes, depending on the amino acid function (Table 1).

P5C dehydrogenase (P5CD) degrades proline via Δ-1-pyrroline-5-carboxylate (P5C) into glutamate[29]. Deficiency of P5CD results in hyperprolinemia with concomitant increase of urinary P5C (hyperprolinemia type II; HPII)[30,31]. These high P5C levels deactivate PLP (vitamin B6), a cofactor for many enzymes[32,33]. An effect of P5CD deficiency on glutamate levels has not been reported. This disorder presents with intellectual disability and fever-provoked PLP-responsive epileptic seizures ascribed to PLP deficiency, which is a common cause of epilepsy[34]. Patients may however also remain free of symptoms.

The reverse reaction, the formation of proline from glutamate, is catalyzed by P5C synthetase (P5CS). P5CS deficiency is further described under 'Disorders of urea-cycle and ammonia metabolism'.

Tyrosine aminotransferase (TAT) transaminates tyrosine, forming p-hydroxyphenylpyruvate and glutamate. TAT deficiency leads to increased levels of tyrosine in plasma and CSF together with increased levels of its catabolic metabolites in plasma and urine[35,36]. Glutamate levels have not been reported in this disease, suggesting that they were not significantly altered. Deposition of tyrosine crystals leads to eye and skin lesions in patients with TAT deficiency, resulting in infancy-onset ophthalmological and dermatological symptoms. The phenotype is further characterized by seizures and self-injuring and difficult behavior.

GABA transaminase (GABAT) converts GABA into succinate semialdehyde and glutamate. Patients with GABAT deficiency show high GABA levels in CSF and on brain MRS and have increased growth hormone release induced by GABA. These children suffer from a severe neurological phenotype including seizures, hypersomnolence and choreoathetosis and accelerated growth. Symptoms are likely due to increased GABA levels, detected in plasma, CSF and basal ganglia[37]. Although no contributed role of potentially altered glutamate levels to the phenotype has been described, a disturbed GABA-glutamate ratio is postulated to contribute to this metabolic disorder[38,39]. Mutations in the GAD1 gene, encoding glutamate decarboxylase which irreversibly decarboxylates glutamate into GABA, have been described in one family with inherited spastic quadriplegic cerebral palsy type 1, seizures and developmental delay[40]. The authors hypothesize that the neurologic phenotype is secondary to an altered glutamate:GABA ratio, however these levels have not been reported.

Branched-chain amino acid transferase 2 (BCAT2) deficiency has been described in a single patient who presented with high plasma levels of the branched-chain amino acids leucine, isoleucine and valine[41]. The patient suffers from paroxysmal occipital headache, mild memory decline and retinal degeneration. A brother and sister with leucine-isoleucine abnormalities presented with seizures, developmental delay, retinal degeneration and died at the age of 3 years. A BCAT mutation was assumed but not validated[42]. Recently, a genome wide association study showed a clear association between BCAT2 missense mutations and increased valine levels, however no phenotypes were described[43]. It is hypothesized that BCAT2 provides nitrogen for optimal glutamate synthesis -which is supported by the finding that BCAT inhibition decreases glutamate levels- and that the clinical phenotype of BCAT2 deficiency is attributed to disturbed glutamate synthesis rather than the increase in branched-chain amino acids[44-46]. However, thus far glutamate levels were not reported in BCAT2 deficient patients, precluding definite conclusions.

Alanine transaminase 2 (ALT2) deficiency leads to low concentrations of alanine in plasma and in some cases also in CSF[47,48]. Affected patients clinically present with developmental delay, spastic paraplegia and sporadically with seizures. It has been postulated that ALT2 deficiency leads to decreased glutamate production in the brain disturbing the glutamate-glutamine/lactate-alanine shuttle and synaptic neurotransmitter release, which might contribute to the pathogenesis[48]. The strictly neurological effect of ALT2 deficiency can be explained by the neuronal expression of ALT2 and possible compensation by ALT1 expressed in other tissues. Although glutamate levels were normal in CSF and plasma, this does not exclude the possibility of deviant levels in the brain and a local effect. There is contradictory data on the preferable direction of ALT2[49,50]. The decreased alanine concentrations in ALT2 deficiency however suggests that the preferable direction of ALT2 is towards alanine synthesis.

Phosphoserine aminotransferase (PSAT) uses the amino-group of glutamate for serine synthesis[51]. PSAT deficiency has been reported in patients with Neu-Laxova syndrome 2, characterized by central nervous system anomalies, facial dysmorphic features, anomalies of limb and genitalia, intrauterine growth retardation, skin disorders, and other congenital abnormalities[52]. An overlapping phenotype caused by PSAT mutations is described in one family under the name phosphoserine aminotransferase deficiency[53]. It is questionable whether this concerns the same syndrome. Neu-Laxova syndrome can also be caused by other genetic defects interfering the serine biosynthesis pathway. Serine is a precursor of important metabolites such as nucleotides, phospholipids and neurotransmitters. Therefore the pathophysiology in PSAT deficiency and in other serine deficiency disorders with similar symptoms is ascribed to the lack of serine[54]. A potential contributing role of

glutamate has not been described.

In conclusion, defects of P5C dehydrogenase and transaminases producing or metabolizing amino acids with concomitant glutamate conversion lead to different metabolic profiles. Glutamate and glutamine levels are not consistently reported, precluding conclusions about their contributing role to the pathophysiology underlying the broad spectrum of clinical phenotypes. The pathophysiology of these disorders is postulated to be due to disturbed metabolic pathways downstream from the particular affected enzyme. Nevertheless, tissue specific abnormalities and pathophysiologic involvement of glutamate and glutamine may still play a role in these inborn errors of glutamate metabolism.

DISORDERS OF UREA-CYCLE AND AMMONIA METABOLISM

The urea cycle is initiated by N-acetyl glutamate synthase (NAGS), which catalyzes the conversion of glutamate into N-acetyl glutamate (NAG), an obligatory co-factor of the first enzyme of the urea cycle, carbamoyl phosphate synthetase 1 (CPS1)[55]. Primary urea-cycle disorders (UCDs) caused by defects in urea cycle enzymes, including NAGS deficiency, are characterized by altered levels of citrulline, ornithine and arginine, depending on the site of the metabolic block. This hampered urea cycle leads to hyperammonemia, which can be detoxified by the formation of glutamine and alanine (non-toxic ammonia carriers) from glutamate and pyruvate respectively. Toxic hyperammonemia results in the typical clinical phenotype characterized by headaches, lethargy and seizures[56]. NAGS deficiency leads to inactive CPS1 and a hampered urea cycle resulting in hyperammonemia, increased glutamine concentrations and hypocitrullinemia. This leads to the typical clinical presentation of UCDs[57]. NAGSD theoretically leads to glutamate excess, which was indeed reported in one patient but remained unreported in other patients[58]. In addition to primary UCDs, four other defects in glutamate metabolism disturbing the urea cycle and ammonia metabolism have been described (Table 1).

Glutamate dehydrogenase (GDH) catalyzes the deamination of glutamate into α-ketoglutarate and free ammonia[59]. Patients with GDH gain-of-function mutations -resulting in increased sensitivity to ADP allosteric activation- present with neonatal-infantile onset hyperinsulinism-hyperammonemia (HI-HA syndrome), also called hyperinsulinism hypoglycaemic 6 syndrome[60,61]. Hyperammonemia is constant and postulated to result either from increased glutamate deamination directly leading to high ammonia or from glutamate deficiency leading to reduced NAG synthesis, although the levels of urea cycle intermediates and of glutamine remain normal. In parallel, increased GDH activity results in a fueled pancreatic TCA cycle through α-ketoglutarate resulting in insulin secretion and hypoglycemia. Patients suffer from epileptic seizures -amenable to diazoxide treatment-

and developmental delay, but typical symptoms of hyperammonemia like headaches and encephalopathy are absent[62]. As epileptic seizures occur independently of glucose concentrations, epileptic seizures are likely cause by hyperammonemia or a disequilibrium of glutamate:GABA[62]. GDH mutations follow an autosomal dominant trait. However, mutations in the sulfonylurea receptor, either recessive or dominant, causing HIHA are also described.

Glutamic oxaloacetic transaminase 2 (GOT2) transfers the amino-group of glutamate to produce aspartate. GOT2 deficiency was recently described in patients who presented with mild hypercitrullinemia, mild hyperammonemia and normal glutamine, arginine and ornithine levels [63]. Additionally, affected patients had secondary serine deficiency as a consequence of a hampered aspartate-malate cycle and suffered from epileptic seizures and acquired microcephaly ascribed to the secondary serine synthesis defect.

Ornithine, substrate in the urea cycle, is synthesized by two enzymes directly metabolizing glutamate. Δ-1-pyrroline-5-carboxylate synthetase (P5CS) converts glutamate into glutamate-γ-semialdehyde. This is in equilibrium with P5C and can be converted into ornithine. P5CS deficiency results in low ornithine and subsequent citrulline and arginine levels with mild fasting hyperammonemia. Despite the hampered urea cycle, glutamine concentrations are not increased in these patients. This defect additionally results in low proline levels, the product of P5C. Patients present with symptoms ranging from severe cutis laxa to adult-onset spastic paraplegia (depending on the presence of mono- or bi-allelic mutations) with concomitant hypermobility of the joints, neurodegeneration and bilateral cataracts or corneal clouding[64-69]. These symptoms are in line with the role of proline in collagen and elastin synthesis, protein synthesis, oxidative stress defense in addition to a possible role as an inhibitory neurotransmitter[70].

Ornithine aminotransferase (OAT) converts glutamate-γ-semialdehyde into ornithine coupled to glutamate transamination. In the neonatal period, the enzyme is ornithine-producing. Neonatal-onset OAT deficiency leads to low ornithine, hyperammonemia, high glutamine concentrations and failure to thrive[71,72]. In infancy and adulthood, the enzyme is ornithine-catabolizing and its deficiency results in increased ornithine levels and concomitant inhibition of creatine synthesis. Patients present mainly with gyrate atrophy of the choroid and retina and other ophthalmological abnormalities, although some have also been described with developmental delay. These symptoms are postulated to result from either creatine deficiency or toxicity of ornithine and its downstream metabolites spermine and spermidine, which induce retinal cell death and photoreceptor degeneration via oxidative stress[73,74].

Taken together, all inborn errors of glutamate metabolism leading to defects of the urea-cycle or ammonia metabolism show hyperammonemia. However, in GOT2 deficiency, P5CS deficiency and GDH hyperactivity hyperammonemia is mild and does not result in glutamine excess. The pathophysiology of the primary UCD's is assigned to hyperammonemia, while the pathophysiology of the other disorders of ammonia metabolism are postulated to be due to disturbed metabolic pathways downstream from the particular affected enzyme.

γ-GLUTAMYL-CYCLE DISORDERS

Glutamate is one of the intermediaries of the γ-glutamyl-cycle, synthesis and degradation of the important anti-oxidant glutathione,. Two of the disorders of the γ-glutamyl-cycle disorders are directly involved in glutamate metabolism (Figure 1, Table 1).

γ-glutamyl-cysteine synthetase (GCLC) catalyzes the conjugation of glutamate and cysteine to γ-glutamyl-cysteine and is the first and rate-limiting step of glutathione biosynthesis[75]. GCLC deficiency leads to extremely low levels of erythrocytic glutathione and γ-glutamyl-cysteine which result in infantile-adult onset hemolytic anemia[76]. Other reported features are neurological problems, amino aciduria, reticulocytosis and hepatosplenomegaly with transient jaundice but whether these are related to the enzyme defect remains unclear[77-79]. 5-oxoprolinase (5-OPase) catalyzes the last degradation step of glutathione into glutamate by the hydrolysis of 5-oxo-proline[80]. 5-OPase deficiency (OPLAHD) leads to 5-oxoprolinuria, normal erythrocytic glutathione levels and an inconsistent -or even no- clinical presentation including gastrointestinal features and hypoglycemia[81,82]. The lack of a consistent clinical picture and the normal glutathione levels lead to the hypothesis that 5-OPase deficiency is a benign disorder, although a pathogenic role of 5-oxoprolinase deficiency remains possible as specific clinical features may only become obvious later in life[82,83].

In these γ-glutamyl-cycle disorders, glutamate and glutamine levels have not been reported. The pathophysiology is likely predominantly based on oxidative stress, as this cycle plays an important role in metabolism of glutathione.

DRAWING PARALLELS BY COMPARISON OF PHENOTYPIC ABNORMALITIES FROM HPO

In order to create insight into the clinical effect of disturbed glutamate metabolism, we explored clinical parallels between the disorders of glutamate metabolism based on a hierarchical database. This database was created based on all phenotypic abnormalities and their correlated superclasses as reported in the Human Phenotype Ontology (HPO) database (Supplemental Table 1). For the recently described GLS hyperactivity, GLS loss-of-function and GOT2 deficiency, this information was obtained from the original articles

as these have not yet been included in HPO. We obtained a hierarchical database of 539 phenotypic abnormalities including the correlated superclasses. To analyze whether disturbed glutamate metabolism leads to specific clinical consequences, the prevalence of phenotypic abnormalities within the seventeen inborn errors of metabolism was plotted against their prevalence within all 10.204 Mendelian disorders listed in HPO. A prevalence rate >2.5 was used. The following phenotypic abnormalities were excluded from the selection: metabolic abnormalities other than glutamate and glutamine (as we focused on clinical phenotypes rather than metabolic phenotypes); duplicates; upper superclasses (as these are non-specific abnormalities); and phenotypic abnormalities that only presented in one of the seventeen inborn errors. The 72 phenotypic abnormalities that were >2.5 times more prevalent within inborn errors of glutamate metabolism than in all Mendelian disorders were used for further analyses.

Perhaps not surprisingly, the phenotypic abnormalities that are remarkably more prevalent within inborn errors of glutamate metabolism than in all Mendelian disorders, are abnormalities of the nervous system. All inborn errors of glutamate metabolism -except for OAT and OPLAH deficiency- result in neurodevelopmental abnormalities, of which GLS hyperactivity and loss, GS, GABAT, ALT2, PSAT, GAD, GOT2, and P5CS deficiency present in a more severe, global developmental delay. This is 2.7x more prevalent than in all Mendelian disorders. Additionally, seizures are 4x more common in patients with defects of GLS, GS, P5CD, GABAT, BCAT2, ALT, PSAT, NASGS, GAD, GOT2 and in patients with HIHA. White matter and myelination abnormalities are frequently reported in these patients. Coma (13.6x), lethargy (10.4x) and vomiting (10.3x) are also more common phenotypic abnormalities, especially -but not only- in disorders of urea cycle and ammonia metabolism. Abnormalities of the lens and skin are also more prevalent in patients with an inborn error of glutamate metabolism. Cataract occurs in patients with GLS hyperactivity and P5CS and OAT deficiencies and is 3x more common in these inborn errors. Different skin abnormalities are seen in patients with GS deficiency, GLS hyperactivity, PSAT and TAT deficiency and are 2.7-3.2x more common in glutamate related disorders compared to other Mendelian disorders (Supplemental Table 1).

TABLE 1. Clinical and laboratory findings of inborn errors of glutamate metabolism based on the Human Phenotype Ontology (HPO) database and original articles.

Disorder (OMIM) enzyme; *gene;* EC code	Number of described cases if <10; Inheritance pattern	Clinical features	Biochemical diagnostics	Ref
Disorders of glutaminase and glutamine synthetase				
Glutaminase hyperactivity GLS; *GLS*; EC 3.5.1.2	n=1 *de novo,* dominant	Development: Profound developmental delay Neurologic: axial hypotonia, kyphosis, agitated and self-injuring behavior. Structural: white matter involvement Ophthalmologic: Neonatal bilateral cataracts	Plasma: mild hyperammonemia Urine: ↑ glutamate, ↓ glutamine CSF: =glutamate, =glutamine MRS brain: ↑ glutamate, ↓ glutamine, ↓ N-acetylaspartate, ↑alanine, ↑ lactate	[18]
Glutaminase loss-of-function GLS; *GLS*; EC 3.5.1.2	n=6 bi-allelic, AR	Development: neonatal death (4/6), regression around age 7 years with dysarthria (2/6) Neurologic: status epilepticus with suppression burst patterns (4/6), truncal ataxia and hypertonia of limbs (4/6) Structural: white matter involvement, simplified gyral pattern, vasogenic cerebral edema with subsequent gliosis and destruction (4/6), cerebellar atrophy with normal white matter (2/6) Opthalmologic: optic bilateral atrophy (2/6) Respiratory: Cheyne–Stokes respiration	Dried blood spot: ↑ glutamine, = glutamate	[21,23]
Glutamine deficiency (610015) GS; *GLUL;* EC 6.3.1.2	n=4 bi-allelic, AR	Development: severe global developmental delay (2/4), neonatal multi-organ failure (2/4), death (2/4 neonatal; 1/4 age 6 years) Neurologic: seizures within first months of life (4/4), hypotonia (2/4), hyperreflexia (1/4) Structural: immature/hypomyelination (3/4), atrophy (3/4), abnormal gyration, hypoplasia corpus callosum (2/4) ventriculomegaly (1/4) subependymal/periventricular cysts (2/4) Dysmorphic features: broad/flat nasal root (2/4), low set ears (2/4), short limbs, flexion contractures, camptodactyly, ulnar deviation of the hands (1/4) Dermatologic: necrolytic erythema (2/4) Respiratory: apneu, decompensation (1/4)	Plasma: hyperammonemia, Borderline ↓ glutamine, = glutamate Urine: ↓ glutamine, = glutamate CSF: ↓ glutamine, = glutamate MRS: ↓ glutamine, =/↓ glutamate	[24,26]

TABLE 1 CONTINUED.

Disorder (OMIM) enzyme; *gene;* EC code	Number of described cases if <10; Inheritance pattern	Clinical features	Biochemical diagnostics	Ref
		Disorders of amino acid metabolism		
Hyperprolinemia II (239510) P5CD; *ALDH4A1;* EC 1.2.1.88	bi-allelic, AR	Development: Intellectual disability Neurologic: Seizures	Plasma: ↑ proline, ↑ hydroxyproline, ↑ glycine (lactic acidosis excluded) ↓ PLP Urine: ↑ proline, ↑ hydroxyproline, ↑ P5C Fibroblasts: ↓ Enzyme activity	31-33,84,85
Hereditary tyrosinaemia II (276600) TAT; *TAT;* EC 2.6.1.5	bi-allelic, AR	Development: Intellectual disability, growth delay Neurological: seizures, microcephaly, self-injury and other behavioral abnormalities, ataxia, tremor, neurological speech impairment Ophthalmologic: bilateral ocular lesions, inflammation conjunctivae, corneal ulcerations, photophobia Dermatologic: skin lesions	Plasma: ↑ tyrosine (>1200µM, otherwise HTIII) ↑ p-hydroxyphenylpyruvate, ↑ phenolic acids, = acids phenylalanine, methionine CSF: ↑ tyrosine Urine: ↑ phenolic acids Liver biopsy: ↓ enzymatic activity	35,36,86
GABA transaminase deficiency (613163) GABAT; *ABAT;* EC 2.6.1.19	bi-allelic, AR	Development: global developmental delay, death age <10 years. Neurological: encephalopathy, seizures, lethargy, hyperreflexia, muscular hypotonia, high pitched cry, Structural: leukodystrophy, agenesis corpus callosum, cerebral atrophy, cerebellar hypoplasia and cysts, posterior fossa cyst Dysmorphic features: retrognathia, downslanted palpebral fissues, tall stature	CSF: ↑ GABA MRS: ↑ GABA, ↓ glutamine-glutamate semi-oval region Serum: ↑ growth hormone	38,39,87,88
Cerebral palsy, spastic quadriplegic, 1 (605363) GAD; *GAD1;* EC 4.1.1.15	n=6 ni-allelic, AR	Development: global developmental delay Neurological: seizures, hyperreflexia, cerebral palsy, Babinski sign	Not available	40

TABLE 1 CONTINUED.

Disorder (OMIM) enzyme; *gene;* EC code	Number of described cases if <10; Inheritance pattern	Clinical features	Biochemical diagnostics	Ref
		Disorders of amino acid metabolism		
Hypervalinemia and hyperleucine-isoleucinemia (238340) BCAT2; *BCAT2;* EC 2.6.1.42	n=3 bi-allelic, AR	Development: normal - delay Neurological: paroxysm occipital headache, mild memory decline, seizures Structural: white matter involvement Opthalmologic: retinal degeneration	Plasma: ↑ valine, ↑ isoleucine, ↑ leucine Urine: = branched-chain α-keto acids (excluding MSUD) MRS brain: ↓ n-acetylaspartate	41,42,44,45
Mental retardation 49 (616281) ALT2; *GPT2;* 138210	bi-allelic, AR	Development: Global developmental delay, failure to thrive Neurological: seizures, postnatal microcephaly, hypotonia with progressive spastic di/paraplegia with hyperreflexia, dysarthria Structural: subcortical hypomyelination, hypoplasia corpus callosum	Plasma: ↓ alanine, = glutamate, = glutamine Urine: = pyruvate, = lactate CSF: = glutamate, = glutamine, =/↓ alanine, = pyruvate, = lactate	47,48,89
Neu-laxova syndrome 2 / phosphoserine aminotransferase deficiency (616038/610992) PSAT; *PSAT1;* EC 2.6.1.52	bi-allelic, AR	Development: intrauterine growth retardation, decreased fetal movement, neonatal death Dysmorphic features: depressed nasal ridge, low set ears,abnormal pinna, short neck, high/cleft palate, micrognathia, sloping forehead, hypertelorism, acquired microcephaly, scoliosis, limb malformations, Dermatologic: ichthyosis, hyperkeratosis, edema of acra.	Plasma: ↓ serine ↓ glycine CSF: ↓ serine ↓ glycine	51-53,90
		Disorders of urea-cycle and ammonia metabolism		
N-acetylglutamate synthase deficiency (237310) NAGS; *NAGS;* EC 2.3.1.1	bi-allelic, AR	Development: Developmental delay, failure to thrive, neonatal death Neurologic: Seizures, hypotonia, coma, aggressive behavior, lethargy, vomiting Respiratory: respiratory distress	Plasma: hyperammonemia, ↓ citrulline, ↑ alanine, ↑ glutamine, ↑ glutamate (1 patient), Liver biopsy: ↓ enzyme activity	58,91,92
Hyperinsulinemia-hyperammonemia / hypoglycaemia 6 (606762) GDH; *GLUD;* EC 1.4.1.2	*de novo* / AD	Development: Intellectual disability Neurologic: hypoglycemic generalized absence-type epileptic seizures, hypoglycemic coma, generalized dystonia	Plasma: hypoglycemia (provoked at protein intake), hyperammonemia (constant), = glutamine CSF: GABA normal (only measured in 4 patients) Lymphoblasts: ↑ GDH activity by reduced sensitivity to GTP	62,93,94

TABLE 1 CONTINUED.

Disorder (OMIM) enzyme; *gene;* EC code	Number of described cases if <10; Inheritance pattern	Clinical features	Biochemical diagnostics	Ref
Disorders of urea-cycle and ammonia metabolism				
Glutamic-Oxaloacetic Transaminase 2 deficiency AST/GOT2; *GOT2;* EC 2.6.1.1	n=2 bi-allelic, AR	Development: Developmental delay Neurologic: clonic seizures upper limbs, acquired microcephaly, hypotonia	Plasma: ↓ serine, =/↑ glycine, ↑ citrulline, ↑ lactate, hyperammonemia, = glutamine, = glutamate	63
Cutis laxa 3A/3 (219150/616603) **Spastic paraplegia 9A/B (adult phenotype)** (601162/616586) P5CS; *ALDH18A1;* EC 2.7.2.41	bi- mono-allelic, AR/AD/ *de novo*	Development: Developmental delay, pre-postnatal growth retardation Neurologic: neurodegeneration, hypotonia, microcephaly, movement disorder Structural: hypomyelination, cortical atrophy and hypoplastic corpus callosum, tortuosity of brain vessels, cerebellar abnormalities Dermatologic (only cutis laxa): thin wrinked skin with visible veins. Ophthalmologic: neonatal cataract, corneal clouding, nystagmus	Plasma: hyperammonemia, ↓ proline, ↓ornithine, ↓citrulline (SP), ↓ arginine, = glutamine, = alanine MRS: ↓ creatine SP specific: ↓ citrulline, low sum of involved amino acids	65,66,68,70
Gyrate atrophy choroid & retina (258870) OAT; *OAT;* EC 2.6.1.13	bi-allelic, AR	Development: failure to thrive Neurologic: proximal muscle weakness Ophthalmologic: myopia, nyctalopia, infantile cataracts, progressive chorioretinal atrophy, adult blindness	Plasma: ↑ ornithine, ↓ creatine Urine: ↓ creatine, ↑ ornithine, ↑ lysine ↑ arginine Muscle biopsy: ↓ creatine, type II muscle fiber atrophy with tubular aggregates. Fibroblasts, leukoblasts: ↓ OAT activity Neonatal: reversed enzyme direction → ↓ citrulline, ↑ proline, ↓ ornithine, ↓ arginine, hyperammonemia , ↑ glutamine. Diagnosis: ↑ ratio proline/ citrulline	71-73

TABLE 1 CONTINUED.

Disorder (OMIM) enzyme; *gene;* EC code	Number of described cases if <10; Inheritance pattern	Clinical features	Biochemical diagnostics	Ref
		γ-glutamyl-cycle disorders		
γ-glutamyl-cysteine synthetase deficiency (230450) GCLC; *GCLC;* EC: 6.3.2.2	bi-allelic, AR	Development: Developmental delay Neurologic: late onset spinocerebellar degeneration, peripheral neuropathy, myopathy. Haematologic: infantile onset hemolytic anemia Gastro-intestinal: hepatosplenomegaly with transient jaundice	Erythrocytes: ↓ glutathione (<5%) ↓ y-glutamyl-cysteine Erythrocytes, leukocytes, fibroblasts: ↓GCLC activity (<10%) Urine: ↑ 5-oxoproline (excluding GSS deficiency)	75,77-79
5-oxoprolinase deficiency (260005) 5-OPase; *OPLAH;* EC: 3.5.2.9	n≥20 bi-allelic, AR	Unaffected / Inconsistent Gastro-intestinal: enterocolitis, diarrhea, vomiting, abdominal pain Nephrologic: unephrolithiasis	Urine: ↑ 5-oxoproline Erythrocytes: = glutathione (excluding GSS deficiency)	80-83

= normal levels; ↓ decreased levels; ↑ increased levels. Abbreviations: AR autosomal recessive; AD autosomal dominant; CSF cerebrospinal fluid; GLS glutaminase; GS glutamine synthetase; GLUL glutamate-ammonia ligase; P5CD pyrroline-5-carboxylate dehydrogenase; ALDH aldehyde dehydrogenase; TAT tyrosine aminotransferase; GABAT gamma-aminobutyric acid transferase; GAD1 glutamate decarboxylase; BCAT Branched-chain amino acid aminotransferase; ALT alanine aminotransferase; GPT glutamate pyruvate transferase; PSAT phosphoserine transaminase; NAGS N-acetylglutamate synthase; GDH; GLUD glutamate dehydrogenase; AST aspartate transaminase, GOT glutamic oxaloacetic transaminase; P5CS pyrroline-5-carboxylate synthetase; OAT ornithine aminotransferase; GCLC Glutamate-Cysteine Ligase Catalytic Subunit; 5-OPase 5-oxoprolinase.

DISCUSSION

Inborn errors in enzymes of glutamate metabolism lead to distinct clinical and biochemical phenotypes, which can be classified in disorders affecting amino acid metabolism, the urea cycle or ammonia metabolism and the γ-glutamyl cycle. In this review, we provide an overview of the clinical and biochemical phenotype of these defects in an effort to ease the recognition of these ultra-rare metabolic disorders and to create insight into their pathophysiology and the contributing role of deviant glutamate and glutamine concentrations.

Glutamate and glutamine concentrations are most aberrant in defects of the two enzymes directly interconverting these amino acids: GLS and GS. Interestingly, in GLS hyperactivity, glutamate and glutamine levels are normal in plasma and CSF, while both are deviant when analyzed using brain MRS and in urine in line with tissue specific expression of GLS[18]. The discrepancy between CSF and brain MRS might be explained by the degree to which glutamate and glutamine levels are controlled by GLS. CSF is formed out of plasma by the plexus choroid, which consists of glial cells in which glutamate and glutamine levels are regulated by GS rather than GLS[95 96]. This illustrates that normal CSF values do not exclude the possibility of abnormal glutamate values in the brain. Brain MRSI might therefore be indicated when a defect in glutamate metabolism is suspected. MRSI clinical field strength is a suitable approach for this. A higher magnetic field can even distinguish the closely positioned glutamine and glutamate peaks better and can even show regional differences of these metabolites.

In patients with GLS or GS loss-of-function, glutamine concentrations were deviant in blood-spots or plasma, while glutamate was normal, possibly due to dietary intake and other glutamate metabolizing enzymes. Local glutamate deficiency in the brain may, however, contribute to the epileptic phenotype in GLS loss-of-function, given the role of glutamate as the main neurotransmitter.

Interestingly, both glutamine deficiency and glutamate excess may disturb the cellular redox status. In GS deficiency, glutamine deficiency results in reduced NAD^+ synthesis, which plays an important role in redox reactions[6]. In GLS hyperactivity, glutamate excess is postulated to decreased redox buffer capacity[18]. As oxidative stress is associated with cataract, neurodegenerative disorders and epilepsy, this is a likely key player in the pathophysiology of these inborn errors of glutamate metabolism[10,19,97].

In UCDs, glutamine concentrations are increased as a consequence of hyperammonemia.

It is remarkable that both glutamine excess (in these UCDs) and glutamine deficiency (in GS deficiency) can be accompanied by hyperammonemia, which is likely to play a pathophysiological role in these inborn errors. In primary UCD's, glutamine concentrations are increased putatively as a consequence of hyperammonemia-induced GS in an attempt to detoxify ammonia[5,98]. Conversely, glutamine concentrations remain normal despite hyperammonemia in GOT2 deficiency, P5CS deficiency and GDH hyperactivity. In these disorders, hyperammonemia is mild and might therefore not trigger excess glutamine formation.

In all other inborn errors of glutamate metabolism, glutamate concentrations have not been reported, therefore being presumed to be normal. If true, this points to the regulation of glutamate levels by other enzymes of glutamate metabolism. The pathogenesis of these other errors is often ascribed to deficiency or toxic accumulation of substrate or product of the defective enzyme, as explicated in the main text above. However, as seen in GLS hyperactivity, normal concentrations of glutamate and glutamine in plasma and CSF do not exclude local alterations, which might contribute to the pathophysiology as well. Even more locally oriented, in the patient with GABAT deficiency no abnormalities were detected in plasma or CSF, but locally decreased glutamate concentrations in the semi-oval region of the brain were detected on brain MRS and might possibly play a pathogenic role[99]. Also, mildly decreased glutamine concentrations or mildly increased glutamate concentrations may have been detected but attributed to pre-analytical conditions rather than a reflection of *in vivo* metabolism as glutamine is easily spontaneously interconverted into glutamate therefore. The study of glutamate and glutamine and their ratio in carefully collected body fluids -as performed in GS deficiency and GLS hyperactivity- may elucidate alterations of glutamate and glutamine levels in inborn errors of glutamate metabolism. Several *in vivo* techniques are available to study glutamate and glutamine separately, for an overview see Ramadan et al[100].

Inborn errors of metabolism that have a related biochemical ground often have similar clinical features. Drawing phenotypic parallels of all seventeen inborn errors (both HPO phenotypic subclasses and their correlated superclasses) provided interesting leads towards similar pathophysiology. Neurologically, developmental delay, seizures and hypotonia are more common in these inborn errors compared to the prevalence in Mendelian disorders in general, in line with the role of glutamate as the main neurotransmitter (Supplemental Table 1). It is however remarkable that the patient with GLS hyperactivity and glutamate excess in the brain did not develop seizures. Glutamate induces myelination of axons and it is therefore not surprising that white matter and myelin abnormalities are frequently reported in patients with an inborn error of glutamate metabolism[2]. Although this is an

a-specific sign seen in many disorders, it is 4.6-37.5x more prevalent in glutamate related disorders than in all Mendelian disorders.

Interestingly, ectodermal structures seem more affected in inborn errors of glutamate metabolism as both neurologic abnormalities, skin and lens abnormalities are seen. Other ophthalmological features that are seen in glutamate related disorders are optic atrophy in some GLS loss patients; herpetiform corneal ulcerations in patients with TAT deficiency; chorioretinal atrophy in OAT deficient patients; and retinal degeneration in BCAT2 deficient patients. Interestingly, the brain, skin, lens, optic nerve, cornea, and retina are all of ectodermal origin and therefore share similarities in expression and regulation of glutamate receptors[101-103]. This suggests that disturbed glutamate homeostasis might not only affect the brain, but also these other ectodermal structures.

Altogether, seventeen defects of enzymes that directly metabolize glutamate have been described so far, affecting amino acid metabolism, the urea cycle and the γ-glutamyl cycle. Data on glutamate and glutamine concentrations in patients with inborn errors in enzymes of glutamate metabolism should be measured and collected as they provide additional insight into the contributing role of deviant concentrations of these amino acids in the pathophysiology.

SUPPLEMENTARY FILES

TABLE S1.

REFERENCES

1. Yelamanchi SD, Jayaram S, Thomas JK, et al. A pathway map of glutamate metabolism. *J Cell Commun Signal.* 2016;10(1):69-75.
2. Mount CW, Monje M. Wrapped to Adapt: Experience-Dependent Myelination. *Neuron.* 2017;95(4):743-756.
3. Zhou Y, Danbolt NC. Glutamate as a neurotransmitter in the healthy brain. *J Neural Transm (Vienna).* 2014;121(8):799-817.
4. Lu SC. Regulation of glutathione synthesis. *Mol Aspects Med.* 2009;30(1-2):42-59.
5. Hakvoort TB, He Y, Kulik W, et al. Pivotal role of glutamine synthetase in ammonia detoxification. *Hepatology.* 2017;65(1):281-293.
6. Hu L, Ibrahim K, Stucki M, et al. Secondary NAD+ deficiency in the inherited defect of glutamine synthetase. *J Inherit Metab Dis.* 2015;38(6):1075-1083.
7. Cory JG, Cory AH. Critical roles of glutamine as nitrogen donors in purine and pyrimidine nucleotide synthesis: Asparaginase treatment in childhood acute lymphoblastic leukemia. *In Vivo.* 2006;20(5):587-589.
8. Altman BJ, Stine ZE, Dang CV. From Krebs to clinic: glutamine metabolism to cancer therapy. *Nat Rev Cancer.* 2016;16(10):619-634.
9. Zhang J, Pavlova NN, Thompson CB. Cancer cell metabolism: the essential role of the nonessential amino acid, glutamine. *EMBO J.* 2017;36(10):1302-1315.
10. Dong XX, Wang Y, Qin ZH. Molecular mechanisms of excitotoxicity and their relevance to pathogenesis of neurodegenerative diseases. *Acta Pharmacol Sin.* 2009;30(4):379-387.
11. Miladinovic T, Nashed MG, Singh G. Overview of Glutamatergic Dysregulation in Central Pathologies. *Biomolecules.* 2015;5(4):3112-3141.
12. Scott TR, Kronsten VT, Hughes RD, Shawcross DL. Pathophysiology of cerebral oedema in acute liver failure. *World J Gastroenterol.* 2013;19(48):9240-9255.
13. Krebs HA. Metabolism of amino-acids: The synthesis of glutamine from glutamic acid and ammonia, and the enzymic hydrolysis of glutamine in animal tissues. *Biochem J.* 1935;29(8):1951-1969.
14. Haussinger D, Gerok W. Regulation of hepatic glutamate metabolism. Role of 2-oxoacids in glutamate release from isolated perfused rat liver. *Eur J Biochem.* 1984;143(3):491-497.
15. Meister A. Glutamine synthetase from mammalian tissues. *Methods Enzymol.* 1985;113:185-199.
16. Aledo JC, Gomez-Fabre PM, Olalla L, Marquez J. Identification of two human glutaminase loci and tissue-specific expression of the two related genes. *Mamm Genome.* 2000;11(12):1107-1110.
17. Curthoys NP, Watford M. Regulation of glutaminase activity and glutamine metabolism. *Annu Rev Nutr.* 1995;15:133-159.
18. Rumping L, Tessadori F, Pouwels PJW, et al. GLS hyperactivity causes glutamate excess, infantile cataract and profound developmental delay. *Hum Mol Genet.* 2019;28(1):96-104.
19. Spector A. Oxidative stress-induced cataract: mechanism of action. *FASEB J.* 1995;9(12):1173-1182.
20. Brodie MJ, Besag F, Ettinger AB, et al. Epilepsy, Antiepileptic Drugs, and Aggression: An Evidence-Based Review. *Pharmacol Rev.* 2016;68(3):563-602.

21. Rumping L, Buttner B, Maier O, et al. Identification of a Loss-of-Function Mutation in the Context of Glutaminase Deficiency and Neonatal Epileptic Encephalopathy. *JAMA Neurol.* 2018.
22. Butterworth RF. Pathophysiology of brain dysfunction in hyperammonemic syndromes: The many faces of glutamine. *Mol Genet Metab.* 2014;113(1-2):113-117.
23. Lynch DS, Chelban V, Vandrovcova J, Pittman A, Wood NW, Houlden H. GLS loss of function causes autosomal recessive spastic ataxia and optic atrophy. *Ann Clin Transl Neurol.* 2018;5(2):216-221.
24. Spodenkiewicz M, Diez-Fernandez C, Rufenacht V, Gemperle-Britschgi C, Haberle J. Minireview on Glutamine Synthetase Deficiency, an Ultra-Rare Inborn Error of Amino Acid Biosynthesis. *Biology (Basel).* 2016;5(4).
25. Haberle J, Shahbeck N, Ibrahim K, et al. Glutamine supplementation in a child with inherited GS deficiency improves the clinical status and partially corrects the peripheral and central amino acid imbalance. *Orphanet J Rare Dis.* 2012;7:48.
26. Unal O, Ceylaner S, Akin R. A Very Rare Etiology of Hypotonia and Seizures: Congenital Glutamine Synthetase Deficiency. *Neuropediatrics.* 2018.
27. Braissant O, McLin VA, Cudalbu C. Ammonia toxicity to the brain. *J Inherit Metab Dis.* 2013;36(4):595-612.
28. Eelen G, Dubois C, Cantelmo AR, et al. Role of glutamine synthetase in angiogenesis beyond glutamine synthesis. *Nature.* 2018;561(7721):63-69.
29. Hu CA, Lin WW, Valle D. Cloning, characterization, and expression of cDNAs encoding human delta 1-pyrroline-5-carboxylate dehydrogenase. *J Biol Chem.* 1996;271(16):9795-9800.
30. Valle D, Goodman SI, Harris SC, Phang JM. Genetic evidence for a common enzyme catalyzing the second step in the degradation of proline and hydroxyproline. *J Clin Invest.* 1979;64(5):1365-1370.
31. Valle DL, Phang JM, Goodman SI. Type 2 hyperprolinemia: absence of delta1-pyrroline-5-carboxylic acid dehydrogenase activity. *Science.* 1974;185(4156):1053-1054.
32. Farrant RD, Walker V, Mills GA, Mellor JM, Langley GJ. Pyridoxal phosphate de-activation by pyrroline-5-carboxylic acid. Increased risk of vitamin B6 deficiency and seizures in hyperprolinemia type II. *J Biol Chem.* 2001;276(18):15107-15116.
33. Walker V, Mills GA, Peters SA, Merton WL. Fits, pyridoxine, and hyperprolinaemia type II. *Arch Dis Child.* 2000;82(3):236-237.
34. Stockler S, Plecko B, Gospe SM, Jr., et al. Pyridoxine dependent epilepsy and antiquitin deficiency: clinical and molecular characteristics and recommendations for diagnosis, treatment and follow-up. *Mol Genet Metab.* 2011;104(1-2):48-60.
35. Scott CR. The genetic tyrosinemias. *Am J Med Genet C Semin Med Genet.* 2006;142C(2):121-126.
36. Pena-Quintana L, Scherer G, Curbelo-Estevez ML, et al. TYROSINEMIA TYPE II: Mutation update, eleven novel mutations and description of five independent subjects with a novel founder mutation. *Clin Genet.* 2017.
37. Ichikawa K, Tsuji M, Tsuyusaki Y, Tomiyasu M, Aida N, Goto T. Serial Magnetic Resonance Imaging and (1) H-Magnetic Resonance Spectroscopy in GABA Transaminase Deficiency: A Case Report. *JIMD Rep.* 2018.
38. Koenig MK, Hodgeman R, Riviello JJ, et al. Phenotype of GABA-transaminase deficiency. *Neurology.*

2017;88(20):1919-1924.

39. Tsuji M, Aida N, Obata T, et al. A new case of GABA transaminase deficiency facilitated by proton MR spectroscopy. *J Inherit Metab Dis.* 2010;33(1):85-90.
40. Lynex CN, Carr IM, Leek JP, et al. Homozygosity for a missense mutation in the 67 kDa isoform of glutamate decarboxylase in a family with autosomal recessive spastic cerebral palsy: parallels with Stiff-Person Syndrome and other movement disorders. *BMC Neurol.* 2004;4(1):20.
41. Wang XL, Li CJ, Xing Y, Yang YH, Jia JP. Hypervalinemia and hyperleucine-isoleucinemia caused by mutations in the branched-chain-amino-acid aminotransferase gene. *J Inherit Metab Dis.* 2015;38(5):855-861.
42. Jeune M, Collombel, C., Michel, M., David, M., Guibaud, P., Guerrier, G., Albert, J. . Hyperleucinisoleucinemie par defaut partiel de transamination associee a une hyperprolinemie de type 2: observation familiale d'une double aminoacidopathie. *Ann. Pediat.* 1970;17: 85-99.
43. Teslovich TM, Kim DS, Yin X, et al. Identification of seven novel loci associated with amino acid levels using single-variant and gene-based tests in 8545 Finnish men from the METSIM study. *Hum Mol Genet.* 2018;27(9):1664-1674.
44. Hull J, Hindy ME, Kehoe PG, Chalmers K, Love S, Conway ME. Distribution of the branched chain aminotransferase proteins in the human brain and their role in glutamate regulation. *J Neurochem.* 2012;123(6):997-1009.
45. Hull J, Patel VB, Hutson SM, Conway ME. New insights into the role of the branched-chain aminotransferase proteins in the human brain. *J Neurosci Res.* 2015;93(7):987-998.
46. McBrayer SK, Mayers JR, DiNatale GJ, et al. Transaminase Inhibition by 2-Hydroxyglutarate Impairs Glutamate Biosynthesis and Redox Homeostasis in Glioma. *Cell.* 2018.
47. Ouyang Q, Nakayama T, Baytas O, et al. Mutations in mitochondrial enzyme GPT2 cause metabolic dysfunction and neurological disease with developmental and progressive features. *Proc Natl Acad Sci U S A.* 2016;113(38):E5598-5607.
48. Celis K, Shuldiner S, Haverfield EV, et al. Loss of function mutation in glutamic pyruvate transaminase 2 (GPT2) causes developmental encephalopathy. *J Inherit Metab Dis.* 2015;38(5):941-948.
49. DeRosa G, Swick RW. Metabolic implications of the distribution of the alanine aminotransferase isoenzymes. *J Biol Chem.* 1975;250(20):7961-7967.
50. Glinghammar B, Rafter I, Lindstrom AK, et al. Detection of the mitochondrial and catalytically active alanine aminotransferase in human tissues and plasma. *Int J Mol Med.* 2009;23(5):621-631.
51. Baek JY, Jun DY, Taub D, Kim YH. Characterization of human phosphoserine aminotransferase involved in the phosphorylated pathway of L-serine biosynthesis. *Biochem J.* 2003;373(Pt 1):191-200.
52. Acuna-Hidalgo R, Schanze D, Kariminejad A, et al. Neu-Laxova syndrome is a heterogeneous metabolic disorder caused by defects in enzymes of the L-serine biosynthesis pathway. *Am J Hum Genet.* 2014;95(3):285-293.
53. Hart CE, Race V, Achouri Y, et al. Phosphoserine aminotransferase deficiency: a novel disorder of the serine biosynthesis pathway. *Am J Hum Genet.* 2007;80(5):931-937.
54. de Koning TJ, Klomp LW. Serine-deficiency syndromes. *Curr Opin Neurol.* 2004;17(2):197-204.

55. Caldovic L, Morizono H, Gracia Panglao M, et al. Cloning and expression of the human N-acetylglutamate synthase gene. *Biochem Biophys Res Commun.* 2002;299(4):581-586.
56. Ah Mew N, Simpson KL, Gropman AL, Lanpher BC, Chapman KA, Summar ML. Urea Cycle Disorders Overview (updated 2017). In: Adam MP, Ardinger HH, Pagon RA, et al., eds. *GeneReviews((R)).* Seattle (WA)1993.
57. Sancho-Vaello E, Marco-Marin C, Gougeard N, et al. Understanding N-Acetyl-L-Glutamate Synthase Deficiency: Mutational Spectrum, Impact of Clinical Mutations on Enzyme Functionality, and Structural Considerations. *Hum Mutat.* 2016;37(7):679-694.
58. Caldovic L, Morizono H, Panglao MG, Cheng SF, Packman S, Tuchman M. Null mutations in the N-acetylglutamate synthase gene associated with acute neonatal disease and hyperammonemia. *Hum Genet.* 2003;112(4):364-368.
59. Plaitakis A, Kalef-Ezra E, Kotzamani D, Zaganas I, Spanaki C. The Glutamate Dehydrogenase Pathway and Its Roles in Cell and Tissue Biology in Health and Disease. *Biology (Basel).* 2017;6(1).
60. Palladino AA, Stanley CA. The hyperinsulinism/hyperammonemia syndrome. *Rev Endocr Metab Disord.* 2010;11(3):171-178.
61. Grimaldi M, Karaca M, Latini L, Brioudes E, Schalch T, Maechler P. Identification of the molecular dysfunction caused by glutamate dehydrogenase S445L mutation responsible for hyperinsulinism/hyperammonemia. *Hum Mol Genet.* 2017;26(18):3453-3465.
62. Bahi-Buisson N, Roze E, Dionisi C, et al. Neurological aspects of hyperinsulinism-hyperammonaemia syndrome. *Dev Med Child Neurol.* 2008;50(12):945-949.
63. Ramos RJJK, C; Tarailo-Graovac, M; Skrypnyk, C; Lee van der, R; Drogemoller, B.I; Koster, J; Campeau, P; Ruiter, J; Ciapate, J; Kluijtmans, L.A.J; Jans, J.J.M; Ross, C.J; Wintjes, L.T; Rodenburg, R.J; Waterham, H.R; Wasserman, W.W; Wanders, R.J.A; Verhoeven-Duif, N.M; Wevers, R.A GOT2 deficiency: a novel disorder of the malate aspartate shuttle resulting in serine deficiency. *JIMD abstracts SSIEM 2018.* 2018.
64. Fischer-Zirnsak B, Escande-Beillard N, Ganesh J, et al. Recurrent De Novo Mutations Affecting Residue Arg138 of Pyrroline-5-Carboxylate Synthase Cause a Progeroid Form of Autosomal-Dominant Cutis Laxa. *Am J Hum Genet.* 2015;97(3):483-492.
65. Baumgartner MR, Rabier D, Nassogne MC, et al. Delta1-pyrroline-5-carboxylate synthase deficiency: neurodegeneration, cataracts and connective tissue manifestations combined with hyperammonaemia and reduced ornithine, citrulline, arginine and proline. *Eur J Pediatr.* 2005;164(1):31-36.
66. Martinelli D, Haberle J, Rubio V, et al. Understanding pyrroline-5-carboxylate synthetase deficiency: clinical, molecular, functional, and expression studies, structure-based analysis, and novel therapy with arginine. *J Inherit Metab Dis.* 2012;35(5):761-776.
67. Panza E, Escamilla-Honrubia JM, Marco-Marin C, et al. ALDH18A1 gene mutations cause dominant spastic paraplegia SPG9: loss of function effect and plausibility of a dominant negative mechanism. *Brain.* 2016;139(Pt 1):e3.
68. Coutelier M, Goizet C, Durr A, et al. Alteration of ornithine metabolism leads to dominant and recessive

hereditary spastic paraplegia. *Brain.* 2015;138(Pt 8):2191-2205.

69. de Koning TJ. Amino acid synthesis deficiencies. *J Inherit Metab Dis.* 2017;40(4):609-620.
70. Baumgartner MR, Hu CA, Almashanu S, et al. Hyperammonemia with reduced ornithine, citrulline, arginine and proline: a new inborn error caused by a mutation in the gene encoding delta(1)-pyrroline-5-carboxylate synthase. *Hum Mol Genet.* 2000;9(19):2853-2858.
71. de Sain-van der Velden MG, Rinaldo P, Elvers B, et al. The Proline/Citrulline Ratio as a Biomarker for OAT Deficiency in Early Infancy. *JIMD Rep.* 2012;6:95-99.
72. Cleary MA, Dorland L, de Koning TJ, et al. Ornithine aminotransferase deficiency: diagnostic difficulties in neonatal presentation. *J Inherit Metab Dis.* 2005;28(5):673-679.
73. Ginguay A, Cynober L, Curis E, Nicolis I. Ornithine Aminotransferase, an Important Glutamate-Metabolizing Enzyme at the Crossroads of Multiple Metabolic Pathways. *Biology (Basel).* 2017;6(1).
74. Ohashi K, Kageyama M, Shinomiya K, et al. Spermidine Oxidation-Mediated Degeneration of Retinal Pigment Epithelium in Rats. *Oxid Med Cell Longev.* 2017;2017:4128061.
75. Sierra-Rivera E, Summar ML, Dasouki M, Krishnamani MR, Phillips JA, Freeman ML. Assignment of the gene (GLCLC) that encodes the heavy subunit of gamma-glutamylcysteine synthetase to human chromosome 6. *Cytogenet Cell Genet.* 1995;70(3-4):278-279.
76. Kondo T. [Impaired glutathione metabolism in hemolytic anemia]. *Rinsho Byori.* 1990;38(4):355-359.
77. Konrad PN, Richards F, 2nd, Valentine WN, Paglia DE. Glutamyl-cysteine synthetase deficiency. A cause of hereditary hemolytic anemia. *N Engl J Med.* 1972;286(11):557-561.
78. Ristoff E, Augustson C, Geissler J, et al. A missense mutation in the heavy subunit of gamma-glutamylcysteine synthetase gene causes hemolytic anemia. *Blood.* 2000;95(7):2193-2196.
79. Almusafri F, Elamin HE, Khalaf TE, Ali A, Ben-Omran T, El-Hattab AW. Clinical and molecular characterization of 6 children with glutamate-cysteine ligase deficiency causing hemolytic anemia. *Blood Cells Mol Dis.* 2017;65:73-77.
80. Watanabe T, Abe K, Ishikawa H, Iijima Y. Bovine 5-oxo-L-prolinase: simple assay method, purification, cDNA cloning, and detection of mRNA in the coronary artery. *Biol Pharm Bull.* 2004;27(3):288-294.
81. Larsson A, Mattsson B, Wauters EA, van Gool JD, Duran M, Wadman SK. 5-oxoprolinuria due to hereditary 5-oxoprolinase deficiency in two brothers--a new inborn error of the gamma-glutamyl cycle. *Acta Paediatr Scand.* 1981;70(3):301-308.
82. Sass JO, Gemperle-Britschgi C, Tarailo-Graovac M, et al. Unravelling 5-oxoprolinuria (pyroglutamic aciduria) due to bi-allelic OPLAH mutations: 20 new mutations in 14 families. *Mol Genet Metab.* 2016;119(1-2):44-49.
83. Calpena E, Deshpande AA, Yap S, et al. New insights into the genetics of 5-oxoprolinase deficiency and further evidence that it is a benign biochemical condition. *Eur J Pediatr.* 2015;174(3):407-411.
84. Pavone L, Mollica F, Levy HL. Asymptomatic type II hyperprolinaemia associated with hyperglycinaemia in three sibs. *Arch Dis Child.* 1975;50(8):637-641.
85. Wyse AT, Netto CA. Behavioral and neurochemical effects of proline. *Metab Brain Dis.* 2011;26(3):159-172.

86. Rettenmeier R, Natt E, Zentgraf H, Scherer G. Isolation and characterization of the human tyrosine aminotransferase gene. *Nucleic Acids Res.* 1990;18(13):3853-3861.

87. Roberts E, Frankel S. gamma-Aminobutyric acid in brain: its formation from glutamic acid. *J Biol Chem.* 1950;187(1):55-63.

88. Medina-Kauwe LK, Tobin AJ, De Meirleir L, et al. 4-Aminobutyrate aminotransferase (GABA-transaminase) deficiency. *J Inherit Metab Dis.* 1999;22(4):414-427.

89. Yang RZ, Blaileanu G, Hansen BC, Shuldiner AR, Gong DW. cDNA cloning, genomic structure, chromosomal mapping, and functional expression of a novel human alanine aminotransferase. *Genomics.* 2002;79(3):445-450.

90. Shapira Zaltsberg G, McMillan HJ, Miller E. Phosphoserine aminotransferase deficiency: imaging findings in a child with congenital microcephaly. *J Matern Fetal Neonatal Med.* 2018:1-3.

91. Takanashi J, Barkovich AJ, Cheng SF, et al. Brain MR imaging in neonatal hyperammonemic encephalopathy resulting from proximal urea cycle disorders. *AJNR Am J Neuroradiol.* 2003;24(6):1184-1187.

92. Caldovic L, Morizono H, Tuchman M. Mutations and polymorphisms in the human N-acetylglutamate synthase (NAGS) gene. *Hum Mutat.* 2007;28(8):754-759.

93. Hsu BY, Kelly A, Thornton PS, Greenberg CR, Dilling LA, Stanley CA. Protein-sensitive and fasting hypoglycemia in children with the hyperinsulinism/hyperammonemia syndrome. *J Pediatr.* 2001;138(3):383-389.

94. De Lonlay P, Benelli C, Fouque F, et al. Hyperinsulinism and hyperammonemia syndrome: report of twelve unrelated patients. *Pediatr Res.* 2001;50(3):353-357.

95. Bak LK, Schousboe A, Waagepetersen HS. The glutamate/GABA-glutamine cycle: aspects of transport, neurotransmitter homeostasis and ammonia transfer. *J Neurochem.* 2006;98(3):641-653.

96. Blau N, Duran M, Gibson KM. *Laboratory Guide to the Methods in Biochemical Genetics.* Heidelberg Berlin: Springer; 2008.

97. Shin EJ, Jeong JH, Chung YH, et al. Role of oxidative stress in epileptic seizures. *Neurochem Int.* 2011;59(2):122-137.

98. Suarez I, Bodega G, Fernandez B. Glutamine synthetase in brain: effect of ammonia. *Neurochem Int.* 2002;41(2-3):123-142.

99. Bahi-Buisson N, El Sabbagh S, Soufflet C, et al. Myoclonic absence epilepsy with photosensitivity and a gain of function mutation in glutamate dehydrogenase. *Seizure-Eur J Epilep.* 2008;17(7):658-664.

100. Ramadan S, Lin A, Stanwell P. Glutamate and glutamine: a review of in vivo MRS in the human brain. *NMR Biomed.* 2013;26(12):1630-1646.

101. Farooq M, Kaswala RH, Kleiman NJ, Kasinathan C, Frederikse PH. GluA2 AMPA glutamate receptor subunit exhibits codon 607 Q/R RNA editing in the lens. *Biochem Biophys Res Commun.* 2012;418(2):273-277.

102. Genever PG, Maxfield SJ, Kennovin GD, et al. Evidence for a novel glutamate-mediated signaling pathway in keratinocytes. *J Invest Dermatol.* 1999;112(3):337-342.

103. Skerry TM, Genever PG. Glutamate signalling in non-neuronal tissues. *Trends Pharmacol Sci.* 2001;22(4):174-181.

Chapter 6

Fluorescence microscopy with UV-illumination allows accurate visualization of cataract in zebrafish embryos *in vivo*

Submitted

Lynne Rumping, Anko M. de Graaff, Peter A.W. Schellekens, Federico Tessadori, Melanie Kalee, Jeroen Bakkers, Gijs van Haaften, Roderick H.J. Houwen, Judith J.M. Jans, Nanda M Verhoeven-Duif, Peter M van Hasselt

ABSTRACT

The zebrafish (*Danio rerio*) is a powerful model system to study ophthalmological disease caused by genetic defects. Several microscopic methods have been developed to study cataract in zebrafish *in vivo*. These however require either advanced microscopic techniques, staining or genetic modification to emit fluorescence, or detect cataract indirectly. To address this issue, we developed Fluorescence microscopy with UV-light Illumination (FUVI). To study its potential, this method was applied to visualize the lens of *Cloche*^{m39} and *GLS1*-S482C zebrafish embryos -postulated to develop different types of cataract- and compared with confocal reflection microscopy, an established method to detect cataract in zebrafish. Confocal microscopy detected lens abnormalities in *Cloche*^{m39} zebrafish, as well as gross lens abnormalities in *GLS1*-S482C zebrafish. It could however not detect the more subtle abnormalities in *GLS1*-S482C zebrafish. FUVI allowed accurate visualization of the lens and of detailed and dispersed structures likely representing protein aggregation in the *GLS1*-S482C zebrafish lens, as well as diffuse opacity in the *Cloche*^{m39} zebrafish lens representing the remaining presence of a nucleus. These findings illustrate that FUVI allows sensitive and detailed imaging of lens abnormalities in living zebrafish embryos, without the need of staining or genetic engineering to create a fluorescence reporter. As one image represents a large depth of field, serial section imaging is not required, allowing high-speed data acquisition. The false negative results of confocal microscopy in *GLS1*-S482C zebrafish request awareness for false negative conclusions, therefore applying additional microscopic methods before drawing conclusions should be considered. Hereby, we provide a valuable method to visualize different types of cataracts *in vivo* in zebrafish embryos, which can be used to identify new genetic causes of cataract and to study its pathophysiology.

INTRODUCTION

Cataract, opacification of the lens, is one of the main causes of visual impairment and affects approximately 94 million people worldwide[1]. Lens transparency is important for optimal vision and is achieved by embryonic devascularization of the lens, denucleation of its cells and a protective mechanism in which crystallins prevent damaged proteins from aggregation [2,3]. Genetic mutations disrupting any of these elements can initiate opacification of the lens in specific appearance. The zebrafish (*Danio rerio*) is a powerful model organism to study ophthalmological pathology. The zebrafish eye closely resembles the human eye with regard to gene expression and morphology. Additionally, the relatively large eyes, transparent embryos and the fast reproduction and *ex-utero* development make the zebrafish a very suitable model organism [4,5]. Indeed, the zebrafish has been used as a model system in the elucidation of 7 novel genetic diseases [6-15].

Several microscopic methods have been developed to detect cataract in zebrafish *in vivo*, all with their own properties and advantages. These however require advanced microscopes, staining or genetic modification to emit fluorescence, they detect cataract indirectly or they provide images with low acquisition speed and resolution. Confocal reflection microscopy uses laser light which is reflected by lens opacities and imaged as scattering by a detector [6]. Although this indirect detection of cataract enables quantification of opacity, the scattering is an inaccurate visualization of the lens. Negative results are pictured as black fields, thereby hampering the interpretation of the data. Additionally, serial sections are required to create a large depth of field. Coaxial reflected light stereomicroscopy also uses reflected light, positioned in a different angle enabling detailed imaging of the whole lens [16]. This method is easily accessible and resembles slit lamp microscopy used to diagnose human cataract. The resolution of light microscopy is however low. Selective plane illumination microscopy also uses a narrow light beam, but additionally needs fluorescence staining to image the lens *in vivo* [17].

We developed a Fluorescence microscopy method based on UV-light Illumination (FUVI) to visualize the zebrafish lens and previously applied this method to identify a new genetic cause of infantile cataract[15]. Here, we enlighten this microscopic method and illustrate that it allows sensitive and high-speed imaging of different kinds of lens opacities in living zebrafish embryos, without the need for staining or genetic engineering to create a fluorescence reporter.

MATERIALS AND METHODS

ANIMALS

Animal experiments were approved by the Animal Experimentation Committee of the Royal Netherlands Academy of Arts and Sciences (KNAW). Tübingen Longfin (TL) wild-type zebrafish were used. *Cloche*^{m39} zebrafish embryos were kindly obtained from professor Stainier[18]. *GLS1*-S482C mutant zebrafish embryos were obtained as previously described by Rumping et al[15]. *Cloche*^{m39} siblings (heterozygous or wildtype) and unmodified wildtype zebrafish were used as controls. The zebrafish were kept under standard laboratory conditions in E3 medium at a temperature of 28.5°C. Before *in vivo* imaging at 5 days post fertilization (dpf), the zebrafish were anaesthetized in 16mg/ml Tricaine (MS22) in E3 and mounted in 0.25% agarose (w/v) prepared in E3.

CONFOCAL REFLECTION MICROSCOPY

Confocal reflection microscopy was performed as previously described using a Leica TCS SP8 (Leica Microsystems) confocal laser-scanning microscope fitted to a DMI6000 inverted microscope with a 488nm solid state laser[6]. Serial sections were obtained at 1µm intervals under the reflected light mode.

FLUORESCENCE MICROSCOPY WITH UV-LIGHT ILLUMINATION

Images were acquired using a Leica AF7000 fluorescence microscope equipped with a Leica DFC365FX camera, 20x NA 0.4 objective, Leica EL6000 External light source and a Leica A4 filter cube (BP340-380/400/BP450-490). The Leica LAS-AF software was used to capture the images. The acquired images were linearly edited with ImageJ and Adobe Photoshop.

DESIGN

Fluorescence microscopy induces auto-fluorescence which allows *in vivo* visualization of the eye. The depth at which auto-fluorescence is induced is wavelength dependent. The optimum combination of excitation and emission filters -selecting light with specific wavelengths that characteristically penetrate structures- were selected to reach the optimum depth in the eye to most accurately image the lens. The UV-light created with the BP340-380 UV-filter allows excitation of molecules from the deeper part of the lens, generating auto-fluorescence. This emitted light is blocked by lens opacities -when present- allowing detailed visualization of these structures. Reflected excitation light is blocked by a dichroic mirror before it reaches the camera and is thereby not visualized (fig. 1).

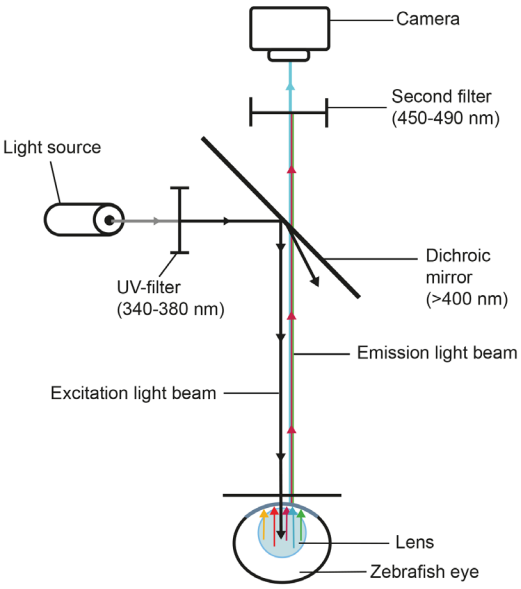

FIGURE 1. Experimental setup of fluorescence microscopy with UV-illumination. The light source is a mercury-vapor lamp and produces white light. This excitation light passes a UV-filter -letting light pass with a wavelength between 340 and 380nm- and is reflected towards the specimen by a dichroic mirror. Molecules in the deeper part of the lens of the zebrafish are excited and emit light with a broad spectrum of wavelengths. Light with wavelengths above 400nm passes through the dichroic mirror and a 450-490nm filter and is detected by a digital camera.

RESULTS

Two genetic zebrafish models known to develop cataract were studied: *Cloche*^{m39} and *GLS1*-S482C zebrafish. *Cloche*^{m39} zebrafish develop cataract due to the absence of denucleation of lens cells[6,7,18]. In *GLS1*-S482C zebrafish, cataract is postulated to develop due to protein aggregation secondary to oxidative stress[15]. We applied both confocal reflection microscopy -an established technique to detect cataract in zebrafish - and FUVI to the same zebrafish lenses[6,7].

CONFOCAL MICROSCOPY

Lens opacities were visualized using confocal microscopy in *Cloche*^{m39} zebrafish by the detection of reflected light in the center of the lens (9/12), while these were absent in wildtype *Cloche*^{m39} siblings (0/9) (fig. 2A.1, S1A.1) (fig. 2A.2, S1A.2). It thereby illustrated its

ability to detect diffuse cataract. Confocal microscopy however did not detect reflected light in *GLS1*-S482C zebrafish (fig. 2A.3, S2A.1), with the exception of one zebrafish (fig. 2A.4). No cataract was detected in wildtype zebrafish (0/3) used as controls (fig. 2A.5 and S2A.2).

TESTING THE ABILITY OF FUVI FOR DETECTION OF DIFFERENT TYPES OF CATARACTS

FUVI visualized diffuse opacities in *Cloche*^{m39} zebrafish (12/12) in the whole surface of the lens, corresponding to the remaining presence of a nucleus. Additionally, increased central auto-fluorescence was detected (fig. 2B.1, S1B.1) at the same location as the reflected light detected by confocal microscopy. This is likely due to an optimum of opacities in this deepest location of the cylindrically shaped lens. No cataract was detected in *Cloche*^{m39} siblings (0/9) (fig. 2B.2, S1B.2). In *GLS1*-S482C zebrafish, FUVI allowed visualization of dispersed, subtle structures in the lens in detail (8/8) (fig 2B.3, 2B.4, S2B.1). These structures most likely represent protein aggregation. The one zebrafish lens in which confocal microscopy detected reflected light, exhibited extensive opacities when visualized by fluorescence microscopy (fig. 2B.4). In the other lenses, in which confocal microscopy could not detect opacities, these were milder but could be visualized by FUVI. Opacities were not detected in wildtype zebrafish (fig. 2B.5, S2B.2).

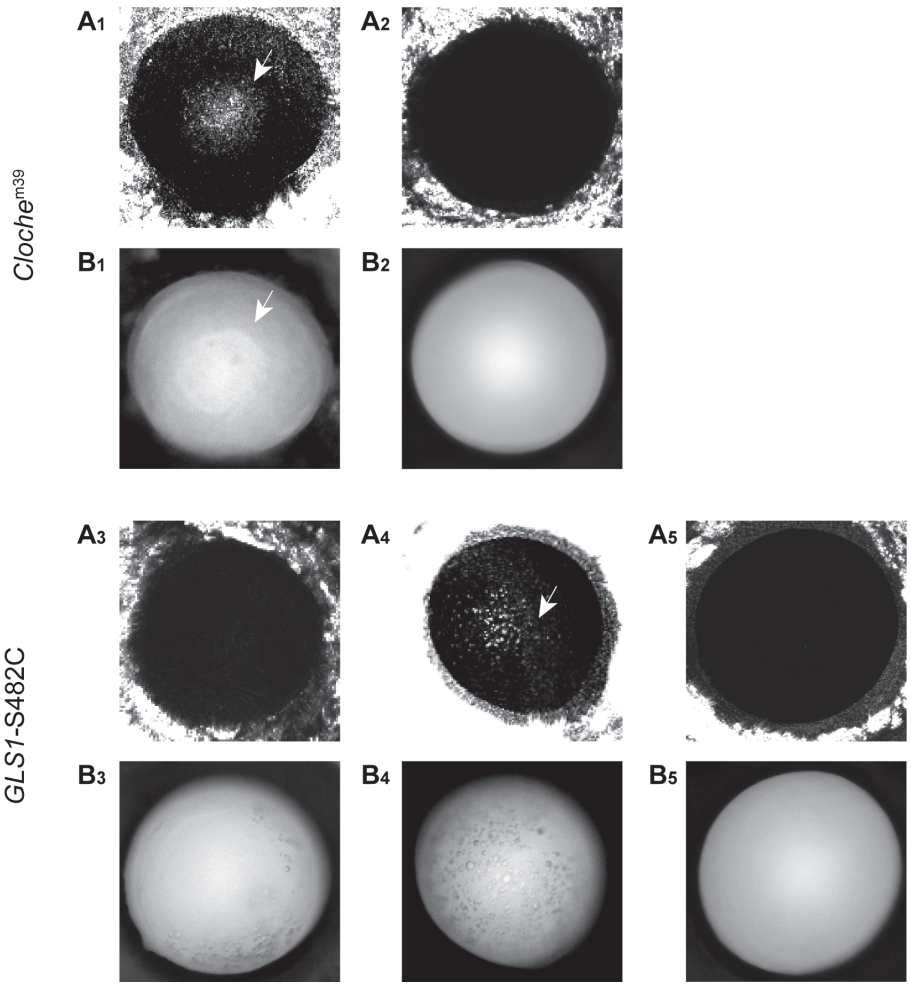

FIGURE 2. *Cloche*^{m39} and *GLS1*-S482C zebrafish lenses imaged by confocal reflection microscopy (A) and FUVI (B). Images aligned vertically represent the same lens. Additional results are shown in supplementary figures S1 and S2. **(A)** Confocal reflection microscopy. In *Cloche*^{m39} zebrafish, reflected light was detected in 9/12 lenses (A1). In all siblings, a clear lens was visualized (A2). In *GLS1*-S482C zebrafish, reflected light was not detected in 7/8 lenses (A3). In one lens, confocal microscopy did detect reflected light (white arrow) (A4). In all wildtype zebrafish a clear lens was visualized (A5). **(B)** Fluorescent microscopy with UV-Illumination. In *Cloche*^{m39} zebrafish, FUVI visualized diffuse opacity and increased central auto-fluorescence in all lenses (white arrow). This image is representative for 12 lenses (B1). In all 9 wildtype *Cloche*^{m39} siblings, a clear lens was visualized (B2). In the *GLS1*-S482C zebrafish lens, dispersed structures were imaged. This image is representative for 8 lenses (B3). In one of these lenses in which confocal microscopy did detect reflected light, extensive abnormalities were visualized with FUVI (B4). In all 3 wildtype zebrafish a clear lens was imaged (B5).

DISCUSSION

This study shows that fluorescence microscopy with UV-light allows sensitive and detailed visualization of the zebrafish lens *in vivo* by detecting lens abnormalities ranging from local subtle structures to diffuse opacity. The method was compared to the established confocal reflection microscopic method.

FUVI offers a number of advantages, complementary to current techniques. First, it is easily accessible as it does not require serial section imaging since one image represents a large depth of field. Second, staining or genetic engineering to create fluorescence are not required, as UV-illumination generates auto-fluorescence by excitation of molecules in the lens. Both these properties allow high-speed data acquisition. Third, fluorescence microscopy contains high quality objectives and uses a camera instead of a detector, allowing high resolution imaging.

In this study, FUVI allowed sensitive visualization of cataract in both *GLS1*-S482C and *Cloche*^{m39} zebrafish. Confocal microscopy enabled to detect these subtle structures in the lens of *GLS1*-S482C zebrafish as well, but only when extensively present. The higher sensitivity of FUVI is also illustrated by the observation that FUVI could detect diffuse opacities in all *Cloche*^{m39} zebrafish embryos, while confocal microscopy could only detect opacities in 6/9 zebrafish embryos. The higher sensitivity of fluorescence microscopy may be explained by a more efficient blockade of emitted fluorescence light -generated in the whole lens with low intensity- by lens opacities compared to laser light used in confocal microscopy, which is focused and has high intensity and therefore needs denser structures to be reflected. Conversely, the false negative results for more subtle opacities in *GLS1*--S482C zebrafish by confocal microscopy can be regarded as a cautionary note: not lens abnormalities can be detected with the same microscopic method, therefore a causal correlation between a genetic defect and cataracts should not be withdrawn without the application of additional microscopic methods. The potential of FUVI to study different types of cataracts in other zebrafish models, such as those developing osmotic cataract in addition to cataracts caused by oxidative stress and the absence of denucleation, are needed to verify whether all types of cataract can be detected with this imaging technique.

FUVI might be valuable for both the study of genetic causes of cataracts and the pathophysiology. By applying it to genetically altered zebrafish, new genetic causes of cataracts can be identified as previously accomplished for the *GLS1*-S482C mutation[15]. The ability to sensitively visualize opacities in detail might furthermore contribute to create insight into the pathogenicity of cataract formation, as the appearance and localization

of opacities might provide information about the cause. In *Cloche*^{m39} zebrafish, cataract is caused by the absence of denucleation in all lens cells [6]. The visualization of diffuse cataract by FUVI therefore aligns with the pathophysiology of the cataract formation. In *GLS1*-S482C zebrafish, cataract is hypothesized to be caused by protein aggregation secondary to oxidative stress. The visualization of dispersed, subtitle structures by FUVI is therefore in line with the pathogenicity of cataract formation. The potential of FUVI to create insight into the pathogenicity of cataract formation increases when applied to high-content screenings. This might not only enable follow-up of cataract formation, but also the disappearance of cataract during drug treatments in time. The effect of UV-light on the lens should however be explored.

In conclusion, we describe Fluorescence microscopy with UV-Illumination as a sensitive technique which allows rapid and detailed visualization of the lens and cataracts in zebrafish embryos.

ACKNOWLEDGEMENTS

We thank professor D. Stainier for his generous gift of the *Cloche*^{m39} zebrafish and siblings and thank N. Fukuda and A. Karczewska for their technical assistance. This project has been funded by ODAS Stichting.

SUPPLEMENTARY FILES

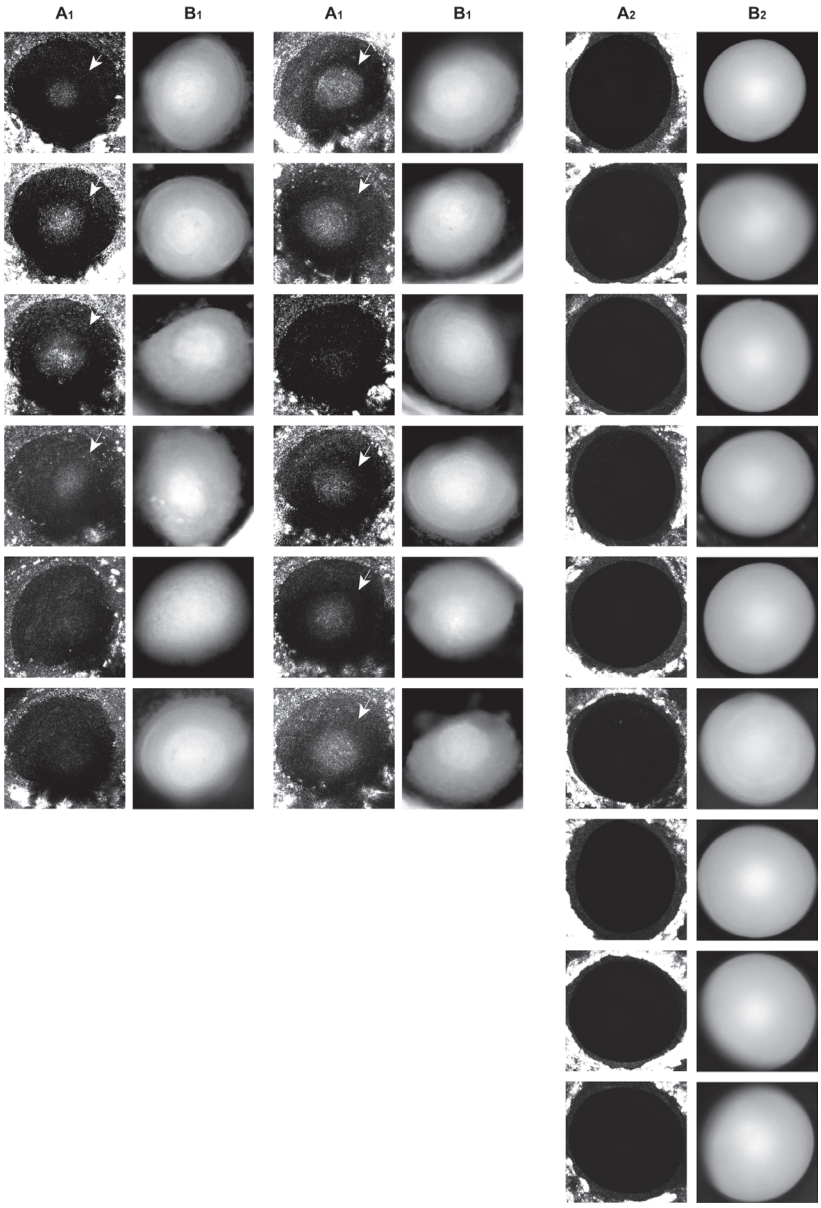

FIGURE. S1 *Cloche* ^{m39} zebrafish and siblings lenses imaged by confocal microscopy and FUVI. (A) Confocal microscopy visualized the lens of *Cloche*^{m39} zebrafish and opacities in 6/9 lenses (white arrow) (A1) and its siblings (A2). **(B)** Fluorescent microscopy with UV-illumination visualized the lens of *Cloche*^{m39} zebrafish op opacities in 9/9 lenses (B1) and its siblings (B2). Images aligned horizontally represent the same lens.

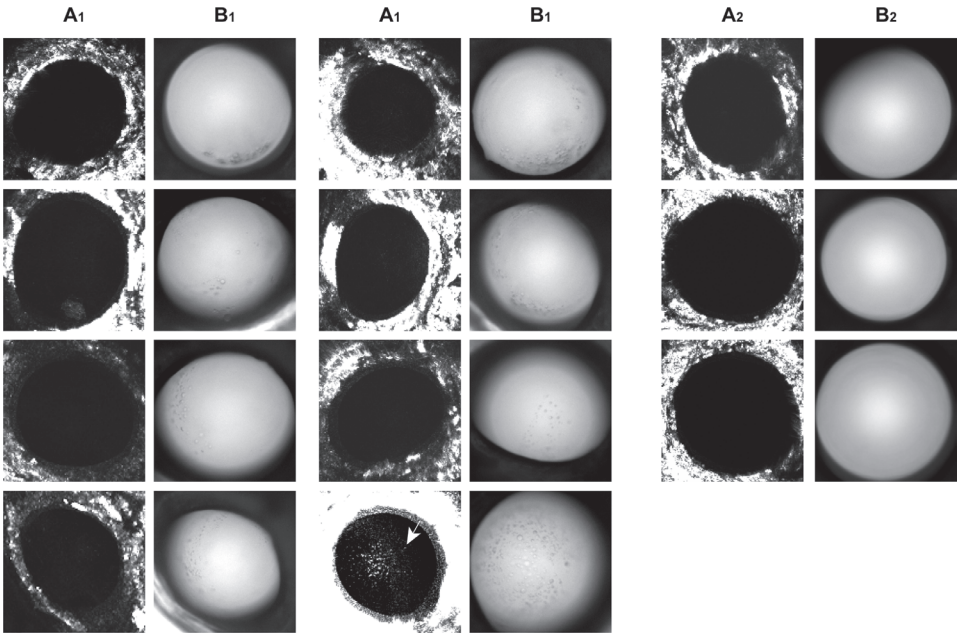

FIGURE. S2 *GLS1*-S482C and wildtype zebrafish lenses imaged by confocal microscopy and FUVI. **(A)** Confocal microscopy visualized the lens of *GLS1*-S482C zebrafish (A1) and wildtype zebrafish (A2). Confocal microscopy only detected reflectance in 1 *GLS1*-S482C zebrafish lens (white arrow). **(B)** Fluorescent microscopy with UV-Illumination visualized the lens of *GLS1*-S482C zebrafish (B1) and wildtype zebrafish (B2). Images aligned horizontally represent the same lens.

REFERENCES

1. SP M. Global data on visual impairments 2010. *World Health Organization.* 2012;20.
2. Bassnett S. On the mechanism of organelle degradation in the vertebrate lens. *Exp Eye Res.* 2009;88(2):133-139.
3. Graw J. Genetics of crystallins: cataract and beyond. *Exp Eye Res.* 2009;88(2):173-189.
4. Dahm R, Schonthaler HB, Soehn AS, van Marle J, Vrensen GF. Development and adult morphology of the eye lens in the zebrafish. *Exp Eye Res.* 2007;85(1):74-89.
5. Haffter P, Nusslein-Volhard C. Large scale genetics in a small vertebrate, the zebrafish. *Int J Dev Biol.* 1996;40(1):221-227.
6. Goishi K, Shimizu A, Najarro G, et al. AlphaA-crystallin expression prevents gamma-crystallin insolubility and cataract formation in the zebrafish cloche mutant lens. *Development.* 2006;133(13):2585-2593.
7. Dhakal S, Stevens CB, Sebbagh M, et al. Abnormal retinal development in Cloche mutant zebrafish. *Dev Dyn.* 2015;244(11):1439-1455.
8. Vihtelic TS, Yamamoto Y, Springer SS, Jeffery WR, Hyde DR. Lens opacity and photoreceptor degeneration in the zebrafish lens opaque mutant. *Dev Dyn.* 2005;233(1):52-65.
9. Murphy TR, Vihtelic TS, Ile KE, et al. Phosphatidylinositol synthase is required for lens structural integrity and photoreceptor cell survival in the zebrafish eye. *Exp Eye Res.* 2011;93(4):460-474.
10. Hansen L, Comyn S, Mang Y, et al. The myosin chaperone UNC45B is involved in lens development and autosomal dominant juvenile cataract. *Eur J Hum Genet.* 2014;22(11):1290-1297.
11. Semina EV, Bosenko DV, Zinkevich NC, et al. Mutations in laminin alpha 1 result in complex, lens-independent ocular phenotypes in zebrafish. *Dev Biol.* 2006;299(1):63-77.
12. Froger A, Clemens D, Kalman K, Nemeth-Cahalan KL, Schilling TF, Hall JE. Two distinct aquaporin 0s required for development and transparency of the zebrafish lens. *Invest Ophthalmol Vis Sci.* 2010;51(12):6582-6592.
13. Clemens DM, Nemeth-Cahalan KL, Trinh L, Zhang T, Schilling TF, Hall JE. In vivo analysis of aquaporin 0 function in zebrafish: permeability regulation is required for lens transparency. *Invest Ophthalmol Vis Sci.* 2013;54(7):5136-5143.
14. Cheng S, Shakespeare T, Mui R, White TW, Valdimarsson G. Connexin 48.5 is required for normal cardiovascular function and lens development in zebrafish embryos. *J Biol Chem.* 2004;279(35):36993-37003.
15. Rumping L, Tessadori F, Pouwels PJW, et al. GLS hyperactivity causes glutamate excess, infantile cataract and profound developmental delay. *Hum Mol Genet.* 2019;28(1):96-104.
16. Tschopp M, Takamiya M, Cerveny KL, et al. Funduscopy in adult zebrafish and its application to isolate mutant strains with ocular defects. *PLoS One.* 2010;5(11):e15427.
17. Jarrin M, Young L, Wu W, Girkin JM, Quinlan RA. In vivo, Ex Vivo, and In Vitro Approaches to Study Intermediate Filaments in the Eye Lens. *Methods Enzymol.* 2016;568:581-611.
18. Reischauer S, Stone OA, Villasenor A, et al. Cloche is a bHLH-PAS transcription factor that drives haemato-vascular specification. *Nature.* 2016;535(7611):294-298.

Chapter 7

General discussion

Samenvatting

Summary

Dankwoord

Curriculum Vitae

List of publications

Abbreviations

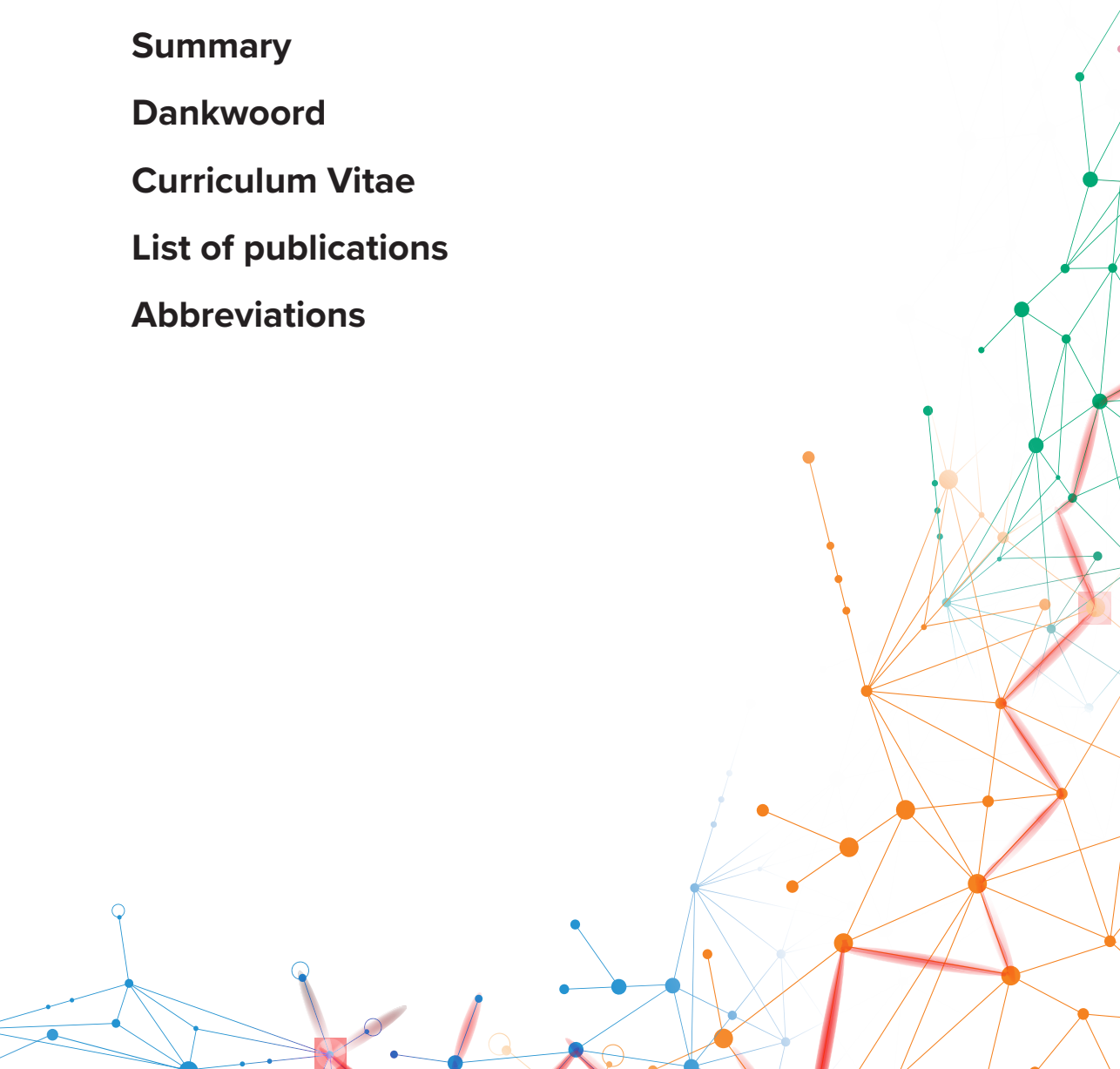

GENERAL DISCUSSION

The research presented in this thesis focuses on the pathophysiology of enzyme defects involved in glutamate metabolism. It presents the identification of two novel inborn errors of glutamate metabolism and the study of their biochemical and phenotypic consequences by innovative techniques. In this chapter, we discuss the implications of this research, with the focus on the (patho)physiology of glutamate metabolism and future perspectives on disease identification in the era of metabolomics and genomics.

ONE GENE, TWO INBORN ERRORS OF METABOLISM

The two novel inborn errors or metabolism (IEMs) described in this thesis are caused by mutations in the same gene, *GLS,* encoding the enzyme glutaminase (GLS) (**chapter 2 and 3**). While bi-allelic loss-of-function (LoF) *GLS* variants resulted in glutamine excess and glutamate deficiency, a mono-allelic, hypermorphic *de novo GLS* variant caused GLS hyperactivity with subsequent glutamine deficiency and glutamate excess. Hyperactivity variants are extremely uncommon and two errors causing opposite defects in the same enzyme are even more so. The opposing effects of these variants provide the opportunity to explore the biochemical and clinical consequences of an extensive enzyme activity spectrum.

CLINICAL AND BIOCHEMICAL EXPECTATIONS AND REALITY OF GLS DEFECTS

As the metabolic phenotypes of GLS hyperactivity and LoF are opposite, different clinical phenotypes may be expected for these disorders. At first glance, this is not the case as both diseases present with a predominantly neurological phenotype. This in itself is to be expected given the pivotal functions of glutamate and glutamine in the brain.

Patients with GLS LoF described in **chapter 2** exhibit neonatal respiratory failure, epileptic seizures, abnormalities in both the construction and the maintenance of brain structures and early death. This is in line with the importance of glutamate as a neurotransmitter functioning in the regulation of the respiratory center of the brain, signal transduction and axon myelination[1,2]. The importance of glutamate for respiration was previously illustrated by a GLS knock-out mousce model that also developed respiratory dysfunction[3]. High glutamine concentrations may have also contributed to the clinical phenotype of GLS LoF, since cerebral edema was observed in these patients, which can be secondary to glutamine accumulation[4,5]. GLS LoF is the first IEM that illustrates the importance of

glutamate -and GLS- for human brain function and survival.

On the other end of the spectrum, the patient with GLS hyperactivity described in **chapter 3** has profound developmental delay, axial hypotonia and shows agitated, self-injurious behavior. We postulate that this neurological phenotype is mainly caused by glutamate excess, as glutamate excitotoxicity is associated with neurodegenerative disorders and agitated, self-injurious behavior[6,7]. However, a contributing effect of glutamine deficiency cannot be excluded. In addition to the neurological phenotype, the patient with GLS hyperactivity also developed erythematic subcutaneous nodules and infantile cataract. Interestingly, the direct link between glutamate excess or GLS activity and cataract has not been described before, although causal links between glutamate excess and oxidative stress, and oxidative stress and cataract have been described[6,8]. GLS hyperactivity illustrates a direct link, as we show that GLS hyperactivity causes cataract in both the patient and a zebrafish model, which in the latter could be alleviated by GLS inhibitors. The positive effects of GLS inhibition offers a potential future treatment avenue.

The absence of epilepsy in the patient with GLS hyperactivity is unexpected as glutamate excitotoxicity is considered a critical factor in the initiation of epileptic seizures[9]. These seizures are provoked by increased glutamate levels in the synaptic cleft, which implies that glutamate levels in the synaptic cleft of our patient are unaffected despite overall brain glutamate excess. Magnetic resonance spectroscopy (MRS) cannot distinguish intracellular and extracellular metabolites and therefore cannot be used for further exploration. Microscopic imaging of glutamate by using a fluorescent probe in a neuronal cell model expressing the GLS hyperactivity variant may further address this issue[10].

GLS produces ammonia concomitant with glutamate; therefore, ammonia levels were expected to be affected in patients with GLS defects. Plasma levels of ammonia in patients with both GLS defects however remained unaffected. In GLS LoF this is not surprising, as less ammonia should be produced. However, as one would expect increased ammonia production with GLS hyperactivity, the normal ammonia levels in our patient seem counterintuitive. An explanation might be that GS, which is maintained or even overexpressed (**chapter 3**), captures ammonia by forming glutamine which serves as a nontoxic inter-organ carrier of ammonia[11].

PERSPECTIVES ON THE DIAGNOSIS OF GLS DEFECTS

The identification of GLS LoF and hyperactivity, creates awareness of these novel IEMs. This might help future recognition of undiagnosed patients with a similar biochemical and clinical phenotype. The diagnosis of GLS defects might include 3 factors: clinical

phenotyping, glutamine and glutamate analyzes and GLS genotyping.

Phenotypic spectrum

The phenotypic spectrum of a disease often expands when more patients are diagnosed and reported. The first description of a disease often represents the more severe end of the spectrum of a disease and may not accurately represent the overall phenotype and prognosis. The introduction of Whole Exome Sequencing (WES) into diagnostics accelerates the process of extending the phenotypic spectrum, as additional patients with ”new” phenotypic features, are diagnosed with known disorders.

Variants that result in hyperactivity are extremely uncommon, especially in a well conserved catalytic area as present in GLS. We therefore expect GLS hyperactivity to remain ultra-rare. Two additional patients with GLS variants claimed to induce LoF were recently described[12]. These patients exhibited a milder phenotype, survived and presented with neuronal ataxia and optic atrophy. No GLS mutations were found in these patients, pointing to intronic defects leading to decreased enzyme expression, which, based on the milder clinical presentation, likely have less profound effects than the truncating mutations found in our patients.

By reviewing the phenotypic features observed in patients with inborn errors of glutamate metabolism in **chapter 5**, we showed that neurological, ophthalmological (cataract, optic atrophy, corneal ulcerations and retinal degeneration) and dermatological features were often exhibited. This is especially observed in GLS hyperactivity (developmental delay, cataract and erythematic subcutaneous nodules), GLS LoF (seizures, developmental delay, ataxia and optic atrophy) and GS deficiency (seizures, developmental delay and necrolytic erythema). Interestingly, the brain, skin, lens, optic nerve, cornea, and retina are all of ectodermal origin and therefore share similarities in expression and regulation of glutamate receptors[13-15]. This suggests that disturbed glutamate homeostasis may not only affect the brain, but also affects other ectodermal structures. We therefore expect that the phenotypic spectrum, once other patients with GLS defects are identified, will include features involving these structures.

As glutamate is also involved in energy metabolism, redox homeostasis and the production of other amino acids, it is plausible that clinical consequences of one of these disturbed processes also includes the phenotypic spectrum. Untargeted metabolomics indeed revealed that GLS hyperactivity had downstream consequences for these pathways (**chapter 4**). The effect of GLS loss-of-function on these pathways has not yet been elucidated.

Metabolic phenotyping

Next to clinical phenotyping, metabolic phenotyping will be essential for the diagnosis of GLS errors. For GLS hyperactivity, glutamate excess together with glutamine deficiency points in this direction. Normal levels in plasma and CSF however do not exclude the diagnosis (see below "Tissue specificity for deviant glutamate and glutamine levels"). Measurements in urine and brain with MRSI might be most accurate, as these patient fluids and tissues represent those with high GLS expression[16]. If hyperammonemia is detected as well, GS deficiency should be kept in mind as a differential diagnosis. For GLS LoF, glutamine excess together with glutamate deficiency, without hyperammonemia, is expected. We however only studied these amino acids in blood spots and not in plasma, CSF, urine or by brain MRSI and can therefore not give a definite conclusion about tissue specific alterations in GLS LoF.

Genotyping

The detection of a (likely) pathogenic variant(s) in the *GLS* gene might confirm the diagnosis. However, when absent, intronic variants and mosaicism have not been excluded and should be considered. Whole Genome Sequencing (WGS) and the study of RNA- or protein expression, as well as genotyping of DNA from other sources like saliva or urine, might provide additional insight.

It is possible that the identification of disease causing variants is hampered by the current paradigm that mono-allelic variants in enzyme-encoding genes are usually harmless. GLS hyperactivity illustrates that mono-allelic, dominant enzyme defects can be harmful as well. Other examples of IEMs caused by mono-allelic mutations are hyperinsulinism-hyperammonia syndrome caused by hypermorphic mutations in *GDH* and cutis laxa and spastic paraplegia caused by *de novo* mutations in *ALDH18A1*[17,18]. This expands our classical paradigm of recessive IEMs towards that of (*de novo*) dominant IEMs. We therefore advocate to consider pathogenicity in cases of mono-allelic variants. Pathogenicity of a variant should especially be considered when the clinical and metabolic phenotype are compatible and when the variant co-segregates within the family.

GLS DEFECTS VERSUS GS DEFECT

While GS deficiency and GLS hyperactivity both lead to glutamine deficiency, their phenotypes differ significantly. One of the major differences is that patients with GS deficiency present with neonatal lethal epilepsy, while the patient with GLS hyperactivity described in chapter 3 did not[19]. This might be explained by biochemical differences other than glutamine deficiency. For instance, patients with GS deficiency are not reported to have glutamate excess. Furthermore hyperammonemia was reported in these patients,

which is known to cause epilepsy. The GLS hyperactivity patient characterized in chapter 3 did exhibit glutamate excess, but did not show hyperammonemia. These factors may provide an explanation for the phenotypical differences.

In GS deficiency, the lack of glutamine leads to NAD^+ deficiency[20]. NAD^+ is important for redox homeostasis. We showed in **chapter 3** that the redox buffer capacity is reduced in GLS hyperactivity, in line with the disturbed γ-glutamyl cycle intermediaries observed with untargeted metabolomics in **chapter 4**. Although not studied in our work, NAD^+ deficiency secondary to glutamine deficiency might have contributed (in addition to glutamate excitotoxicity) to a disturbed redox homeostasis in GLS hyperactivity.

Interestingly, patients with GLS LoF described in chapter 2 and GS deficiency show clinical similarities, while they exhibit opposite metabolic effects: they developed neonatal epilepsy and died shortly after birth. This shows that disturbed glutamine-glutamate homeostasis, in either direction, is detrimental and indicates that homeostasis is extremely important for human brain function and survival.

GLUTAMATE METABOLISM REVISITED

REGULATION OF GLUTAMATE METABOLISM

Unraveling the mechanisms behind GLS hyperactivity has provided new insights into the regulation of glutamate metabolism. By aligning +/- 12.000 GLS protein sequences from >1000 genera, we revealed that the substituted residue Ser482 had an extremely high degree of conservation, comparable to the conservation of residues directly involved in the enzymatic activity (**chapter 3**). Substitution of this highly conserved residue leads to GLS hyperactivity. This suggests that Ser482 serves as a built-in restrictor, ensuring submaximal activity rather than maximal enzyme activity of GLS.

Next to the regulation of glutamate homeostasis on genetic level, we showed that metabolic compensatory mechanisms are activated in a state of GLS hyperactivity (**chapter 3**). Increased glutamate concentrations induced downregulation of GLS expression. This effect supports the observation by Krebs, who in 1935 showed that glutamate acts as a sensor for GLS regulation, and reveals that glutamate not only affects GLS enzyme kinetics but also its expression. Additionally, we observed that protein levels of the reciprocal enzyme GS were upregulated to maintain glutamate homeostasis.
Whether compensatory mechanisms also occur in GLS LoF was not determined in our

work. Hypothetically, downregulation of GS may prevent glutamine excess and glutamate deficiency. Upregulation of GLS enzyme expression is ineffective to compensate for GLS LoF since GLS function is lost. This ineffective mechanism is also observed in GS deficiency, in which upregulation of GS enzyme expression could not prevent glutamine deficiency[21]. Future work involving the use of patient cells or a GLS LoF knock-out cell model will increase the understanding of compensatory mechanisms in GLS LoF.

In **chapter 5**, we reviewed inborn errors in enzymes of glutamate metabolism and studied their effect on glutamate and glutamine levels. Deviant glutamate and glutamine levels were however scarcely reported in these IEMs, other than in GLS and GS defects and urea cycle defects. These levels were therefore presumed to be normal. If true, this points to compensatory regulation of these levels by either transport or other enzymes of glutamate metabolism. It is important that glutamate and glutamine levels are measured in different patient sources and are reported. Dissemination of this knowledge could benefit from an open access database for the controlled registration of these data.

TISSUE SPECIFICITY FOR DEVIANT GLUTAMATE AND GLUTAMINE LEVELS

Under certain conditions, metabolite concentrations in the cerebrospinal fluid (CSF) can provide surrogate information on the metabolic status of the brain. However, glutamate and glutamine levels in the patient with GLS hyperactivity described in **chapter 3** were normal in CSF, while MRS(I) detected extremely high levels of glutamate and almost undetectable levels of glutamine in the brain. This discrepancy may be explained by the degree to which glutamate and glutamine levels are controlled by GLS in different cell types. CSF is formed by the choroid plexus consisting of glial cells, in which glutamate and glutamine levels are regulated by GS rather than GLS. In brain tissue, these metabolites are mainly regulated by GLS[22,23]. This striking contrast can be regarded as a cautionary note: CSF should not be readily regarded as a representation for the brain if it concerns glutamine and glutamate. If aberrant metabolite levels are expected in a patient, we advise additional MRS measurements to be performed to inform on the metabolic status of the brain. Regional differences of these metabolites (obtained by MRSI) might create additional insight into the expression of GLS and pathology.

In our patients with GLS LoF described in **chapter 2**, glutamate and glutamine levels were only measured in bloodspots as these patients died shortly after birth. Although glutamate levels were normal in bloodspots, we expect deviant levels in brain given high neuronal GLS expression and the neurologic phenotype observed in these patients. MRS might provide valuable information about glutamate metabolism in the brain of patients with GLS LoF and we therefore recommend to perform brain MRS as soon as possible when a new

patient with this IEM is diagnosed.

Alterations of glutamate and glutamine levels seem tissue specific. These levels not only remained unaffected in the CSF. In plasma of the patient affected with GLS hyperactivity, glutamate and glutamine values remained unaffected as well. This can be likely explained by the expression of the isoenzyme GLS2[16]. In urine, glutamate and glutamine values were altered, in accordance to tissue-specific GLS expression[16]. This points to tissue specificity for glutamate and glutamine levels, dependent on tissue specific GLS expression and on compensatory mechanisms. This can be regarded as a second cautionary note: the absence of these altered metabolites does not always exclude pathology.

BLOOD SPOTS: TREASURE, NOT TRASH. A MESSAGE TO THE GOVERMENT

Co-segregation of a genetic variant and the clinical or biochemical phenotype within a family is essential for disease identification. In **chapter 2** we describe how segregation of GLS variants and the clinical and metabolic phenotype within a family, using bloodspots saved from newborn screening, led to the proof of causality and the retrospective diagnosis of a family member that died 10 years prior. This case illustrates the potential of bloodspots for the retrospective identification of rare metabolic diseases in undiagnosed, deceased patients. It is therefore important that bloodspots remain available for diagnostics.

In the other family we described in **chapter 2**, from South-Asian descent, co-segregation with deceased family members was not possible, since bloodspots were unavailable. In the Netherlands, the law “Wet zeggenschaps en lichaamsmateriaal” states that bloodspot cannot be stored for longer than 5 years. It is therefore impossible to perform retrospective analyses beyond 5 years of age. To enable doctors and researchers to diagnose patients and identify novel, rare diseases, it is important that this law will be amended. We therefore make an appeal to store all blood spots for at least 16 years [24,25].

FLUORESCENCE MICROSCOPY WITH UV-ILLUMINATION (FUVI)

Innovative techniques to study to pathophysiology and causality of a genetic variant are important. We developed a Fluorescence microscopic method with UV-Illumination (FUVI)

to image lens opacities in zebrafish. We show in **chapter 3 and 6** that FUVI accurately visualizes the zebrafish lens with high sensitivity. It is easily accessible and does not require genetic engineering or staining for visualization. One image represents a large depth of field, allowing high-speed data acquisition. We anticipate that this method can be valuable for multiple purposes: discovering new genetic causes of cataracts; creating insight into the pathophysiology of cataracts; and (as we have illustrated metabolic intervention in zebrafish as a potential strategy for cataract treatment in chapter 3) enabling the study and follow-up of therapeutic chemical potentials. The question remains as to whether other kinds of cataracts can be detected using FUVI. As it accurately visualizes the whole lens, other lens disorders, such as micro- or aphakia and ectopia lentis can likely be depicted in zebrafish embryos by FUVI as well. Together, FUVI might create possibilities for the further study of the genetic causes and pathophysiology of cataract as well as other lens abnormalities.

IEM IDENTIFICATION IN THE ERA OF GENOMICS AND METABOLOMICS

This thesis illustrates the value of the “genome first approach” for the identification of new diseases and to unravel their pathophysiology. Variant interpretation is extremely important now that with NGS a large number of variants are detected, which might or might not underlie a disorder. Incorrect interpretation of variant pathogenicity might lead to misdiagnosis of the patient and family, with severe implications. Clinical phenotyping and metabolomics are essential for the interpretation of variants and to provide evidence for causality and pathophysiology. The “genome first approach” should therefore not be mistaken by a “genome only approach”.. The importance of phenotyping is illustrated by a recent study, in which clinical reviewing alone provided a diagnosis in 11% of the patients which were re-evaluated in a multidisciplinary setting, because they did not have a diagnosis despite extensive medical evaluation[26]. Metabolomics provides a functional readout of the consequences of genetic variation and therefore creates both evidence for causality and insight into pathophysiology.

Untargeted metabolomics provides an extensive “metabolic fingerprint” of the metabolic response to a pathogenic stimuli, which does not require *a priori* knowledge of the clinical or metabolic phenotype. **Chapter 5**, in which untargeted metabolomics is performed on a GLS hyperactivity cell model, is a good illustration of the power of this approach. With only one test, our in-house developed DI-HRMS pipeline enabled us to detect thousands of metabolites within a few minutes. We learned that GLS hyperactivity has numerous

downstream metabolic consequences, in line with the multiple functions of glutamine and glutamate. This not only created insight into the possible contributing pathologic factors, but it also provided interesting leads to possible treatment. It suggested that targeting the source would be more accurate than multiple downstream targeting. Indeed, targeting GLS activity with the GLS inhibitor CB-839 effectively maintained a balanced metabolome in this cell model.

Untargeted metabolomics is currently used for research purposes. However, it is increasingly being valued as a means for disease recognition and might eventually progress towards a tool for diagnostics. There remain some challenges: specificity and reproducibility should be improved and a structured workflow to select specific metabolites (out of the thousands provided metabolites) should be created. Recently, such a workflow was suggested for semi-untargeted data, comparable with the approach of WES analysis[27]. This involves 3 steps: targeted evaluation based on identified genetic variants of uncertain significance in metabolic pathways, followed by a panel of IEM-related metabolites and, if needed, by an 'open the metabolome' analysis. Although untargeted metabolomics should currently still be confirmed by targeted metabolomics, its role in the genomic and metabolomics era will likely grow.

COLLABORATION: THE KEY TO SUCCESS

Multidisciplinary teams are a key element to diagnose patients with rare disorders in this era of genomics and metabolomics. Projects with the aim to solve unsolved cases are arising fast. In the United States, the Undiagnosed Disease Network is established to apply a multidisciplinary model in the evaluation undiagnosed patients with the aim to identify new diseases and their biologic characteristics[26]. In the Netherlands, similar projects are started, in which pediatricians, clinical geneticists, laboratory specialists and other academics collaborate to reach this prime aim. These projects bridge the gap between clinical care and research, which is necessary for successful collaboration.

As IEMs are scarce, international collaboration is of increasing importance to identify similar patients. This is easier now that communication all over the world is accessible with social media and other communication tools. GeneMatcher, for instance, is a website that enables the connection between clinicians and researches who share an interest in the same gene[28]. This tool enabled us to find multiple patients with GLS mutations, which strengthened the evidence of pathogenicity of GLS dysfunction. We collaborated with scientists and doctors from Germany, Switzerland and England not only to find multiple patients but also to share valuable knowledge.

Not only international, also local, interdisciplinary collaboration is essential to provide a complete view of a disease from phenotype to genotype. Collaboration of patients and their family are crucial for this process, as are clinical geneticists, pediatricians and metabolic and molecular laboratory specialists, molecular biologists, zebrafish experts and many other specialists. As can be seen in the author list, we highly uphold this principle of strong collaborations.

REFERENCES

1. Mount CW, Monje M. Wrapped to Adapt: Experience-Dependent Myelination. *Neuron.* 2017;95(4):743-756.
2. Nedergaard M, Takano T, Hansen AJ. Beyond the role of glutamate as a neurotransmitter. *Nat Rev Neurosci.* 2002;3(9):748-755.
3. Masson J, Darmon M, Conjard A, et al. Mice lacking brain/kidney phosphate-activated glutaminase have impaired glutamatergic synaptic transmission, altered breathing, disorganized goal-directed behavior and die shortly after birth. *J Neurosci.* 2006;26(17):4660-4671.
4. Takahashi H, Koehler RC, Brusilow SW, Traystman RJ. Inhibition of brain glutamine accumulation prevents cerebral edema in hyperammonemic rats. *Am J Physiol.* 1991;261(3 Pt 2):H825-829.
5. Butterworth RF. Pathophysiology of brain dysfunction in hyperammonemic syndromes: The many faces of glutamine. *Mol Genet Metab.* 2014;113(1-2):113-117.
6. Dong XX, Wang Y, Qin ZH. Molecular mechanisms of excitotoxicity and their relevance to pathogenesis of neurodegenerative diseases. *Acta Pharmacol Sin.* 2009;30(4):379-387.
7. Brodie MJ, Besag F, Ettinger AB, et al. Epilepsy, Antiepileptic Drugs, and Aggression: An Evidence-Based Review. *Pharmacol Rev.* 2016;68(3):563-602.
8. Spector A. Oxidative stress-induced cataract: mechanism of action. *FASEB J.* 1995;9(12):1173-1182.
9. Barker-Haliski M, White HS. Glutamatergic Mechanisms Associated with Seizures and Epilepsy. *Cold Spring Harb Perspect Med.* 2015;5(8):a022863.
10. Marvin JS, Borghuis BG, Tian L, et al. An optimized fluorescent probe for visualizing glutamate neurotransmission. *Nat Methods.* 2013;10(2):162-170.
11. Hakvoort TB, He Y, Kulik W, et al. Pivotal role of glutamine synthetase in ammonia detoxification. *Hepatology.* 2017;65(1):281-293.
12. Lynch DS, Chelban V, Vandrovcova J, Pittman A, Wood NW, Houlden H. GLS loss of function causes autosomal recessive spastic ataxia and optic atrophy. *Ann Clin Transl Neurol.* 2018;5(2):216-221.
13. Farooq M, Kaswala RH, Kleiman NJ, Kasinathan C, Frederikse PH. GluA2 AMPA glutamate receptor subunit exhibits codon 607 Q/R RNA editing in the lens. *Biochem Biophys Res Commun.* 2012;418(2):273-277.
14. Genever PG, Maxfield SJ, Kennovin GD, et al. Evidence for a novel glutamate-mediated signaling pathway in keratinocytes. *J Invest Dermatol.* 1999;112(3):337-342.
15. Skerry TM, Genever PG. Glutamate signalling in non-neuronal tissues. *Trends Pharmacol Sci.* 2001;22(4):174-181.
16. Aledo JC, Gomez-Fabre PM, Olalla L, Marquez J. Identification of two human glutaminase loci and tissue-specific expression of the two related genes. *Mamm Genome.* 2000;11(12):1107-1110.
17. Fischer-Zirnsak B, Escande-Beillard N, Ganesh J, et al. Recurrent De Novo Mutations Affecting Residue Arg138 of Pyrroline-5-Carboxylate Synthase Cause a Progeroid Form of Autosomal-Dominant Cutis Laxa. *Am J Hum Genet.* 2015;97(3):483-492.
18. Palladino AA, Stanley CA. The hyperinsulinism/hyperammonemia syndrome. *Rev Endocr Metab Disord.* 2010;11(3):171-178.

19. Spodenkiewicz M, Diez-Fernandez C, Rufenacht V, Gemperle-Britschgi C, Haberle J. Minireview on Glutamine Synthetase Deficiency, an Ultra-Rare Inborn Error of Amino Acid Biosynthesis. *Biology (Basel).* 2016;5(4).
20. Hu L, Ibrahim K, Stucki M, et al. Secondary NAD+ deficiency in the inherited defect of glutamine synthetase. *J Inherit Metab Dis.* 2015;38(6):1075-1083.
21. Haberle J, Gorg B, Rutsch F, et al. Congenital glutamine deficiency with glutamine synthetase mutations. *N Engl J Med.* 2005;353(18):1926-1933.
22. Bak LK, Schousboe A, Waagepetersen HS. The glutamate/GABA-glutamine cycle: aspects of transport, neurotransmitter homeostasis and ammonia transfer. *J Neurochem.* 2006;98(3):641-653.
23. Blau N, Duran M, Gibson KM. *Laboratory Guide to the Methods in Biochemical Genetics.* Heidelberg Berlin: Springer; 2008.
24. Oproep om hielprikbloed langer te bewaren. 2018; www.stofwisselingsziekten.nl/oproep-om-hielprikbloed-langer-te-bewaren/. Available at: www.stofwisselingsziekten.nl/oproep-om-hielprikbloed-langer-te-bewaren/. Accessed 14-11-2018.
25. Pelt S. Kinderarts: bewaar hielprikbloed langer, het kan zeldzame ziektes helpen ontrafelen. *de Volkskrant*30-10-2018.
26. Splinter K, Adams DR, Bacino CA, et al. Effect of Genetic Diagnosis on Patients with Previously Undiagnosed Disease. *N Engl J Med.* 2018;379(22):2131-2139.
27. Coene KLM, Kluijtmans LAJ, van der Heeft E, et al. Next-generation metabolic screening: targeted and untargeted metabolomics for the diagnosis of inborn errors of metabolism in individual patients. *J Inherit Metab Dis.* 2018;41(3):337-353.
28. Sobreira N, Schiettecatte F, Valle D, Hamosh A. GeneMatcher: a matching tool for connecting investigators with an interest in the same gene. *Hum Mutat.* 2015;36(10):928-930.

NEDERLANDSE SAMENVATTING

Metabole ziekten (stofwisselingsziekten) zijn erfelijke ziekten. Deze worden veroorzaakt door mutaties (veranderingen in genen van het DNA) die er voor zorgen dat metabole (biochemische) processen in het lichaam worden verstoord. Dit uit zich vaak op kinderleeftijd al met ernstige symptomen en leidt soms tot het overlijden van de patiënten. Het is belangrijk dat patiënten zo vroeg mogelijk gediagnosticeerd worden, omdat veel metabole ziekten behandeld kunnen worden met medicijnen, leefregels of dieetadviezen. Het stellen van een diagnose is bovendien belangrijk voor het inzicht in het ziektebeloop en de levensverwachting en daarmee de verwerking voor de patiënt en familieleden. Hiernaast opent dit de weg naar familiescreening.

Het identificeren van nieuwe metabole ziekten en het ontrafelen van het ziektemechanisme is belangrijk. Het stelt artsen in staat deze ziekten te herkennen bij toekomstige patiënten met vergelijkbare klachten en verstoorde biochemische processen. Het kan tevens inzicht geven in mogelijke behandelingen. Door het bestuderen van het ziektemechanisme van nieuw ziekten kan ook kennis verkregen worden over het normale functioneren van biochemische processen in het lichaam en het belang hiervan voor de gezondheid.

Het werk gepresenteerd in dit proefschrift beschrijft de ontdekking en de ziektemechanismen van twee nieuwe metabole ziekten die beiden worden veroorzaakt door mutaties in het GLS gen. Het GLS gen codeert voor het eiwit glutaminase, dat het aminozuur glutamine omzet in het aminozuur glutamaat. Glutamine is een bouwsteen voor vele eiwitten en is belangrijk voor de detoxificatie van de giftige stof ammoniak. Glutamaat is belangrijk voor de signaaloverdracht van zenuwen, voor energie metabolisme en voor het behoud van een goede balans tussen oxidanten en anti-oxidanten. Een teveel aan glutamine en glutamaat kan echter ook schadelijk zijn. Een balans tussen deze aminozuren is daarom essentieel.

In **hoofdstuk 1** wordt ingegaan op de benodigde stappen voor het ontdekken van nieuwe metabole ziekten. Tevens wordt toegelicht hoe de ontwikkeling van genetische en analytische technieken ons vermogen om nieuwe genetische metabole ziekten te ontdekken sterk heeft verbeterd.

In **hoofdstuk 2** beschrijven wij een nieuwe metabole ziekte bij vier kinderen van twee onverwante families, veroorzaakt door mutaties in het GLS gen. Hierdoor gaat de functie van het eiwit glutaminase verloren. Dit leidt in pasgeboren kinderen tot ademhalingsproblematiek, epileptische aanvallen en het kort daarna overlijden van deze

patiënten. Deze ziekte is ontdekt met een 'genoom-eerst aanpak', waarbij DNA analyse gevolgd werd door analyse van glutamine en glutamaat, welke het verlies van glutaminase functie bevestigde. Deze nieuwe metabole ziekte, genaamd 'GLS loss-of-function' is de eerste metabole ziekte die het belang van glutamaat en GLS voor een goede functie van de hersenen in mensen aantoont. Door het analyseren van opgeslagen hielprikkaartjes in Zwitserland van broertjes en zusjes van een van de patiënten, kon ook van deze kinderen bepaald worden of ze al dan niet aangedaan waren. Deze benadering illustreert de toegevoegde waarde van het langdurig bewaren van hielprikkaarten. In Nederland worden hielprikkaartjes maar tot 5 jaar na de geboorte bewaard. Op grond van ons onderzoek hebben wij daarom een oproep aan de regering gedaan om deze gedurende langere tijd op te slaan.

In **hoofdstuk 3** beschrijven wij een andere nieuwe metabole ziekte in een patiënt die ook veroorzaakt wordt door een GLS gen mutatie. Deze mutatie veroorzaakt juist een versterkte functie van glutaminase, wat leidt tot verlaagde glutamine en verhoogde glutamaat waarden. Deze patiënt met 'GLS hyperactiviteit' had staar sinds de leeftijd van 3 maanden, dermatologische afwijkingen, verlaagde spierspanning in de romp en een ernstige ontwikkelingsachterstand. In een celmodel waarin deze GLS mutatie is nagebootst, toonden wij aan dat compensatiemechanismen aangezet werden om de balans tussen glutamine en glutamaat te herstellen: het glutaminase eiwit was verlaagd aanwezig en glutamine synthetase (het eiwit dat de tegenovergestelde reactie uitvoert) was verhoogd aanwezig. Tevens toonden wij aan dat de capaciteit om oxidanten onschadelijk te maken, verlaagd werd door GLS hyperactiviteit. Het was al uit eerder onderzoekbekend dat zeer hoge glutamaat waarden leiden tot hoge oxidanten waarden, en dat hoge oxidanten waarden leiden tot staar. Dat GLS hyperactiviteit daadwerkelijk de oorzaak is van de staar in onze patiënt, toonden wij aan doordat zebravissen met GLS hyperactiviteit ook staar ontwikkelden, wat voorkomen kon worden door het remmen van de GLS activiteit.

Om de lens van de zebravisembryo (kleiner dan 0.1mm) en de staar goed in beeld te kunnen krijgen, hebben wij een fluorescentie microscopie methode op basis van illuminerend UV-licht ontwikkeld (FUVI). In **hoofdstuk 6** omschrijven wij deze methode door deze toe te passen op verschillende zebravis modellen die staar ontwikkelen en deze te vergelijken met reguliere microscopie.

Glutamaat en glutamine vervullen beiden veel verschillende functies in het lichaam en zijn hierdoor verweven in vele metabole paden. In **hoofdstuk 4** werden de uitgebreide metabole gevolgen van GLS hyperactiviteit bestudeerd door gebruik te maken van 'untargeted metabolomics'. Bij deze methode is de specificiteit lager dan bij het doelgericht

meten van een selectie van metabolieten, maar met deze methode wordt in één keer een profiel gemaakt van meer dan duizend metabolieten en kan daarbij tot nieuwe inzichten leiden.. Wij toonden hiermee aan dat GLS hyperactiviteit niet alleen gevolgen heeft voor glutamine en glutamaat waarden, maar verstrekkende gevolgen heeft voor vele metabole paden.

GLS loss-of-function en GLS hyperactiviteit zijn niet de enige stofwisselingsziekten waarbij glutamaat direct betrokken is. Wij vroegen ons af in hoeverre er vanwege de betrokkenheid van glutamaat ook klinische overenkomsten waren. In **hoofdstuk 5** bestudeerden wij daarom 17 metabole ziekten, veroorzaakt door defecten in eiwitten die glutamaat direct metaboliseren. Door een overzicht te creëren van de klinische en biochemische eigenschappen van deze patiënten, hopen wij dat deze metabole ziekten makkelijker herkend zullen worden bij toekomstige patiënten. Deze metabole ziekten konden verdeeld worden in drie grote groepen: ziekten veroorzaakt door een verstoorde aanmaak of afbraak van andere aminozuren; ziekten in de ammoniak stofwisseling; en ziekten met een verstoorde oxidanten-antioxidanten balans. Door het vergelijken van de symptomen van patiënten met deze metabole ziekten, kon informatie verkregen worden over de gevolgen van een verstoorde glutamaat stofwisseling. Opvallend was dat deze patiënten vooral klachten van het zenuwstelsel, de ogen en de huid hadden. Deze observatie geeft ons inzicht in het belang van reguleerde glutamaat waarden voor deze organen.

Tenslotte bediscussiëren we in hoofdstuk 7 de ziektemechanismen van GLS loss-of-function en GLS hyperactiviteit door de symptomen en biochemie van de patiënten te vergelijken met elkaar, en verwante metabole ziekten. We bespreken vervolgens welke kennis over het normale glutamaat metabolisme en de regulatie ervan opgedaan kan worden uit deze metabole ziekten. Vervolgens wordt geëindigd met mijn toekomstperspectief (dat niet zover vooruit ligt) betreffende het identificeren van nieuwe metabole ziekten: de combinatie van fenotypering en metabole en genetische analyse van meerdere patiënten met eenzelfde ziektebeeld is hiervoor vereist, waarbij een goede interdisciplinaire en internationale samenwerking van essentieel belang is.

SUMMARY

Inborn Errors of Metabolism (IEMs) are a class of inherited genetic disorders caused by variants in genes coding for proteins that function in metabolism. As IEMs can affect a wide range of metabolic pathways, the biochemical and clinical presentations vary widely but these patients often have early, severe onset. Early diagnosis is essential for optimal outcome of children with an IEM, as treatment is possible for many IEMs. It provides insight into prognosis and is important for the psychological processing of the patient and family. It furthermore enables the screening of family members.

Not all IEMs are known yet, therefore some patients still remain undiagnosed. Identification of these new IEMs and their disease mechanism is important. It creates awareness for these new IEMs, which helps recognition of future patients with a similar clinical and biochemical phenotype. It might additionally provide leads to treatment and knowledge about normal physiology and its importance for health.

The research presented in this thesis describes the identification and disease mechanisms of two novel IEMs caused by mutations in the GLS gene. This gene encodes the protein glutaminase, which converts the amino acid glutamine into glutamate. Glutamine is a source for many proteins and is important for ammonia detoxification. Glutamate is an important neurotransmitter and plays a pivotal role in energy metabolism and redox homeostasis. Excess of these amino acids however can be harmful. A balance between these amino acids is therefore essential.

In **chapter 1**, the required steps for the identification of new IEMs are elaborated. Furthermore, it is exemplified how the development of genetic and analytical techniques improved our ability to discover the genetic cause of IEMs.

In **chapter 2**, we describe a new IEM in 4 children of 2 unrelated families, caused by bi-allelic loss-of-function mutations in GLS. This leads to neonatal, respiratory insufficiency, epilepsy and death. This was achieved through a “genome first approach”, in which Whole Exome Sequencing identified the variants in the GLS gene, which co-segregated within the family, and targeted metabolic analyses confirmed loss-of-function. This is the first IEM that illustrates the importance of glutamate and GLS for human brain function and survival. Through analysis of bloodspots stored from neonatal screening (in Switzerland), deceased siblings of the patients could retrospectively diagnosed. This illustrated the importance to store bloodspots. In the Netherlands, bloodspots are only stored for 5 years after birth. We therefore made an appeal to the government to store all blood spots for at least 16 years.

In **chapter 3**, we describe another novel IEM caused by a GLS mutation. This mutation caused GLS hyperactivity, resulting in low glutamine and high glutamate levels. This patient had early onset cataract diagnosed at age 3 months, dermatological abnormalities, axial hypotonia and profound developmental delay. In a cell model in which the GLS hyperactivity mutation was expressed, we showed that metabolic compensatory mechanisms were activated: glutaminase protein expression was decreased, while glutamine synthetase (the reciprocal enzyme) protein expression was increased. We furthermore demonstrated that redox capacity buffer was decreased. The causal links between glutamate excess and oxidative stress, and oxidative stress and cataract are known. We confirmed the causality of GLS hyperactivity for cataract formation, as zebrafish with GLS hyperactivity developed cataract, which could be alleviated with GLS activity inhibition.

To visualize the lens of the zebrafish embryo (smaller than 0.1mm) and lens opacities, we developed a fluorescence microscopic method based on UV-Illumination (FUVI). In **chapter 6**, we describe this method and applied it to different zebrafish models that are known to develop cataract. We compared FUVI with confocal microscopy, an established method .

Glutamate and glutamine have several important functions and are involved in a variety of metabolic pathways. In **chapter 4** the extensive downstream metabolic consequences of GLS hyperactivity were examined by untargeted metabolomics. This method provides an extensive “metabolic fingerprint”. It is less specific than targeted metabolic techniques, but enables the detection of thousands of metabolites with one test. We demonstrated that GLS hyperactivity not only affected glutamine and glutamate levels, but that it has far-reaching downstream metabolic consequences.

GLS loss-of-function and GLS hyperactivity are not the only inborn errors of glutamate metabolism. In **chapter 5** we review all reported inborn errors of enzymes of glutamate metabolism and provide an overview of their clinical and biochemical characteristics. By drawing phenotypic and biochemical parallels, we attempt to create insight into the clinical effect of disturbed glutamate metabolism. These IEMs could be divided in three main groups, affecting amino acid metabolism, the urea cycle- and ammonia metabolism or the γ-glutamyl cycle. By drawing parallels between phenotypic features of these patients, we showed that neurological, ophthalmological and dermatological features were often exhibited. This provides us with knowledge about the importance of regulated glutamate homeostasis for these tissues.

Finally, in **chapter 7**, I discuss the underlying disease mechanisms of GLS loss-of-function and GLS hyperactivity by comparing clinical and biochemical features of these and related

IEMs. I furthermore elucidate what novel knowledge can be extracted from these IEMs concerning physiologic glutamate metabolism and its regulation. I end with my near future perspectives regarding the identification of all novel IEMs: the combination of deep phenotyping, metabolic and genetic diagnostics of patients with a similar phenotype is required. Interdisciplinary and international collaboration is essential to reach this prime aim.

DANKWOORD

Het is zover. Mijn proefschrift met het resultaat van ruim 4 jaar onderzoek is af. De eindbestemming van een uitdagende, leerzame periode waarin ik veel inspirerende mensen heb leren kennen die mij allen geholpen hebben om mijn doel, promoveren, te bereiken.

Allereerst wil ik graag de leden van de leescommissie, prof. dr. **V.V.A.M. Knoers**, prof. dr. **E.E.S. Nieuwenhuis**, prof. dr. **J.P.H. Burbach**, prof. dr. **M.M. van Genderen** prof. dr. **H.R. Waterham** bedanken voor het lezen en beoordelen van dit proefschrift. **Johannes Häberle** and **Eric Kalkhoven**, I would also like to thank you for your participation in my PhD committee.

Mijn onderzoek op de afdeling van **Nanda Verhoeven**, Genetica sectie Metabole Diagnostiek, begon als wetenschappelijke stage onder begeleiding van **Peter van Hasselt, Berthil Prinsen** en **Gijs van Haaften** en zette zich voort als PhD-traject met ook de begeleiding van **Judith Jans** en **Roderick Houwen**. **Nanda**, ik wil je bedanken voor de ruimte die ik heb gekregen om mij naast mijn promotie ook op andere vlakken te ontwikkelen. Je bent daarnaast een mooi voorbeeld voor mij van een krachtige vrouw met hoge functie, die ook tijd neemt voor haar sociale leven. **Roderick**, dank voor het mogelijk maken van deze promotie. **Judith**, jij hebt mij integriteit in de wetenschap geleerd. Natuurlijk stond ik niet altijd te springen om de experimenten in triplo in drievoud uit te voeren om reproductiviteit aan te tonen, maar hierdoor staan wij allen sterk achter onze stellingen. **Peter**, jouw creatieve geest werkt inspirerend en heeft het onderzoek een stuk verder gebracht. Onze koppigheid botste zo nu en dan, maar daar kwamen we met wat onderhandelingen wel uit. Je hebt je erg voor mij ingezet en hebt ook altijd aandacht gehad voor mijn persoonlijke ontwikkeling. Ik waardeer dit erg.

Rúben, for about three years we spent most hours of our days together as graduate students. We have worked really hard together but also have had many nice moments (coffees, museum, congresses in Rome and of course Lyon). Thank you for your help with the mass spectrometer and for letting me sing in our room. I hope you are having a great time and career in New York.

Toen ik begon met mijn wetenschappelijke stage, kon ik pipeteren en cellen kweken. Maar daar hield het qua labskills ook wel een beetje bij op. Ik heb ontzettend veel hulp gehad van vele mensen waaronder **alle laboranten van het laboratorium metabole ziekten**. Ik ben jullie allemaal dankbaar voor deze hulp en jullie gezelligheid! Graag bedank ik enkele

mensen specifiek: **Ans**, **Mirjam**, **Gerda** en **Birgit**, jullie hebben mij vanaf het begin tot eind op weg geholpen. **Johan**, **Yuen-Fung**, **Maria**, **Marcel** en **Mia**, dank voor jullie technische en biostatische ondersteuning bij de untargeted metabolomics. **Can**, well…we tried. Unfortunately glutathion measurements remain a mystery. **Martin**, bedankt voor de GABA analyses en dat ik je ook in de weekenden kon bellen. **Deena**, **Raymond**, **Isa**, **Harrold**, **Suzana**; deze periode was zoveel minder leuk geweest zonder al jullie kletspraatjes!

Glen, Monique, Jolita, **Sanne en met name ook Hanneke**: jullie hebben mij tijdens de onderzoeksbesprekingen weer een stapje vooruit, of een stapje terug, laten zetten. Sanne en **Karen**, naast dit ook ontzettend bedankt voor alle ondersteuning in het lab! Zoals bij de meeste onderzoeken, staat niet alles opgeschreven. Zo staat in dit boekje bijvoorbeeld niet omschreven dat ik (mislukte) experimenten uitgevoerd heb op de muizenogen die **Judith** en Lena over hadden van hun cardiologische experimenten (in het kader van duurzaamheid). Meiden, bedankt hiervoor! **Esmee**, jij was echt een top student met veel inzicht en doorzettingsvermogen! Je hebt mij ontzettend geholpen bij alle ROS metingen. **Melanie** en **Willem**, bedankt voor het mooie overzicht over microscopie bij zebravissen en de technische hulp bij de microscopische methoden. **Maaike**, de Seahorse experimenten zijn niet gelukt, maar we hebben er wel leuke koffiemomenten aan overgehouden. Ook de **genetica groep in het Stratenum** wil ik bedanken. **Chris** en **Christina** ik ben blij dat wij onze ontbijtjes voortzetten zodat we zo nu en dan bij kunnen kletsen. **Saskia** en **Marijn**, bedankt dat jullie mij geïntroduceerd hebben met de klinische genetica. Door jullie enthousiasme is mijn interesse aangewakkerd en ben ik waar ik nu ben!

Zoals ik mijn discussie afsloot: samenwerking is de sleutel tot succes. Wij hebben samengewerkt op zowel multidisciplinair niveau (artsen, onderzoekers, biologen, statistici enzovoorts) als op internationaal niveau. Ik wil **alle co-auteurs** die hebben bijgedragen aan dit onderzoek bedanken. **Federico** en **Anko**, dank voor alle hulp bij de zebravis experimenten. **Fried**, jij kwam erachter dat mijn celmodel niet klopte, 1 dag voor submissie van het onderzoek. Ik kan niet zeggen dat ik toen erg blij was, maar ik ben je wel erg dankbaar voor al je hulp om het onderzoek weer op de rails te krijgen. **Holger**, het moment dat wij samen met 3D bril op de structuur van GLS bestudeerden, zal ik niet snel vergeten. Bedankt voor de enthousiaste uitleg en hulp hierbij. **Tobias**, bedankt voor de hulp bij de ROS metingen en interpretatie hiervan. **Maarten Lequin** en **Peter Schellekens** bedankt voor jullie radiologische resp. oogheelkundige deskundigheid. **Petra Pouwels**, **Marjo van der Knaap**, **Jannie Wijnen** en **Alex Bhogal**, bedankt voor jullie metingen inzicht in MRS en MRSI. **Benjamin Büttner, Rami Jamra**, **Oliver Maier, Jan-Ulrich Schlump, Bernhard Schmitt, Michele Losa, Ralph Fingerhut, Johannes Lemke** and **Graeme Black**: international collaboration is important, but a challenge, we did it!

Alex, met jouw MRSI passie en deskundigheid heb je mij veel geleerd en het onderzoek naar een hoger level getild. Ik ben blij dat je er voor mij was in de laatste stressvolle periode.

Speciaal wil ik ook stilstaan bij de **patiënten en familieleden**. Zonder hun verhaal en toestemming dit te mogen delen met de academische wereld, was dit onderzoek niet mogelijk geweest.

Het laatste jaar van mijn promotie heb ik gecombineerd met mijn opleiding tot klinisch geneticus in het Amsterdam UMC. Deze combinatie was niet altijd gemakkelijk. Ik wil **alle assistenten klinische genetica** bedanken voor de gezelligheid op de werkvloer, dit maakte de periode zoveel lichter! Ook wil ik de **stafleden,** met name mijn opleidster **Eline**, bedanken voor de ruimte die ik gekregen heb voor de laatste loodjes van mijn boekje.

Pilli's: **Britt**, **Lenneke**, **Zoë**, **Karin**, **Frederieke**, wij zijn samen begonnen met onze bachelor Biomedische Wetenschappen en hebben sindsdien allemaal ons eigen pad gevolgd. Ik geniet ontzettend van alles wat jullie meemaken en wat wij samen doen. **Free** zelfs met de oceaan ertussen zijn wij dichter naar elkaar gegroeid! **Britt**, jou ken ik al als tiener. Samen fotomodellen, liefdesverdriet, wonen, ruziën, gieren, reizen: ik ben zo blij om jou als vriendin te hebben. Ik hoop je snel weer te zien uit Australië. **Emerens**, **Ruben** en **Mantre**: ook jullie hebben van mijn studietijd inclusief co-schappen zo'n ontzettende leuke tijd gemaakt!

Naast al het werken is ontspanning natuurlijk belangrijk en dit heb ik in zoveel leuke dingen gevonden. Bovenal in het salsadansen bij Union. Ik heb genoten van het lesgeven en alle feestjes. **Alle dansers**: bedankt! Golly Gee Girls, wat krijg ik veel energie van het zingen met jullie. Vier verschillende stemmen en karakters die samen een match vormen. **Lex**, there ain't no valley low enough girl. Je bent recht door zee en doortastend. Ik heb genoten van alle optredens samen en kijk uit naar de volgende! **Willemijn**, geen toon is té complex voor jou. Met jouw harmonie laat jij alle tonen in het midden ontmoeten. Ik mis je als huisgenoot! **Inge**, jij verdient eigenlijk een eigen bladzijde. Niet alleen vanwege je krachtige stem, ook vanwege je krachtige en zachte persoonlijkheid. Je geeft mij zelfinzicht en naast dit alles kan ik vooral heel lekker met je lachen. **Willem**, wij zouden de kakelende kippetjes moeten heten zonder jouw jazzy leiding. Bedankt! **Pain du pudding** peoples: de weekendjes, festivals en vakanties met z'n allen hebben mij heel veel energie gegeven om weer een periode te kunnen knallen. Ik kijk weer uit naar het volgende weekendje weg!

Anne: studiegenoot, huisgenoot, vakantiegenoot, vriendin: ik ben blij met jou! **Bart**, je bent een topper. Je maakt onze Annie zowaar wat minder pittig en je vrolijke energie is aanstekend. **Roel**, jij staat expres los van Inge hier omdat ik je ook los van Inge als goede vriend zie waar ik altijd terecht kan voor een goede borrel en een goed gesprek. Fiesta Macumba baby! **Freark**, ook jou wil ik onwijs bedanken voor je gezelligheid en de heerlijke Lindyhop dansjes!

Lieve **(oud)huisgenoten**. Door jullie was er altijd wel wat te beleven in huis. **Marloes**, wij hebben elkaar in korte tijd goed leren kennen. Samen aan de BBB (nice and firm) en de avonden doorwerken aan ons onderzoek met theetje en kaarsjes erbij maakten mijn thuis een stuk gezelliger! **Geertrude**, ik heb zoveel met je gelachen, en ja ik weet dat ik vooral óm jou gelachen heb, maar het spijt me niet want ik heb het zo leuk met je gehad. **Bob**, ik heb genoten van jouw verhalen, muzikale bezigheden en alle spelletjes samen.

Lieve **pap** en **mam**. Jullie hebben mij de basis gegeven om het ver te schoppen met mijn carrière. Zowel in opvoeding als in genen! En nog steeds steunen jullie mij. Zo mochten de muizenogen en zebravislenzen met kerst bij jullie overnachten zodat ik niet op en neer hoefde te reizen. Ik geniet van alle verwennerijen als ik bij jullie ben en niet aan mijn promotie hoef te werken: het ophalen van en naar de trein, roomcroissantjes, massages, kopjes thee op de bank en natuurlijk het lekkere eten. **Merel** en **Bibi**, lieve zussen, wij zijn alle drie heel verschillend en toch zo hetzelfde. Ik vind het heel tof om te zien hoe wij ons alle drie onafhankelijk ontwikkeld hebben. Bieb, ontzettend bedankt voor je hulp bij het drukken van dit proefschrift! Ik ben altijd weer blij om jullie, en jullie mannen **Niels** en **Yasser**, te zien. **Oma Rumping**, u kunt zo heerlijk verhalen vertellen. Ik geniet altijd van uw gezelligheid! **Oma Willy**, u bent er al van jongs af aan bij als er iets te vieren valt: afzwemmen, dans- en fluitoptredens, afstuderen en nu ook mijn promotie-verdediging. Helaas kan **opa Ferry** er niet bij zijn, want wat zal hij ervan genoten hebben! In gedachten zijn hij en **opa Rumping** erbij.

Lena en **Nina**, mijn lieve paranimfen! Wij begonnen onze arts-onderzoekers carrière samen met de opleiding SUMMA en vervolgden deze gelijktijdig met onze PhD's in het UMC Utrecht en zijn nu alle drie in opleiding tot specialist. Ik ben zo trots op ons en zo ontzettend blij met jullie. **Nin**, met jouw luisterend oor en empathie kan ik altijd bij jou aankloppen. Tevens ook voor taartjes en 10-kazengerechten. **Leen**, alles is leuk met jou: weekendjes weg, wintersport, Suriname, zero heroo's, diners enz. Je bent een krachtig persoon en ziet en benoemt ook de kracht in anderen. Ik kijk uit naar alle aankomende gezellige diners met jullie lieve mannen **Job** en **Lars**. Ik ben ontzettend benieuwd waar wij over 10 jaar staan in onze carrière en sociale leven samen!

CURRICULUM VITAE

Lynne Rumping was born on 8 March 1988 in Beverwijk, the Netherlands. In 2007, Lynne started her bachelor Biomedical Sciences at the University of Amsterdam. During her bachelor, she was involved in research at the department of human antropogenetics, where her interest in clinical genetics arose. After her bachelor, Lynne was accepted for the Selective Utrecht Medical Master (SUMMA) in Utrecht. During medical school, her interest for pediatric genetics further developed. She started a research project at the departments of pediatrics and genetics, section metabolic diseases. Together with pediatrician metabolic diseases dr. van Hasselt, she obtained funding from ODAS to start her PhD-project in 2014 under supervision of prof.dr. Nanda Verhoeven-Duif and prof.dr. Roderick Houwen and her co-promotors dr. Judith Jans and dr. Peter van Hasselt. Her research mainly focused on the pathophysiology of novel metabolic diseases with disturbed glutamate homeostasis. During her PhD-project, she followed the training program 'Cancer, Stem cells and Developmental Biology' at the Graduate School of Utrecht. Furthermore, she was trained as a clinical scientist by the PhD training program of TULIPS (Teaching Upcoming Leaders of Pediatric Science) which focusses on bridging the gap between science and the clinic. Lynne combined the end of her PhD-project with her work as an in-training resident at the department of Clinical Genetics at the Amsterdam UMC under the supervision of dr. Eline Nannenberg. Her ambition is to combine her training as a clinical geneticist with translational science, by studying disease mechanisms of patients with unsolved genetic etiology.

LIST OF PUBLICATIONS

Rumping L*, Büttner B*, Maier O, Rehmann H, Lequin M, Schlump J.U, Schmitt B, Schiebergen-Bronkhorst B, Prinsen H.C.M.T, Losa M, Fingerhut R, Lemke J.R., Zwartkruis F.J.T, Houwen R.H.J, Jans J.J.M, Verhoeven-Duif N.M, van Hasselt P.M *, Jamra R*. Identification of a Loss-of-Function Mutation in the Context of Glutaminase Deficiency and Neonatal Epileptic Encephalopathy. *JAMA Neurol.* 2018.
*These authors contributed equally

Rumping L*, Tessadori F*, Pouwels P.J.W, Vringer E, Wijnen J.P, Bhogal A.A, Savelberg S.M.C, Duran K.J, Bakkers M.J.G, Ramos R.J.J, Schellekens P.A.W, Kroes H.Y, Klomp D.W.J, Black G.C.M, Taylor R.L, Bakkers J.P.W, Prinsen H.C.M.T, van der Knaap M.S, Dansen T.B, Rehmann H, Zwartkruis F.J.T, Houwen R.H.J, van Haaften G, Verhoeven-Duif NM, Jans JJM*, van Hasselt PM*. GLS hyperactivity causes glutamate excess, infantile cataract and profound developmental delay. *Hum Mol Genet.* 2019;28(1):96-104.
*These authors contributed equally

Rumping L, Waterman H.R, Kok I, van Hasselt P.M., Visser G. Hereditaire fructose Intolerantie. *Ned Tijdschr Geneeskd*. 2014.

Dijkman R, Mulder H.L, **Rumping L,** Kraaijvanger I, Deijs M, Jebbink M.J., Verschoor E.J., van der Hoek L. Seroconversion to HCoV-NL63 in Rhesus Macaques. *Viruses*. 2009.

SUBMITTED MANUSCRIPTS

Rumping L, Pras-Raves M.L, Gerrits J, Tang Y.F, Willemsen M.A, Houwen R.H.J, van Haaften G, van Hasselt P.M, Verhoeven-Duif N.M, Jans J.J.M. Metabolic fingerprinting reveals extensive consequences of GLS hyperactivity. Manuscript submitted.

Rumping L, van Hasselt P.M., Vringer E, Houwen R.H.J., Jans J.J.M., Verhoeven-Duif N.M.. Review: Inborn errors of glutamate metabolism. Manuscript submitted.

Rumping L, de Graaff A.M, Schellekens P.A.W, Tessadori F, Kalee M, Bakkers J, van Haaften G, Roderick H.J. Houwen, Jans J.J.M, Verhoeven-Duif N.M, van Hasselt P.M. Fluorescence microscopy with UV-illumination allows accurate visualization of cataract in zebrafish embryos *in vivo*. Manuscript submitted.

ABBREVIATIONS

IEM	Inborn error of metabolism
5-Opase	5-oxoprolinase
AD	Autosomal Dominant
ALDH	Aldehyde dehydrogenase
ALT	Alanine Aminotransferase
AR	Autosomal Recessive
AST	Aspartate transaminase
BCAT	Branched-chain amino acid aminotransferase
CSF	Cerebrospinal fluid
DI-HRMS	Direct infusion high resolution mass spectrometry
DNA	Deoxyribonucleic acid
DPF	Days Post Fertilization
EC code	Enzyme commission code
EV	Empty Vector
FUVI	Fluorescence microscopy with UV-light Illumination
GABAT	Gamma-aminobutyric acid transferase
GAC	Kidney-type glutaminase
GAD1	Glutamate decarboxylase
GCLC	Glutamate-Cysteine Ligase Catalytic Subunit
GDH/GLUD	Glutamate dehydrogenase
GLS/GLS1	Glutaminase
GLUL	Glutamate-ammonia ligase
GoF	Gain-of-function
GOT	Glutamic oxaloacetic transaminase
GPT	Glutamate pyruvate transferase
GS	Glutamine synthetase
HPO	Human Phenotype Ontology
KGA	Kidney-type glutaminase
LoF	Loss-of-function
MRI	Magnetic resonance image
MRS	Magnetic resonance spectroscopy
MRSI	Magnetic resonance spectroscopic imaging
NAGS	N-acetylglutamate synthase

NGS	Next Generation Sequencing
OAT	Ornithine aminotransferase
P5CD	Pyrroline-5-carboxylate dehydrogenase;
P5CS	Pyrroline-5-carboxylate synthetase
PDB	Protein Data Bank
PSAT	Phosphoserine transaminase
RNA	Ribonucleic acid
ROS	Reactive Oxygen Species
SNP	Single nucleotide polymorphism
TAT	Tyrosine aminotransferase
TCA	Tricarboxylic acid
UCD	Ureum Cycle Defect
VUS	Variant of Unknown Significance
WES	Whole Exome Sequencing
WGS	Whole Genome Sequencing